IDENTIFICATION AND CONTROL STRATEGY APPLIED IN LOAD MANAGEMENT OF RESIDENTIAL AIR-CONDITIONERS

SYED AMEENUDDIN HUSSAIN

SYSTEMS ENGINEERING

JANUARY 2004

KING FAHD UNIVERSITY OF PETROLEUM AND MINERALS

DHAHRAN 31261, SAUDI ARABIA

DEANSHIP OF GRADUATE STUDIES

This thesis, written by **SYED AMEENUDDIN HUSSAIN** under the direction of his Thesis Advisor and approved by his Thesis Committee, has been presented to and accepted by the Dean of College of Graduate Studies, in partial fulfillment of the requirements for the degree of **MASTER OF SCIENCE IN SYSTEMS ENGINEERING.**

Thesis Committee

Dr. SAMI EL – FERIK (Chairman)

Dr. FOUAD AL – SUNNI (Co – Chairman)

Dr. UMAR AL – TURKI
(Department Chairman)

Dr. CHOKRI B. AHMED (Member)

Prof. OSAMA A. JANNADI
(Dean of Graduate Studies)

Dr. MANSOUR AL – DAJANI (Member)

Date

Dr. SAMIR C. NASSIF (Member)

Dedicated

to

My Dear Parents

Whose Prayers, Guidance and Inspiration led to this

Accomplishment.

ACKNOWLEDGEMENTS

All praise is for ALLAH (S.W.T.), the most compassionate, the most merciful. May peace and blessings be upon Prophet Muhammed (S.A.W.), his family and companions. I thank almighty ALLAH (S.W.T.) for giving me the knowledge and patience to complete this work.

I would like to acknowledge the facilities provided by King Fahd University of Petroluem & Minerals during my stay at Dhahran. I would also like to acknowledge the support provided by the Chairman, Systems Engineering department, for the completion of this work.

I would like to express my profound gratitude and appreciation to my advisor Dr. Sami El-Ferik, for his consistent help, guidance and attention that he devoted throughout the course of this work. He was always kind, understanding and sympathetic to me. His valuable suggestions and useful discussions made this work interesting for me.

I would also like to thank Dr. Fouad Al-Sunni for his constant appreciation, attention and words of encouragement throughout my thesis work. I would also take opportunity to express my gratitude to Dr. Chokri Belhaj Ahmed for giving access

to share the setup in Rabee Courts, KFUPM. Thanks are also due to my thesis committee members Dr. Mansour Al-Dajani and Dr. Samer Nassif for their interest, cooperation, and constructive advice.

I would also like to acknowledge valuable suggestions given by Dr. Shafiq and Mr. Anas Viqar during the implementation stage of this work.

Thanks are due to my friends Noman, Farooq, Asif, Amjad, Naveed, Ahsan, Sanaullah, Faheem, Ashfaq, Khaleel, Atiul, Jaweed, and to all S.E graduate students, for their moral support, good wishes and the memorable days shared together.

Special thanks are to my parents Mrs & Dr. Syed Hafeezuddin Hussain, my sister and brother-in-law Mrs & Mr Arshad Alam Khan, my brothers Syed Aleemuddin Hussain and Syed Viquaruddin Hussain and sister Miss Syeda Asma for their love, sacrifices, prayers and understanding.

Contents

List of Tables

List of Figures

THESIS ABSTRACT

Name: SYED AMEENUDDIN HUSSAIN

Title: Identification and Control Strategy applied in Load management of Residential Air-Conditioners

Degree: MASTER OF SCIENCE

Major Field: SYSTEMS ENGINEERING

Date of Degree: JANUARY 2004

Saudi power utilities are under increasing need for controlling the power demand because of severe limitations of power generation resources. Loads with energy storage characteristics like Air-conditioners, Space heaters, etc. are considered as best suited for Demand-side load management scheme having the objective of changing the power demand profile. In this work the steps towards Direct Load Control (DLC) which have shown promising results are addressed. These steps involve identifying the parameters of systems and applying the control strategies as forced duty cycles. An integrated simulation environment was developed wherein the identification and control algorithm were implemented. Also, foundation was laid for carrying out the implementation of this simulated environment on a real Air-Conditioner (A/C) system.

Keywords: *Physically based load models, Load management, Identification, Optimal control.*

Master of Science Degree

King Fahd University of Petroleum & Minerals, Dhahran.

JANUARY 2004

Chapter 1

INTRODUCTION

1.1 Overview

Electric Power demand is growing rapidly throughout the globe. For Saudi Arabia, it has increased by almost 25 times from 1975 to 1998 and it is expected that the peak load will reach 60,000 MW by year 2020. Of all the total load the residential Air-Conditioner (A/C) load contributes to almost half of the total power demand satisfied by Saudi Electric Company (SEC) [1]. The increase in A/C load is mainly attributed to technological advances and rapid urbanization during the last decade in the Kingdom.

In Saudi Arabia, the power generation resources are limited and rely on steam generation or natural gas turbine generation. The Kingdom has shown an interest and a sincere commitment to the development of the electrical energy sector. Although

the competition in the electrical market is not comparable, the major company SEC and its customers will benefit greatly from any load management policy aiming at reducing cost and increasing reliability.

These Load Management Schemes can be described as activities oriented to have a desired shape in the profile of the load demand. This allows for better use of the power system resources, ensuring stability in the network and creating advantage of low tariffs for the customer.

The Load Management Schemes could be categorized into two different types. They are described as follows:

1. Direct Load Control (DLC): The utility in this case has direct control over the equipment used by the customer. The equipment taken under consideration are the ones associated with some kind of energy storage like Air-Conditioners, Space Heaters, Water-Heaters, etc. In this kind of control the utility goes for selective "On-Off" of equipment in the group while ensuring

    - the demand profile follows the target curve
    - minimum comfort levels are maintained
    - payback periods are avoided etc.

2. Indirect Load Control (ILC): In this type of control the customers switch on and off their equipment depending on their own price signals like dynamic tariff rates etc.

Direct Load Control are the one which are commonly adopted where the forced utility interruptions to a homogenous groups are implemented to reliably achieve maximum profits, improve and control the load profile. DLC strategies will be addressed through out this work.

Models are needed to predict whether the DLC implemented by the utility produces the desired results or not. These load models should be able to fulfill the following:

1. Provide all the necessary information as to how the DLC provide benefits when implemented.

2. Allow evaluation of each and every control action implemented by the utility from the customers point of view.

Models based on the time-series approach [2, 3, 4, 5] have been implemented but fail in the wake of certain characteristics faced in the load modelling problems. These are sketched in detail in Chapter 2. These liabilities have invoked much interest in the more complex physical based modelling methodologies [6, 7, 8, 9, 10].

The physically based models are decomposed into two parts: modelling is first done at the elementary level, and then various statistical methodologies are applied to obtain an aggregate model. The elementary physically based model encompasses two major components: the functional model and the electric response model as shown in Figure 1.1.

The functional model is associated with energy storage and control whereas the

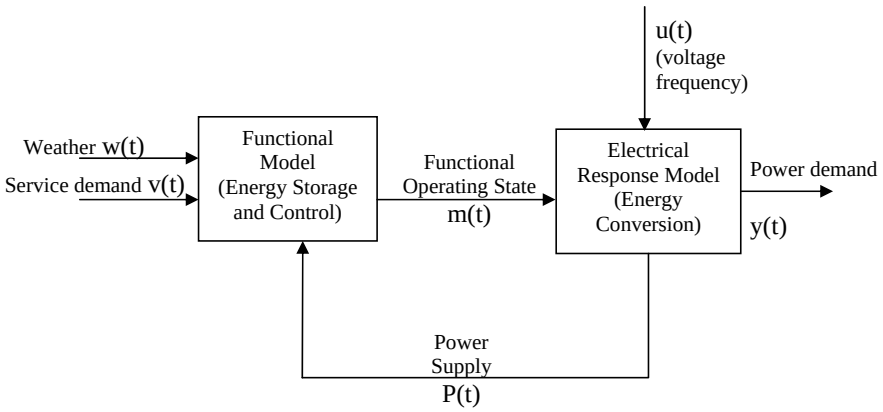

Figure 1.1: An Elementary Physically Based Model.

electric response model portrays the energy conversion in the model.

Different physically based models were proposed for DLC, but Stochastic Hybrid State model proposed by Chong and Debs [8] was adopted for its comprehensiveness. Aggregation was then applied to it and the resulting aggregate load model is a system of Fokker-Plank equations. These equations characterize the dynamics of temperature distributions in dwellings associated with the thermostatic discrete state "On and "Off" respectively. One of the advantages of this approach is that the physical meaning present at the elementary level is preserved at the aggregate level. The methodology presented is exact in a statistical sense [9].

Another important fact about these models is the identifiability from easy to access data. There are two methods discussed in the literature. The maximum likelihood approach addressed by Kamoun and Madame [11] and an identification scheme based on standard device energy consumption measurements over constant time

intervals proposed by Sami El-Ferik and Madame [12]. Maximum Likelihood Estimation Scheme addresses the problem of identification based on the measurements of "On-Off" thermostat durations. The simplest algorithm reduces to recursive computation scheme based on these "On-Off" durations.

Different controller formulation schemes are also important for the DLC strategies. Many of these controllers are based on optimization tools like linear programming, dynamic programming [13, 14, 15, 16, 17] etc. to achieve maximum profits and reduce demand. Pulse Width Modulation (PWM) [18] has also been used in designing a controller. But all the above schemes have presented a shortcoming based on their own assumptions to come up with a controller. For examples, in controllers based on dynamic programming and linear programming, candidate schedules have to be pre-specified and the demand profile cannot be modified according to target load profile. PWM also presents a good controller scheme but does not take into account the customer's minimum comfort level to calculate forced duty cycles. Model Predictive Control based on sequential quadratic programming [19] has also been presented which have eliminated the shortcoming of all the above mentioned controller types.

Implementation architecture for these controller schemes have recently received great importance in DLC programs. This is due to exponential increase in technology in the last decade and availability of sophisticated, inexpensive and high speed equipment. The specific selection of the technology that is to be applied and equipment

to be used is important for success of DLC. The next section describes the problem at hand.

1.2 Description of the Problem

The aim is to have an integrated environment where direct load management simulation scheme is developed in order to reshape electric consumption profiles. Also, the load management strategy must be cost driven and more than ever rely on timely information. In order to fulfill these two objectives, load management system (LMS) is composed of two main parts: the hardware component, and the software component. At the customer side the required hardware includes sensors for the measurement of required output such as power consumption and thermostat on/off cycles, input/output interface card with data collecting units, data transmission, and direct control devices implemented at the load level. At the utility end, a computer program automatically performs the analysis of the collected data, identifies the load model parameters and generates the required control actions. The objective of this work is presented in the following section.

1.3 Objectives

This work is composed of two parts: simulation and experimental. The simulation part of this work aims at reproducing the close dynamics of the load model.

This model will help represent the power changes with respect to the environmental conditions. A sensitivity analysis will evaluate the quality of the identification algorithm and the convergence speed of the estimators and predicting the required power. The control algorithm will be applied to different set of homogenous classes. A feasibility study will be conducted to evaluate the possible power savings.

The experimental part will focus on the real identification of load model parameters in a residential setting. It will deal with data acquisition of various parameters from different instruments and its related programming. The experimentation also aims at developing and designing a device for implementing a DLC environment for a real case. It will include components such as sensors, electronic circuitry for Air-Conditioners state measurement and actuators to apply direct control intervention. The selection and design criteria of the hardware will be preceded by sensitivity analysis to environmental changes.

The objectives could be stated as follows:

1. "Simulation and validation of physically based models that would be used in identification and control strategy for a single and homogenous system"

2. "Simulation and analysis of the identification scheme on a real case and its performance compared and validated with theoretical results"

3. "Analysis of optimal control performance on power savings and payback when reconnected on different homogenous groups"

4. "Devise suitable and practical ways of measuring and transmitting data for identification and implementation of control strategy as forced duty cycles"

5. "Extension of objective 2 to study the effects of solar radiation and humidity levels on identification and if they can be incorporated as noise parameters"

1.4 Thesis Organization

The remainder of this thesis is organized as follows. In Chapter 2 related research articles are first categorized in four different groups depending on their approach. The contribution of various authors was reviewed. Chapter 3 deals with the introduction of the identification scheme and its implementation in simulation for the A/C. In Chapter 4, the control strategy is developed and its analysis is presented with some simulation results. Chapter 5 presents the full experimental work involving instrumentation and data collection. It also reports the hardware design of a low cost computer controlled device needed for load control in DLC. Chapter 6 contains the identification of the load model based on real data collected, and the results compared with the theoretically derived values. It also discusses the effects of humidity and solar radiation on the identification. Finally, conclusions and suggestions for future work are presented in Chapter 7.

Chapter 2

LITERATURE REVIEW

2.1 Introduction

The literature presents the review material in the area of Load Management of residential Air-Conditioners, which could be approached from four different points of view:

1. The Modelling perspective which forms the basis for Load Management Schemes.
2. Identification of model parameters which is critical for implementation.
3. Control strategies that are the core of Load Management Schemes.
4. The implementation architecture for executing Direct Load Control strategy.

The review for each approach is presented in subsequent sections. The following section presents the literature for the Load models used in DLC strategies.

2.2 Modelling

There are two types of load models for electric load consumption. They are:

1. *Load demand model*: This type describes the demand behavior with respect to time. It also characterizes the load demand portion of any component with influence from human-use patterns, environmental changes, etc.

2. *Load response model*: This type describes behavior of load when subjected to changes in external inputs (like the changes in voltage, frequency, operating state etc.) to the electric load.

The above characteristics are present in various power-system operations. Getting a model that combines both the load demand and load response characteristics helps in implementation of online automatic control generation, transient stability analysis, handling emergency situations in power demand etc. Time series approach was extensively used in modelling both types but each was approached separately.

Galiana F. D. et al. [3] & Bunn and Farmer [5] approached the Load Demand Modelling problem traditionally by collecting data and filtering it through some statistical means. This was usually applied for short term load forecasting known as Automatic Generation Control (AGC) where diversified loads were involved.

However, when Load Management Schemes are applied, both of these models have to be jointly considered. The demand behavior of the electric load will have to be studied and analyzed when different control actions are taken on the system. Also,

prediction as to how the demand will evolve has to be done. This has led to the use of more complex physically based models.

The literature mostly presents thermal models of house for investigating the heating and cooling loads of power systems. The literature for these models is presented next.

Chong C.Y. and Debs A. S. [8] in 1979 for the first time proposed physically based models to be used to overcome the problem faced by time-series models. They also provided the basis of aggregation methodology of functional load model, where statistical aggregation of a large number of similar components in electric power system (based on these basic physical models) were done. Of all the models suggested by them, the stochastic hybrid state model is the one of particular importance because it constitutes a significant portion of the load demand.

Ihara S. and Schweppe F. C. [6] in 1981 provided a simplified physical dynamic model for the temperature of a house having a heater regulated by a thermostat. With this model, the transient behavior of the power load when subjected to control actions could easily be accessed.

Madame R. and Chong C. Y. [20] showed the dynamics of electric demand of large aggregate of electric space heaters or air-conditioners. They derived the electrical dynamics of a homogenous group of similar devices as a system of coupled ordinary and partial differential equations known as the Fokker-Planck equation. They claimed that this equation for a particular case of a large aggregate of space heaters

could be generalized to other hybrid-state stochastic systems.

Madame R. and Chong C. Y. [21] studied extensively the statistical properties of the cyclic diffusion process that was used to construct the aggregate load models for power system loads governed by the thermostat(heating or cooling loads). These properties were analyzed using the Renewal Theory and Fokker-Planck equation.

Mortensen R. E. and Haggerty K. P. [7] in 1988 extended the model given by Ihara and Schweppe [6] by two folds. First, they added a white noise forcing term making it a stochastic difference equation model. They proposed this for pure application in computer simulation so as to have an understanding of the system which was not transparent from the theoretical angle. Then, this model was extended where the state was discretized. The model they proposed was relevant from studying loss and recovering diversity of thermostat loads following an outage.

Mortensen R. E. [22] in 1990 studied the class of stochastic process called the alternating renewal processes that appear more suitable for modelling thermostat loads on electric power systems. He studied a particular case for air-conditioners and derived expressions in Laplace transforms for non-stationary mean and stationary autocorrelation functions. He also showed that these results could permit measurements taken under nominal conditions to predict transient behavior after an outage.

Mortensen R. E. and Haggerty K. P. [9] in 1990 compared five different models for cold load pick-up and Direct Load Control strategies. They concluded that the actual utility data has two stages in their transients which they referred to as 'epochs'.

The first epoch is experienced when all the loads are connected to the power grid and the second occurs when the load undergoes thermostatic cycling until a diversified state of cycling is reached. They concluded that the Deterministic Differential equation model and the Stochastic Difference equation model are suited to find out the duration of first epoch, while the Markov Chain Matrix equation model and the Alternating Renewal model is suited to predict the duration of the second epoch. But Hybrid Partial differential equation provided a unifying framework for all the models which makes it important to study it further in terms of identification, control strategies, etc.

Alvarez, Madame and Gabaldon [10, 23] also supported Mortensen and Haggerty's [9] conclusion about hybrid partial differential equations and showed how these models could be used as a tool for load management action evaluation.

Canbolat and Ramazan [24] in addition studied the load parameter dispersion and concluded that thermal capacity and dead band do not alter the magnitude of an aggregated load but the thermal resistant, rating of the Air-Conditioner and the thermostat setting are important parameters in determining the aggregated load level for steady-state.

2.3 Identification

The next important question one faces is how to identify the parameters of power systems for utilities to implement Load Management Schemes. These identification issues i.e. strategies and methologies have been addressed by two papers in the literature. They are presented below.

Kamoun and Madame [11, 25] have addressed this identification issue which reduces the problem of identification to an estimation of the elementary model parameters. This scheme was inspired from the very nature of measurements (i.e. "On-Off" thermostat durations) and the stochastic nature of the model. Evaluation of internal thermal noise which is a key parameter was also adequately addressed along with the deterministic parameters of the model. Given the stochastic nature of the model they found the Maximum-Likelihood method more appropriate when weighed against Least-Squares method as the later viewed the dwelling internal noise as spurious and originating in measurement errors. They also subsequently provided statistical properties of the Maximum-Likelihood estimators for a limited sample. The scheme's advantage is presented in the evaluation of potential benefits of the Load Management by DLC to a given utility before actually investing the required control and communication equipment.

El-Ferik and Malhame's [12, 26] identification scheme was inspired because of non-availability of measurements of thermostat "On" and "Off" durations. This identi-

fication scheme relies on standard energy consumption measurements over constant time intervals wherein the alternating renewal nature of thermostat switching process was exploited. But an increase in length of data record required for identification was observed with gradual loss of identifiability as the constant interval over which energy measurements are collected grows.

2.4 Control Strategies

Control strategies are methodologies whose aim is to influence the demand of the power system according to what is desired by the utilities. These strategies provide means of getting the desired results by governing the decision variables that are to be controlled in the system. The decision variable here is the switching of the power supply to particular thermostatic loads arranged in some kind of homogeneous groups. Various different optimization and other methods of influencing these switching loads have been discussed in the literature, some of which are presented below.

Hsu and Kuo [15] used a dynamic programming algorithm to produce both generation schedule and amount of load control at each control interval. This was part of initial efforts in implementation of control strategies for demand reduction with an objective of integrating Direct Load Control schedules with unit commitment and maximizing fuel cost saving. But this algorithm required high memory and compu-

tation time which makes time horizon for its implementation small.

Wei and Chen [16] presented their algorithm to overcome this limitation of time horizon using the multi-pass dynamic programming methods for dispatching of Air-Conditioner Direct Load Control. Using this approach, they were able to schedule DLC dispatch of Air-conditioners for eight days with very less computation time and memory.

Chen et al. [17] presented a method which first identified a set of candidate control patterns for feasibility and cost benefit and then gives an optimal DLC dispatch via a binary network flow model. However, both of the above methods considered a constant controllable load and specified fixed candidate schedules in their formulation.

Kurucz et al. [13] used linear programming for reducing peak load demand and concluded that linear programming was a powerful and effective tool for scheduling load control. The paper did not consider possibilities for all control duration strategies that could be used.

Ng and Shebé [14] rectified the above liability and considered all the control duration strategies using linear programming. But the method used an assumption of constant controllable load to achieve load reduction which is a drawback in itself. Moreover, the aforementioned strategies did not include the customers comfort index in their formulation, which is considered equally important when compared to demand reduction.

Navid and Banakar [18] presented the Pulse Width Modulation(PWM) to reduce the controlled appliances power demand in accordance with a predefined load reduction profile or target curve. This control strategy had the advantage of scheduling controllable loads with the basic information of peak demand and thermostat cycling which are easily available. The scheduling technique was computationally easy to implement on a PC. While this strategy helped in getting a more flexible Load Management program and an effective use of more sophisticated equipments, it was applied only during control period. A different control strategy was opted after the control period in order to reduce the payback. Apart from this, customer comfort is not taken into consideration which could always lead to customer dissatisfaction. Bhattacharya and Crow [27] introduced fuzzy logic in DLC anticipating the need to implement customer's preferences and needs into consideration in the utility based control. Using the fuzzy logic approach, they tried to optimize the trade-off between customer preferences, utility resources and uncertainty in load.

Huang et al. [28] suggested a fuzzy dynamic programming structure to reduce load as well as total operating costs for scheduling the DLC. Taking the uncertainties of load variation on the basis of the previous load prediction errors, the authors made their method more robust in its structure.

Leether and Hsieh [29] proposed the use of a modified Genetic Algorithm (GA) called as recursive GA to optimize the scheduling of DLC strategies. They showed that the recursive GA tends to level off the accumulated shedding time of each controllable

load group which can avoid customer complaints about the fairness of scheduling. Although this strategy works with good results, it requires the optimal schedules to be set up manually in the load management system. Moreover, it looked at the controllable load profile without taking into consideration the global or the total load profile.

Molina et al. [19] described a new constrained multi-variable predictive control strategy with the objective of scheduling the DLC in accordance with the global or total load curve to be applied in residential Heating, Ventilation and Air-Conditioner (HVAC) DLC. This control algorithm provided a multiobjective framework taking into account customer's comfort, HVAC limits, utility limitations etc., to minimize the discrepancies between controlled load curve and the predefined target load curves. The control problem suggested by them was to optimally control the residential HVAC to modify the global load curve according to a target load profile prefixed previously. They demonstrated the qualities of this scheme by applying it to modify the real load curve profile.

2.5 Implementation

The structure or the architecture of implementing a control scheme on a power system is gaining its own importance in Load Management Schemes. Recent literature has also given some importance to it and their successes, experiences and liabilities

have been discussed. Some of the implementation architecture schemes that are addressed in the literature are presented below.

Anibal and Edward [30] gave an assessment of how different technologies could be used in monitoring the load management schemes with respect to implementation.

Chang et al. [31] shared the experiences on implementing a DLC using ripple signal in Taiwan's power system. They discussed the problems faced in such an implementation and suggested solutions to those problems.

Cho and Huang [32] developed a PC-based energy management system associated with automatic power meter reading and various control functions. In their PC based structure, automatic power meter was configured by a Programmable Logic Controller (PLC) and several software like Visual basic, PLC ladder language and Diamond package were used to integrate all the hardware equipment. They showed that by running with this particular implementation structure for two years, it was possible to effectively achieve peak load cutting and energy saving.

Ming, Gau and Huang [33] suggested a microprocessor based demand control system which contains both the load management software package and the demand controller. Visual Basic combined with C language support were used as software supports for load data retrieval, database management, demand contract evaluation and load characteristic analysis.

Hwang [34] investigated and suggested a load survey system to identify the potential of air conditioner load management. In the survey, he had shown that a rise of 1^{o}C

had resulted an increase in power demand by 490 MW at Taipower systems, Taiwan. The accuracy of this proposed method was verified by knowing actual power demand of the whole Taipower system and using it to derive the temperature sensitivity of power system consumption.

Paul and Harold [35] proposed an internet based architecture for monitoring, controlling and operating HVAC systems. This is the latest in implementation strategies adopted by power system utilities and has come about with the revolutionary advancement in computer and internet technologies. They found that the architecture proposed was achievable given the network protocols and software systems, and could be easily linked with TCP/IP-based office and campus network.

2.6 Summary

In this chapter we have looked at the available literature in the area of Load Management of residential A/C's. The work was classified according to modelling, identification, control strategies and implementation. Major contributions of various authors was briefly discussed.

Chapter 3

IDENTIFICATION SCHEME

3.1 Introduction

Since the model available in the literature deals with the heater, our methodology in the presentation of the identification scheme will be as follows:

- First the heater elementary model proposed in [8] and the aggregate model based on [21] are presented.
- Then the Maximum Likelihood identification scheme proposed in [11] will be presented along with some theoretical sensitivity analysis.
- Identification results obtained through simulation for the heater will then be compared with the theoretical results [11, 25].
- The elementary model and the aggregate model for Air-Conditioner will be

developed on the same analogy as that of the heater.

- Identification scheme and sensitivity analysis will then be developed for the Air-Conditioner Case.
- Simulation results for identification will be performed and compared with the theoretical results.
- Finally, the aggregate simulation A/C model for a single homogenous case will be tested for Cold Load Pickup with the result obtained by [10].

The description of the heater model is explained in the following section.

3.2 Description of Heater Model

3.2.1 The Hybrid Stochastic Model for Heater

The continuous stochastic differential equation Model for the heater is described as follows

$$Cdx(t) = -\acute{a}(x(t) - x_a(t))dt + \acute{R}m(t)b(t)dt + d\acute{v}(t) \tag{3.1}$$

which could be modified by dividing through out by C as

$$dx(t) = -a(x(t) - x_a(t))dt + Rm(t)b(t)dt + dv(t) \tag{3.2}$$

where

C	=	avgerage thermal capacity of the house in joules/^{o}C
$\acute{a}$	=	average heat loss rate of the house in Watts/^{o}C
$x(t)$	=	average temperature of the house in ^{o}C
$x_a(t)$	=	the ambient temperature in ^{o}C
$\acute{R}$	=	rate of heat gain supplied by the heater in Watts
$m(t)$	=	operating state of the device (1 for 'on' or 0 for 'off')
$\acute{v}(t)$	=	noise process
$b(t)$	=	the state of the power supply (1 for 'on' or 0 for 'off')

And the discrete state equation is given by

$$m(t) = m(t) + \Pi(x(t) : x^+, x^-) \tag{3.3}$$

$$\Pi(x(t) : x^+, x^-) = \begin{cases} 0 \text{ for } x^- \leq x \leq x^+ \\ m(t-1) \text{ for } x \geq x^+ \\ 1 - m(t-1) \text{ for } x \leq x^- \end{cases} \tag{3.4}$$

This primitive model is illustrated in Figure 3.1, to which aggregation methodology is applied wherein an aggregate model representing a certain class of system is constructed. The aggregation is discussed in the following section.

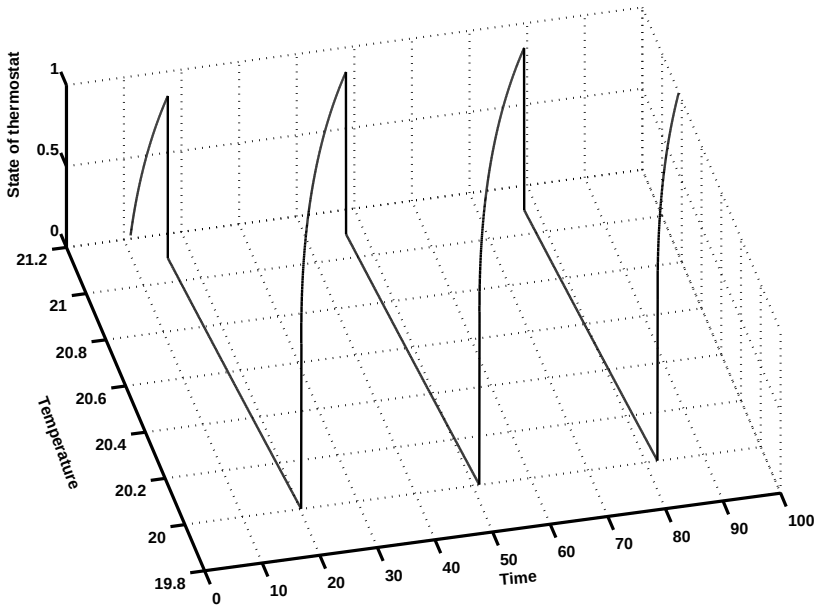

Figure 3.1: Continuous State and Discrete State as Function of Time.

3.2.2 The Aggregate Model

If 'N' devices have the same switching dynamics as in equations (3.1-3.4) then the aggregate demand of the devices i.e. the total power $P(t)$ is

$$P(t) = \sum P_i(t) = \sum \acute{R}_i m_i(t) b_i(t) \tag{3.5}$$

where $i = 0$ to N

Assumptions:

1. Geographically the elements are close which means that the ambient temperature for devices under consideration are almost identical.

2. The next assumption is that the load demand of individual elements are inde-

pendent stochastic processes.

Homogeneous case

Consider a homogeneous group of 'N' devices having identical energy storage capacities and switching dynamics and subjected to the same control strategy.

Therefore

$$b_1(t) = b_2(t) = b_3(t) = ... = b_N(t)$$

Then

$$P(t) = \sum P_i(t) = \acute{R}_i b_i(t) \sum m_i(t) = \acute{R} b(t) N \bar{m}(t) \tag{3.7}$$

where

$$\bar{m}(t) = \frac{1}{N} \sum m_i(t) \tag{3.8}$$

where $\bar{m}(t)$ is called the aggregate operating state. Since $\acute{R}, b(t), N$ are known, the modelling of P(t) suffices for the modelling of $\bar{m}(t)$.

Modelling of $\bar{m}(t)$

With the weather as the time varying input and taking the above two assumptions into consideration, $\bar{m}(t)$ can be treated as N independent and identically distributed random variables at each 't'.

Using Kolmorov's strong law of numbers, as $N \to \infty$

$$\bar{m}(t) \to E_w(m(t)/\zeta) \tag{3.9}$$

where $E_w(./\zeta)$ is the expectation operator conditional on weather information and given the device parameter ζ, then the approximation can be

$$\bar{m}(t) \simeq E_w(m(t)/\zeta) \tag{3.10}$$

This is the basis of aggregation methodology. This variable can be computed once the evolution of probability densities of the stochastic system are known.

Associated with the hybrid state Markov process $[x(t)\ \ m(t)]'$ are two hybrid densities $f_1(\lambda, t)$ and $f_0(\lambda, t)$ which can be defined as

$$f_0(\lambda, t) = Pr[(\lambda < x(t) < \lambda + d\lambda) \bigcap (m(t) = 0)] \tag{3.11}$$

$$f_1(\lambda, t) = Pr[(\lambda < x(t) < \lambda + d\lambda) \bigcap (m(t) = 1)] \tag{3.12}$$

Where $f_1(\lambda, t)$ is the hybrid probability density function for continuous state $x(t)$ and discrete state $m(t)$ when the heater is "On" and $f_0(\lambda, t)$ is the hybrid probability density function for continuous state $x(t)$ and discrete state $m(t)$ when the heater is "Off".

The Aggregate Model

The above hybrid-state probability densities satisfy the Coupled Fokker-Planck Equations (CFPE)

$$T_{\lambda,t}{}^1[f_1(\lambda, t)] = 0 \tag{3.13}$$

$$T_{\lambda,t}{}^{0}[f_0(\lambda,t)] = 0 \tag{3.14}$$

where

$$T^{k}_{\lambda,t}[f] = \frac{\partial}{\partial t}f - \frac{\partial}{\partial \lambda}[(a(\lambda - X_a(t)) - kb(t)R)f] - \frac{\sigma^2}{2}\frac{\partial}{\partial \lambda^2}f \tag{3.15}$$

This is illustrated in Figure 3.2 with the boundary conditions for all 't' defined as follows:

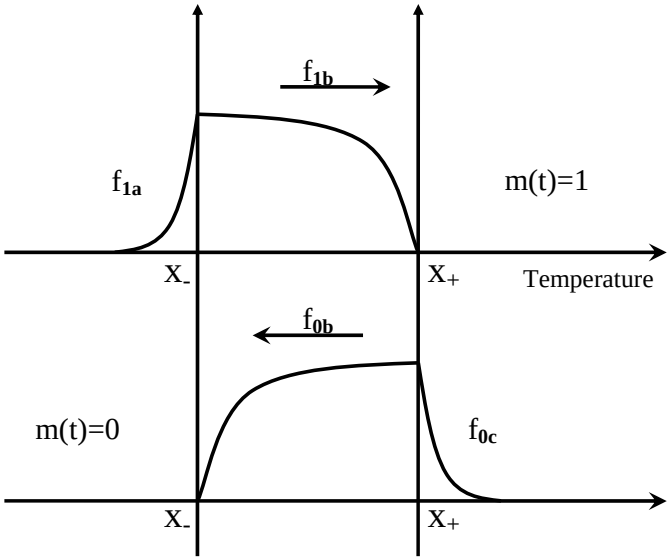

Figure 3.2: Illustration of Dynamical System (Heater).

The absorbing boundary

$$f_{1b}(x_+,t) = f_{0b}(x_-,t) = 0 \tag{3.16}$$

The conditions at infinity

$$f_{1a}(-\infty,t) = f_{0c}(\infty,t) = 0 \tag{3.17}$$

The continuity conditions

$$f_{1a}(x_-, t) = f_{1b}(x_-, t) = 0 \tag{3.18}$$

$$f_{0b}(x_+, t) = f_{0c}(x_+, t) = 0 \tag{3.19}$$

Probability Conservation

$$-\frac{\partial}{\partial\lambda} f_{1a}(x_-, t) + \frac{\sigma^2}{2}\frac{\partial}{\partial\lambda} f_{1b}(x_-, t) + \frac{\sigma^2}{2}\frac{\partial}{\partial\lambda} f_{0b}(x_-, t) = 0 \tag{3.20}$$

$$\frac{\partial}{\partial\lambda} f_{0c}(x_+, t) - \frac{\sigma^2}{2}\frac{\partial}{\partial\lambda} f_{0b}(x_+, t) - \frac{\sigma^2}{2}\frac{\partial}{\partial\lambda} f_{1b}(x_+, t) = 0 \tag{3.21}$$

together with the equation

$$\bar{m}(t) = \int_0^t \frac{\sigma^2}{2}[\frac{\partial}{\partial\lambda} f_1(x_+, \tau) + \frac{\partial}{\partial\lambda} f_0(x_-, \tau)]d\tau + \bar{m}(0) \tag{3.22}$$

is the aggregate load model.

Similarly, the aggregate model for the Air-Conditioner could be arrived at by simple sign changes as shown in further sections.

3.2.3 Probability Density Functions for the "On-Off" Durations

For the space heater, the available variables are the "On-Off" durations and the ambient temperature. When noise is assumed as a Weiner process, then "On-Off" thermostat durations will be independent (first passage times) random variables. The "On" and "Off" duration times corresponding to the first passage times from

x_- to x_+ and x_+ to x_- for a Brownian Motion with time varying drift rates, $r(t)$ and $c(t)$ which are respectively defined as heating and cooling rates

$$r(t) = R - a(x(t) - X_a) \tag{3.23}$$

$$c(t) = a(x(t) - X_a) \tag{3.24}$$

Since the probability density functions are confined within a narrow range of temperatures (typically 1.5^o C), the above drift rates are practically constant (for constant weather conditions and for duration of the control applied). Referring to these as constants r and c with $x(t)$ replaced by the mean $\bar{x} = \frac{x_+ + x_-}{2}$. Then the probability density function for such passage times for this particular case is given by

$$p_{on}(T_{on}, \theta) = \frac{\Delta}{\sigma(2\pi T_{on}^3)^{\frac{1}{2}}} \exp - \frac{(\Delta - rT_{on})^2}{2\sigma^2 T_{on}} \tag{3.25}$$

$$p_{off}(T_{off}, \theta) = \frac{\Delta}{\sigma(2\pi T_{off}^3)^{\frac{1}{2}}} \exp - \frac{(\Delta - cT_{off})^2}{2\sigma^2 T_{off}} \tag{3.26}$$

where T_{on} and T_{off} are respectively the "on" and "off" durations, Δ is the temperature dead-band and θ is the scalar or vector parameter to be estimated. Based on the probability density functions, the identification scheme is developed in the following section.

3.2.4 Identification Scheme for the Heater

A maximum likelihood function, which is the joint probability function of "On" and "Off" probability distributions could be constructed as

$$L = ln \prod_{i=1}^{N} p_{on}(T_{on}, \theta) p_{off}(T_{off}, \theta) \tag{3.27}$$

where N denotes the number of samples of "on-off" durations. On substitution with equations (3.25-3.26) and simplifying we obtain

$$\begin{aligned} L_{(r,c,\sigma^2)} &= \sum_{i=1}^{N} \Bigg[[ln \frac{\Delta}{\sigma(2\pi T_{off}(i)^3)^{\frac{1}{2}}} - \frac{(\Delta - cT_{off}(i))^2}{2\sigma^2 T_{off}(i)}] + \\ &\quad [ln \frac{\Delta}{\sigma(2\pi T_{on}(i)^3)^{\frac{1}{2}}} - \frac{(\Delta - rT_{on}(i))^2}{2\sigma^2 T_{on}(i)}] \Bigg] \end{aligned} \tag{3.28}$$

Differentiating the above likelihood function with respect to the parameters, i.e. the heat drift rate 'r' and the cool drift rate 'c', we get the following expressions for the optimal parameter estimators:

$$r_{opt}(N) = \frac{N\Delta}{\sum_{i=1}^{N} T_{on}(i)} \tag{3.29}$$

$$c_{opt}(N) = \frac{N\Delta}{\sum_{i=1}^{N} T_{off}(i)} \tag{3.30}$$

$$\sigma^2_{opt}(N) = \frac{1}{N} \sum_{i=1}^{N} \left[\frac{(\Delta - r(N)T_{on}(i))^2}{2T_{on}(i)} + \frac{(\Delta - c(N)T_{off}(i))^2}{2T_{off}(i)} \right] \tag{3.31}$$

Using the above three equations, the exact computational scheme of the optimal estimators is possible given a number of observations. This exact scheme will ensure stability and convergence of optimal estimators even in presence of high noise level.

Computational Scheme

The simplest computational algorithm is reduced to the following set of estimator equations:

$$r_{opt}(N) = \frac{N\Delta}{S_{on}(N)} \tag{3.32}$$

$$c_{opt}(N) = \frac{N\Delta}{S_{off}(N)} \tag{3.33}$$

$$\begin{aligned} \sigma^2_{opt}(N) &= \frac{1}{2}\Bigg[\frac{Q_{on}(N)}{N} - 2\Delta r_{opt}(N) + \frac{r_{opt}(N)^2 S_{on}(N)}{N} \\ &\quad + \frac{Q_{off}(N)}{N} - 2\Delta c_{opt}(N) + \frac{c_{opt}(N)^2 S_{off}(N)}{N}\Bigg] \end{aligned} \tag{3.34}$$

where

$$S_{on}(N) = S_{on}(N-1) + T_{on}(N)$$

$$S_{off}(N) = S_{off}(N-1) + T_{off}(N)$$

$$Q_{on}(N) = Q_{on}(N-1) + \frac{\Delta^2}{T_{on}(N)}$$

$$Q_{off}(N) = Q_{off}(N-1) + \frac{\Delta^2}{T_{off}(N)}$$

This section dealt with simple computation scheme that is implemented. The next section presents asymptotic analysis for the estimators.

3.2.5 Theoretical Analysis for the Estimators

For an estimator scheme to be implemented as an online scheme, it is necessary to study some of its asymptotic properties in case of limited samples. The root mean

square relative error in the estimation process is of great importance to measure the time to mean square convergence. According to Kamoun [25], the time to mean square convergence is the number of observations required for the root mean square relative estimation error to reach a prescribed level. This is obtained by first deriving the first and second moments of estimation errors which in turn requires computing different moments of several functions of 'T_{on}' and 'T_{off}' random variables. The Laplace transformations of the probability functions of 'T_{on}' and 'T_{off}' are considered because of the complexity of these density functions. These functions are given by Madame and Chong [21] as

$$f_{T_{on}}(s) = exp\left[\frac{r}{\sigma^2} - \frac{\sqrt{r^2 + 2s\sigma^2}}{\sigma^2}\right] \tag{3.39}$$

$$f_{T_{off}}(s) = exp\left[\frac{c}{\sigma^2} - \frac{\sqrt{c^2 + 2s\sigma^2}}{\sigma^2}\right] \tag{3.40}$$

If 'X' and 'Y' are defined by

$$X = \sum_{i=1}^{N} T_{on}(i) \tag{3.41}$$

$$Y = \sum_{i'=1}^{N} T_{off}(i') \tag{3.42}$$

then the different moments of 'T_{on}' that are to be computed are

$$E[T_{on}] = -\frac{\partial f_{T_{on}}(s)}{\partial s}\bigg|_{s=0} = \frac{\Delta}{r} \tag{3.43}$$

$$E[T_{on}^2] = \frac{\partial^2 f_{T_{on}}(s)}{\partial s^2}\bigg|_{s=0} = \frac{\Delta^2}{r^2} + \frac{\Delta\sigma^2}{r^3} \tag{3.44}$$

$$E\left[\frac{1}{T_{on}}\right] = \int_{s}^{+\infty} f_{T_{on}}(u)du|_{s=0} = \frac{r\Delta + \sigma^2}{\Delta^2} \tag{3.45}$$

$$E\left[\frac{1}{T_{on}^2}\right] = \int_s^{+\infty}\int_v^{+\infty} f_{T_{on}}(u)dudv|_{s=0} = \frac{r^2\Delta^2 + 3r\Delta\sigma^2 + 3\sigma^4}{\Delta^4} \tag{3.46}$$

$$E[X] = -\frac{\partial f_X(s)}{\partial s}\bigg|_{s=0} = \frac{N\Delta}{r} \tag{3.47}$$

$$E[X^2] = \frac{\partial^2 f_X(s)}{\partial s^2}\bigg|_{s=0} = \frac{N\Delta(Nr\Delta + \sigma^2)}{r^3} \tag{3.48}$$

$$E\left[\frac{1}{X}\right] = \int_s^{+\infty} f_X(u)du|_{s=0} = \frac{Nr\Delta + \sigma^2}{N^2\Delta^2} \tag{3.49}$$

$$E\left[\frac{1}{X^2}\right] = \int_s^{+\infty}\int_v^{+\infty} f_X(u)dudv|_{s=0} = \frac{N^2r^2\Delta^2 + 3Nr\Delta\sigma^2 + 3\sigma^4}{N^4\Delta^4} \tag{3.50}$$

Similarly, for 'T_{off}' we have

$$E[T_{off}] = -\frac{\partial f_{T_{off}}(s)}{\partial s}\bigg|_{s=0} = \frac{\Delta}{c} \tag{3.51}$$

$$E[T_{off}^2] = \frac{\partial^2 f_{T_{off}}(s)}{\partial s^2}\bigg|_{s=0} = \frac{\Delta^2}{c^2} + \frac{\Delta\sigma^2}{c^3} \tag{3.52}$$

$$E\left[\frac{1}{T_{off}}\right] = \int_s^{+\infty} f_{T_{off}}(u)du|_{s=0} = \frac{c\Delta + \sigma^2}{\Delta^2} \tag{3.53}$$

$$E\left[\frac{1}{T_{off}^2}\right] = \int_s^{+\infty}\int_v^{+\infty} f_{T_{off}}(u)dudv|_{s=0} = \frac{c^2\Delta^2 + 3c\Delta\sigma^2 + 3\sigma^4}{\Delta^4} \tag{3.54}$$

$$E[Y] = -\frac{\partial f_Y(s)}{\partial s}\bigg|_{s=0} = \frac{N\Delta}{c} \tag{3.55}$$

$$E[Y^2] = \frac{\partial^2 f_Y(s)}{\partial s^2}\bigg|_{s=0} = \frac{N\Delta(Nc\Delta + \sigma^2)}{c^3} \tag{3.56}$$

$$E\left[\frac{1}{Y}\right] = \int_s^{+\infty} f_Y(u)du|_{s=0} = \frac{Nc\Delta + \sigma^2}{N^2\Delta^2} \tag{3.57}$$

$$E\left[\frac{1}{Y^2}\right] = \int_s^{+\infty}\int_v^{+\infty} f_Y(u)dudv|_{s=0} = \frac{N^2c^2\Delta^2 + 3Nc\Delta\sigma^2 + 3\sigma^4}{N^4\Delta^4} \tag{3.58}$$

These are the higher moments of 'T_{on}' and 'T_{off}'. They are needed for the computation at the first and second moments of the estimation errors.

Mean and Variance of 'T_{on}' and 'T_{off}'

The mean and variance which are useful in validating the simulation algorithm are given as follows:

$$Mean(T_{on}) = E[T_{on}] = \frac{\Delta}{r} \tag{3.59}$$

$$Mean(T_{off}) = E[T_{off}] = \frac{\Delta}{c} \tag{3.60}$$

$$\begin{aligned} Variance(T_{on}) &= E[T_{on}^2] - [E(T_{on})]^2 \\ &= \frac{\Delta^2}{r^2} + \frac{\Delta\sigma^2}{r^3} - \left(\frac{\Delta}{r}\right)^2 \\ &= \frac{\Delta\sigma^2}{r^3} \end{aligned} \tag{3.61}$$

$$Variance(T_{off}) = \frac{\Delta\sigma^2}{c^3} \tag{3.62}$$

Bias of the Estimators

The expected values of the optimal estimators are obtained to have first hand information of their potential bias of estimators. According to Kamoun [25], expressions for the expected value are given as follows:

$$\begin{aligned} E[(r_{opt}(N)] &= E\left[\frac{N\Delta}{\sum_{i=1}^{N} T_{on}(i)}\right] \\ &= N\Delta E\left[\frac{1}{\sum_{i=1}^{N} T_{on}(i)}\right] \\ &= N\Delta\left[\frac{Nr\Delta + \sigma^2}{N^2\Delta^2}\right] \\ &= r + \frac{\sigma^2}{N\Delta} \end{aligned} \tag{3.63}$$

Similarly

$$E[(c_{opt}(N)] = c + \frac{\sigma^2}{N\Delta} \tag{3.64}$$

$$E[(\sigma^2_{opt}(N)] = \sigma^2 - \frac{\sigma^2}{N} \tag{3.65}$$

From the above expected values of the estimators it could be said that as the number of observations are increased, i.e. as $N \to \infty$, the bias is eliminated but for finite samples it would be significant.

The Mean Square Convergence Parameters

For N samples, mean square estimation errors are given by various entries in Matrix M(N) where:

$$M(N) = E[(\widehat{\theta}_{opt}(N) - \theta)(\widehat{\theta}_{opt}(N) - \theta)^T] \tag{3.66}$$

with the error terms given by

$$m_{11}(N) = E[(r_{opt}(N) - r)^2] \tag{3.67}$$

$$m_{22}(N) = E[(c_{opt}(N) - c)^2] \tag{3.68}$$

$$m_{33}(N) = E[(\sigma^2_{opt}(N) - \sigma^2)^2] \tag{3.69}$$

The above mean square estimation errors can be written in terms of r, c, σ^2 as

$$m_{11}(N) = \frac{\sigma^2 r}{N\Delta} + \frac{3\sigma^4}{N^2\Delta^2} \tag{3.70}$$

$$m_{22}(N) = \frac{\sigma^2 c}{N\Delta} + \frac{3\sigma^4}{N^2\Delta^2} \tag{3.71}$$

and

$$
\begin{aligned}
m_{33}(N) &= \frac{2}{4N}\left(r^2\Delta^2 + c^2\Delta^2 + \sigma^2 r\Delta + \sigma^2 c\Delta + 2\sigma^2\right) \\
&\quad -\frac{3}{2N^2}\left(\sigma^2 r\Delta + \sigma^2 c\Delta\right) \\
&\quad -\frac{1}{N-1}\left(r^2\Delta^2 + c^2\Delta^2 + \sigma^2 r\Delta + \sigma^2 c\Delta\right) \\
&\quad -\frac{1}{(N-1)^2}\left(\sigma^2 r\Delta + \sigma^2 c\Delta + 2\sigma^4\right) \\
&\quad +\frac{N^3}{4(N-1)^4}\left(r^2\Delta^2 + c^2\Delta^2 + \sigma^2 r\Delta + \sigma^2 c\Delta\right) \\
&\quad +\frac{5N^3}{2(N-1)^5}\left(r\sigma^2 + c\sigma^2 + 2\sigma^4\right) \\
&\quad +\frac{45N^3}{4(N-1)^6}\left(\frac{\sigma^6}{r\Delta} + \frac{\sigma^6}{c\Delta} + 2\sigma^4\right) \\
&\quad +\frac{105N^3}{4(N-1)^7}\left(\frac{\Delta^4\sigma^8}{r^2} + \frac{\Delta^4\sigma^8}{c^2} + \frac{\Delta^5\sigma^6}{r} + \frac{\Delta^5\sigma^6}{c}\right) \\
&\quad +\frac{105N^3}{4(N-1)^8}\left(\frac{\sigma^6}{\Delta^3 r^3} + \frac{\sigma^6}{\Delta^3 c^3}\frac{\sigma^4}{\Delta^2 r^2} + \frac{\sigma^4}{\Delta^2 c^2}\right) \\
&\quad +\sigma^4\left(\frac{1}{4N} + \frac{3}{2N^2}\right)
\end{aligned} \tag{3.72}
$$

The root mean square relative estimation error on the estimators are given by

$$
\rho_i(N) = \frac{\sqrt{m_{ii}(N)}}{\theta_i}, i = 1, 2, 3 \tag{3.73}
$$

where $\theta = [r, c, \sigma^2]$ and $\rho_i(N)$ is the relative estimation error associated with the parameter θ_i. Based on the elementary model developed and proposed identification scheme, the simulation and the sensitivity analysis is carried out. These results are presented in the following section.

3.3 Simulation and Identification

3.3.1 Simulation

Based on equation (3.2-3.4), simulation was conducted with the assumption of Weiner Noise. The exact algorithm of generating the Weiner noise was obtained as explained below.

Weiner Noise

Weiner noise (or Brownian Motion) is a kind of Random walk, which is a stochastic process consisting of a series of independent and identically distributed random variables. A Brownian motion is a random walk, but not all random walks are Brownian motion. Therefore Weiner noise, or Brownian motion starts from zero, takes on values of +1 or -1 in the next period with equal probabilities of 1/2. That is W_0 equals Zero and W_1 equals +1 or -1. Thus the expected value of Weiner noise is 'Zero' with variance equal to 'One'. Thus the model presented could be extended to further time periods. However this would make the variance increase as the time period increases. If constant variance is be achieved, we fix the time and divide it into a fixed number of periods so that the step taken is $\Delta t = 1/n$ where 'n' is the number of periods. Hence the model would become like $\Delta W = \pm\Delta t$. Thus, if we want to capture reality in the model we would like for same time, the number of periods i.e. 'n' to be large. That would leave us selecting 'n' large which makes it

motionless, i.e. the variance would approach 'Zero'. So a different model is tried, which is given as follows

$$\Delta W = \pm\sqrt{\Delta t} \tag{3.74}$$

where $\Delta t = t/n$. This would produce Weiner noise with mean 'Zero' and Variance equals 't'. If 't', the time period under consideration is taken as 'One', the variance obtained thereof would equal 'One'. Thus we can increase and fix a number of periods into which a single time could be divided and obtain a very near to realistic Weiner noise process.

Simulation Results

With the Weiner noise defined, the simulation for the heater was carried out with the following parameters:

$a = 0.02min^{-1}, R = 0.4^oCmin^{-1}, x_+ = 21.1^oC, x_- = 20^oC, x_a = 12^oC$, with noise variance as $\sigma^2 = 0.04^oC^2min^{-1}$. A typical simulation is shown in the Figure 3.3 where the system has already reached steady state.

Different simulations were carried out to verify the theoretical results obtain by Kamoun [25]. The simulation produced 'on' and 'off' time durations and the statistics like mean and variance were verified against the theoretical derived values. For this, two kind of simulations were done: the vertical simulation and the horizontal simulation. The vertical simulation means that the algorithm was executed for a number of parallel runs with different noise vectors. Horizontal simulation means

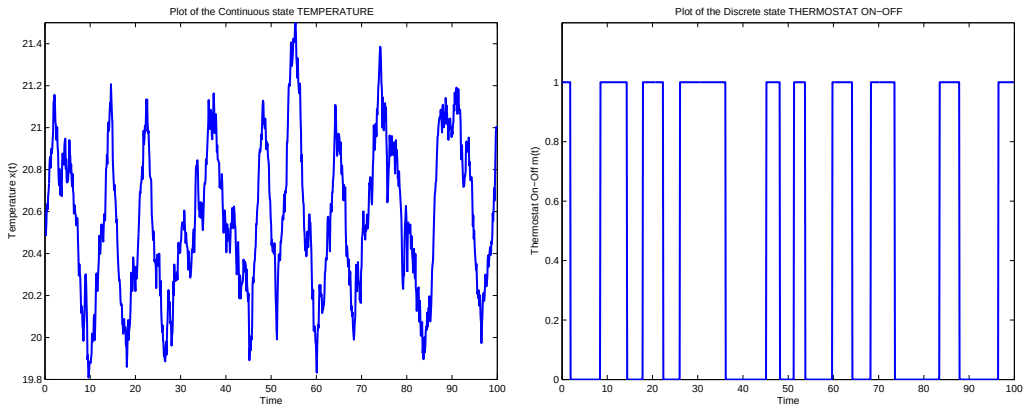

Figure 3.3: Simulation for a System already in Steady State.

that the algorithm was executed once with a long noise vector.

Tables (3.1-3.2) refer to the results obtained through horizontal simulation using the same parameters defined previously. The theoretical mean was calculated as given by equation (3.59) and compared with the mean calculated through simulation. Then the relative error between the theoretically calculated mean and the mean obtained through simulation was evaluated. Similarly the theoretical variance was calculated by equation (3.61) for the parameters defined and compared with variance obtained through simulation and relative error computed.

In this typical horizontal simulation, it could be observed that the relative error generated for mean and variance of samples of 'T_{on}' is less than 3% and 7% respectively and the mean and variance for samples of 'T_{off}' is less than 7% and 8% respectively. The mean and variance of 'T_{on}' and 'T_{off}' converge to their theoretical values as the number of samples are increased.

Table 3.1: Statistics for Horizontal Simulation for 'T_{on}' (Heater).

Sample	Δ/r	Mean	Rel. Err.	$\Delta * \sigma^2/r^3$	Variance	Rel. Err.-Var
10	4.8035	4.12	0.1423	3.6639	9.904	1.7031
20	4.8035	4.405	0.083	3.6639	5.57	0.5202
30	4.8035	4.3467	0.0951	3.6639	3.9012	0.0648
40	4.8035	4.375	0.0892	3.6639	3.2399	0.1157
50	4.8035	4.48	0.0673	3.6639	3.049	0.1678
60	4.8035	4.4417	0.0753	3.6639	2.7913	0.2382
70	4.8035	4.6086	0.0406	3.6639	3.5269	0.0374
80	4.8035	4.6475	0.0325	3.6639	3.3972	0.0728
90	4.8035	4.7944	0.0019	3.6639	3.91	0.0672
100	4.8035	4.867	0.0132	3.6639	3.9287	0.0723

Table 3.2: Statistics for Horizontal Simulation for 'T_{off}' (Heater).

Sample	Δ/c	Mean	Rel. Err.	$\Delta * \sigma^2/c^3$	Variance	Rel. Err.-Var
10	6.4327	8.75	0.3602	8.7996	43.0006	3.8866
20	6.4327	7.62	0.1846	8.7996	24.8901	1.8285
30	6.4327	7.06	0.0975	8.7996	21.517	1.4452
40	6.4327	7.2175	0.122	8.7996	21.9502	1.4944
50	6.4327	7.19	0.1177	8.7996	21.3266	1.4236
60	6.4327	7.3117	0.1366	8.7996	20.0546	1.279
70	6.4327	7.1429	0.1104	8.7996	18.0228	1.0481
80	6.4327	7.065	0.0983	8.7996	16.9094	0.9216
90	6.4327	6.8467	0.0643	8.7996	16.0414	0.823
100	6.4327	6.926	0.0767	8.7996	15.411	0.7513

The next set of tables (3.3-3.6) refer to the results obtained through vertical simulation. Tables (3.3,3.4) represent the individual results obtained in each vertical run and Tables (3.5,3.6) represents the consolidated or the cumulative results. The simulation parameters were same as for the horizontal simulation, but the number of samples were fixed at ten.

At one glance, the results seen show that individual runs for sample length of ten produces an average mean and variance relative error for 'T_{on}' as 12% and 40% re-

Table 3.3: Statistics for Vertical Simulation for 'T_{on}' (Heater).

Sample	Δ/r	Mean	Rel. Err.	$\Delta * \sigma^2/r^3$	Variance	Rel. Err.-Var
10	4.8035	4.5	0.0632	3.6639	2.1378	0.4165
10	4.8035	4.87	0.0138	3.6639	6.0157	0.6419
10	4.8035	5.73	0.1929	3.6639	11.8134	2.2243
10	4.8035	3.12	0.3505	3.6639	1.0707	0.7078
10	4.8035	5.37	0.1179	3.6639	3.1401	0.143
10	4.8035	5.39	0.1221	3.6639	2.6188	0.2853
10	4.8035	5.18	0.0784	3.6639	4.5884	0.2523
10	4.8035	5.1	0.0617	3.6639	1.9067	0.4796
10	4.8035	4.23	0.1194	3.6639	1.8134	0.5051
10	4.8035	5.55	0.1554	3.6639	4.3806	0.1956

Table 3.4: Statistics for Vertical Simulation for 'T_{off}' (Heater).

Sample	Δ/c	Mean	Rel. Err.	$\Delta * \sigma^2/c^3$	Variance	Rel. Err.-Var
10	6.4327	5.78	0.1015	8.7996	4.5662	0.4811
10	6.4327	8.11	0.2607	8.7996	10.9832	0.2481
10	6.4327	5.46	0.1512	8.7996	1.676	0.8095
10	6.4327	6.8	0.0571	8.7996	11.1978	0.2725
10	6.4327	7.8	0.2125	8.7996	8.2889	0.058
10	6.4327	7.26	0.1286	8.7996	9.4316	0.0718
10	6.4327	5.99	0.0688	8.7996	12.4854	0.4189
10	6.4327	6.45	0.0027	8.7996	7.2028	0.1815
10	6.4327	7	0.0882	8.7996	5.06	0.425
10	6.4327	7.28	0.1317	8.7996	6.2551	0.2892
10	6.4327	7.09	0.1022	8.7996	7.3877	0.1605

spectively and for 'T_{off}' as 12% and 30% respectively.

But the cumulative results of the Vertical simulation are important. As observed from tables (3.5,3.6) the relative error in the mean and variance of both 'T_{on}' and 'T_{off}' converges to the theoretical mean and variance as the number of vertical runs(the number of samples) is increased. For 'T_{on}' the relative error in the mean and Variance goes to less than 2% and 7%. Similarly for 'T_{off}' the relative error in

Table 3.5: Cumulative Statistics for Vertical Simulation for 'T_{on}' (Heater).

Sample	Δ/r	Mean	Rel. Err.	$\Delta * \sigma^2/r^3$	Variance	Rel. Err.-Var
10	4.8035	4.5	0.0632	3.6639	2.1378	0.4165
20	4.8035	4.685	0.0247	3.6639	4.0767	0.1127
30	4.8035	5.0333	0.0478	3.6639	6.6556	0.8165
40	4.8035	4.555	0.0517	3.6639	5.2594	0.4355
50	4.8035	4.718	0.0178	3.6639	4.8355	0.3198
60	4.8035	4.83	0.0055	3.6639	4.4661	0.2189
70	4.8035	4.88	0.0159	3.6639	4.4836	0.2237
80	4.8035	4.9075	0.0217	3.6639	4.1614	0.1358
90	4.8035	4.8322	0.006	3.6639	3.9006	0.0646
100	4.8035	4.904	0.0209	3.6639	3.9486	0.0777

Table 3.6: Cumulative Statistics for Vertical Simulation for 'T_{off}' (Heater).

Sample	Δ/c	Mean	Rel. Err.	$\Delta * \sigma^2/c^3$	Variance	Rel. Err.-Var
10	6.4327	5.78	0.1015	8.7996	4.5662	0.4811
20	6.4327	6.945	0.0796	8.7996	7.7747	0.1165
30	6.4327	6.45	0.0027	8.7996	5.7418	0.3475
40	6.4327	6.5375	0.0163	8.7996	7.1058	0.1925
50	6.4327	6.79	0.0555	8.7996	7.3424	0.1656
60	6.4327	6.8683	0.0677	8.7996	7.6906	0.126
70	6.4327	6.7429	0.0482	8.7996	8.3756	0.0482
80	6.4327	6.7062	0.0425	8.7996	8.229	0.0648
90	6.4327	6.7389	0.0476	8.7996	7.8769	0.1049
100	6.4327	6.793	0.056	8.7996	7.7147	0.1233

the mean and Variance is less than 6% and 10%.

These results were obtained to verify the simulation algorithm and to check the convergence with respect to the theoretical results. The convergence is acceptable for the simulation algorithm to be used further for obtaining the optimal estimators.

Simulation of Optimal Estimators

Using the equations (3.32-3.34) simulation was carried out with the parameters defined previously. The computed values of 'r' and 'c' are 0.229^oCmin^{-1} and 0.171^oCmin^{-1} respectively. In this simulation the temperature at the start of the simulation is taken as the mean of x_- and x_+, which means that the system at steady state. The trajectories of the optimal estimators are shown in the figure 3.4.

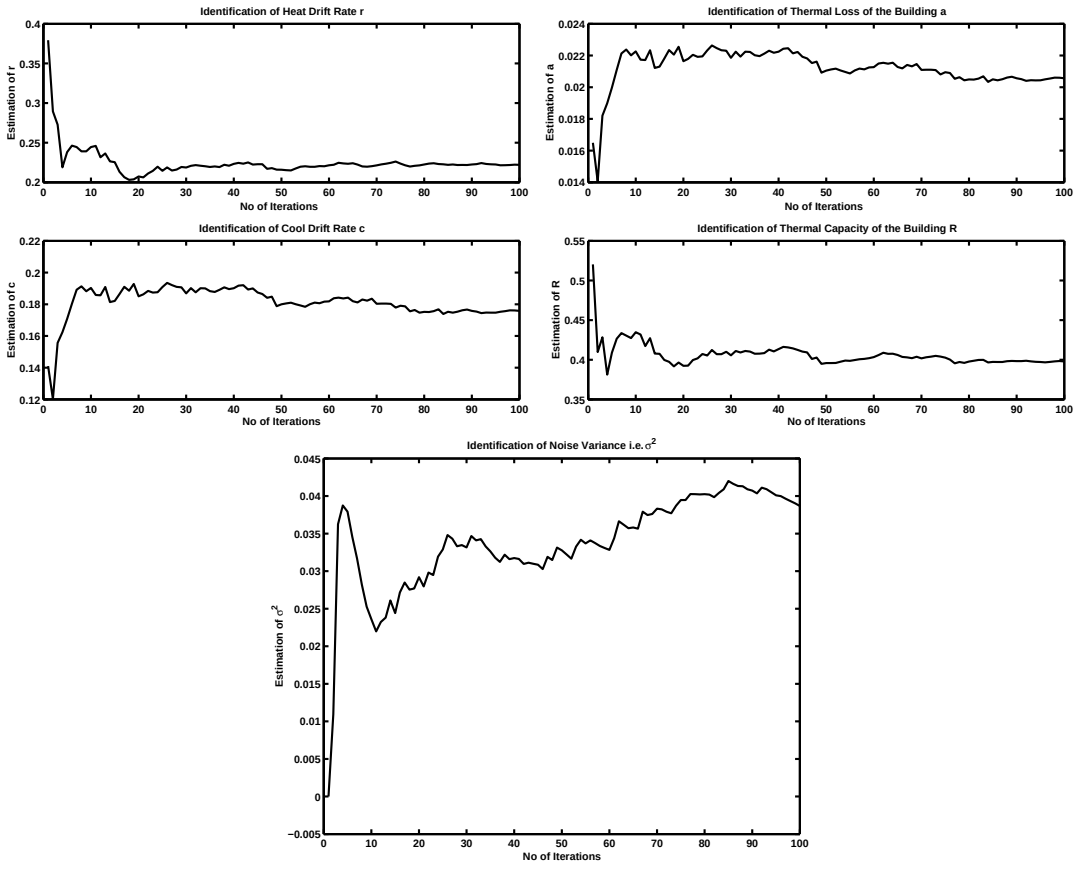

Figure 3.4: Optimal Estimators Trajectories-Steady case (Heater).

The convergence of the optimal estimators is fast and settles down to its respective values. Another simulation was carried out with the simulation starting at temperature other than the interval of switching, for which the simulation was started at temperature equal to the ambient temperature, i.e. $x_1 = x_a = 12^oC$. The results showed that the optimal estimators take longer time to converge to there respective steady-state values. This could be observed in Figure 3.5.

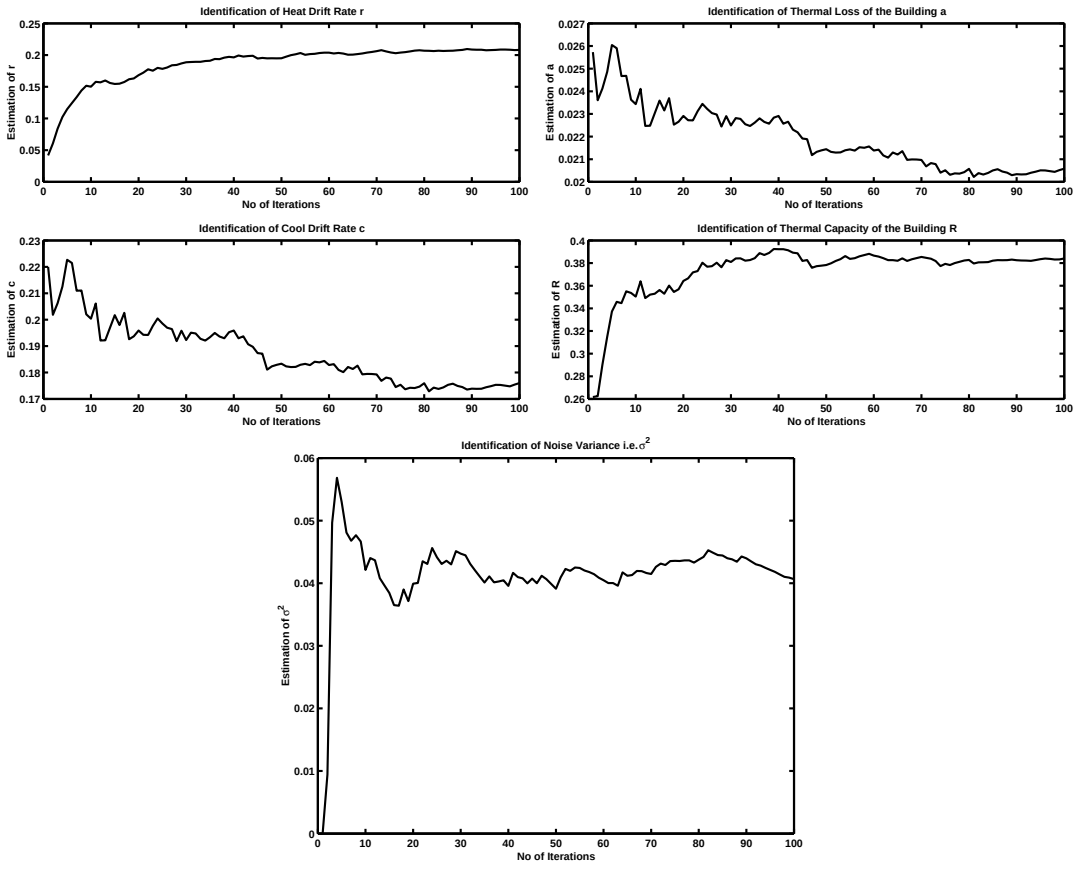

Figure 3.5: Optimal Estimators Trajectories-Unsteady case (Heater).

3.3.2 Sensitivity Analysis

Sensitivity analysis was conducted, to verify the theoretical results for root mean square convergence(MSE) as described by the equations(3.67-3.72) with the one obtained through simulation. Root mean square convergence with respect to simulation is obtained by carrying out the simulation of system for obtaining "On" and "Off" durations. Then these duration are used to calculate the estimators using limited samples and the root mean square relative error with respect to actual parameters calculated. The RMS values thus obtained are compared with the results calculated through theoretical expressions.

Three kind of sensitivity analysis were performed. The first kind of analysis in which the behavior of the optimal estimators as the number of samples are changed was observed. In the second kind of analysis, convergence characteristics with respect to the changes in the parameters of the system was studied and lastly the convergence behavior with respect to noise variance was carried out. The results are shown as follows.

As a Function of the Number of Samples

Using the parameters defined as follows:

$a = 0.02min^{-1}, R = 0.4^oCmin^{-1}, x_+ = 21.1^oC, x_- = 20^oC, x_a = 12^oC$, with noise variance as $\sigma^2 = 0.04^oC^2min^{-1}$

we study the effect of the number of samples used for identification on the quality

of the estimators. The set of plots are shown in figure 3.6. The plot shows root mean square relative error as functions of number of samples. For verification, about twenty parallel simulations where carried out and the results obtained from each simulation about the estimates r, c, σ^2 were taken and the root mean square relative error was compared with the one obtained theoretically.

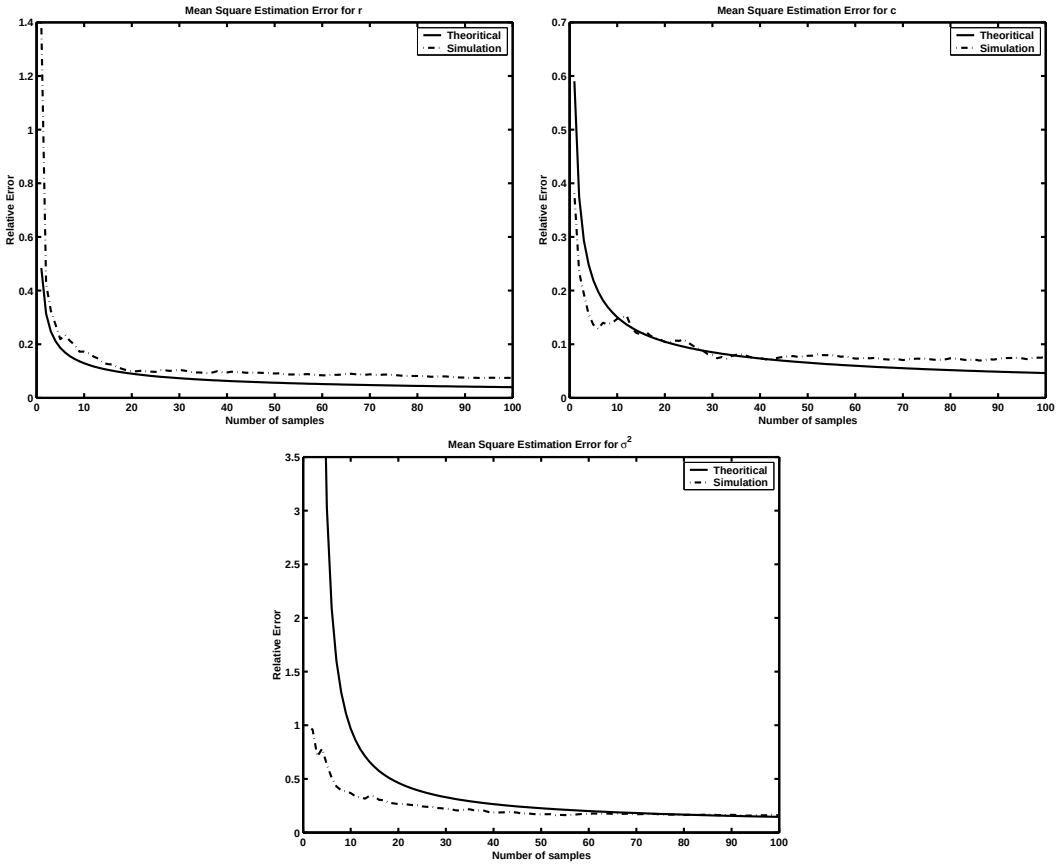

Figure 3.6: MSE as a Function of Number of Samples for Heater.

As seen in the figure the simulation gave good results when compared to theoretical for heat drift rate 'r' and cool drift rate 'c'. For σ the theoretical results show

high values when compared to results obtained through simulation. This could be due to limited number of horizontal simulation(number of heaters) carried out. The theoretical results are for an aggregated load were infinite number of heater system are assumed and hence if we increase the number of heaters we approach the theoretical results. Also, it is obvious that if more number of samples are collected it would give us a better estimation of parameters.

As a function of the Thermal Heat Loss and Heat Rate

In the next set of simulation, the theoretical root mean square relative convergence error and the one obtained through simulation was calculated as a function of thermal heat loss 'a' and Heating rate 'R'. In the simulation, the values of the parameter 'a' was varied from $0.005min^{-1}$ to $0.045min^{-1}$ and for two different values of the parameter 'R' i.e. 0.4^oCmin^{-1} and 0.6^oCmin^{-1}. Also the simulation was carried out for twenty different parallel runs under steady-state and the results are averaged and compared with the theoretical results. The results are shown in the Figure 3.7. As seen from the figure, the simulation follows in the trend of the theoretical results. The plots also suggest that, the estimate of 'r' becomes difficult for high values of 'R' and 'a' which could be attributed to small values of 'on' times. Similarly the estimation of 'c' becomes better because of long and stable values of 'off' times as the parameter 'a' is increased. As for the estimation of σ^2, small values of 'a' makes the 'off' time very small and comparable to noise and high estimation errors and

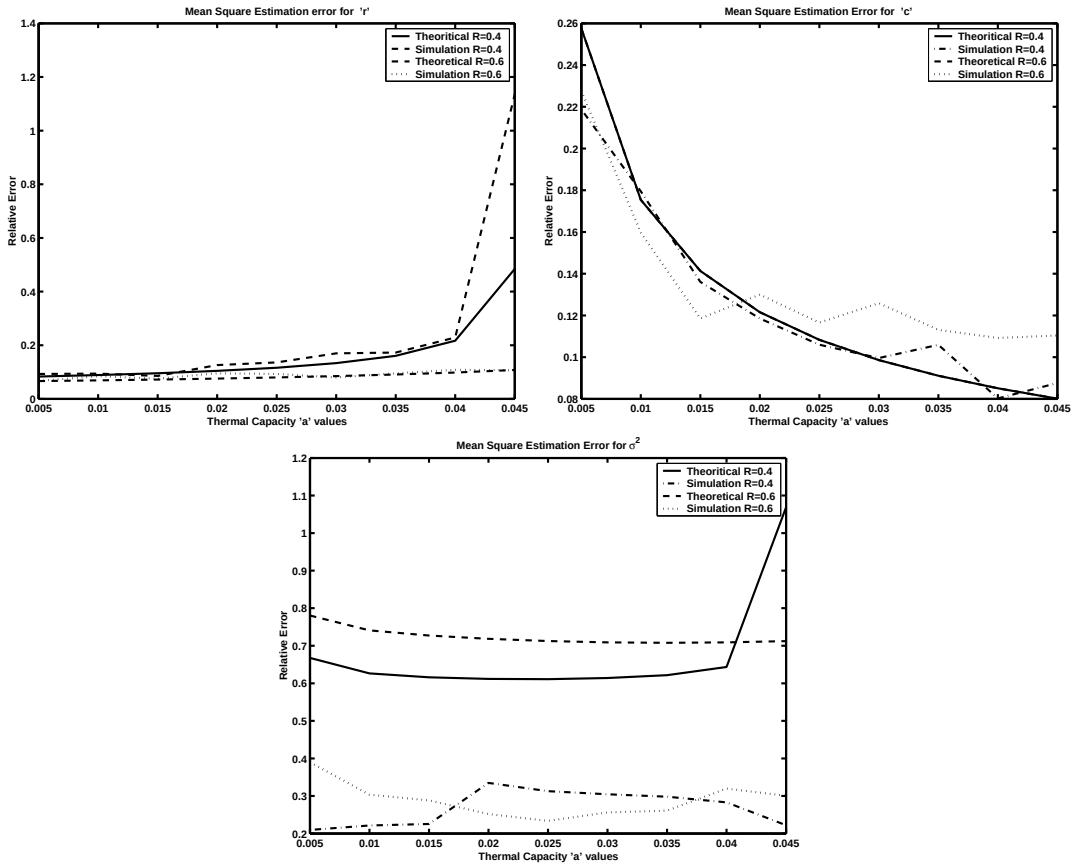

Figure 3.7: MSE as a Function of Thermal Heat Loss 'a' and Heat Rate 'R' for Heater.

large values of 'a' makes 'r' small and hence poor estimates. The estimation errors produced by simulation as compared to theoretical estimation error is less. This might be improved by increasing the number of parallel simulation.

As a Function of Noise Parameter 'σ'

In this simulation, the theoretical root mean square estimation errors and the one obtained through simulation were compared as a function of different values of σ for different samples of 'on' and 'off'. That is in this particular simulation the noise parameter σ was varied from $0.05^oC^2min^{-1}$ to $0.85^oC^2min^{-1}$ for two different sample length of 5 and 15. Also for the simulation, 10 different parallel runs under steady-state were carried out and the root mean square was computed and compared with the theoretical results. The plots of this study are given in Figure 3.8. From the figures, it could be observed that as the noise parameter σ, is increased the relative error in the estimation of 'r' and 'c' for fixed sample size also increases. This is because the noise pollutes the estimation and the estimation error increases. As for the estimation of σ^2 the relative error is very high for small values of σ because the systems dynamics are not excited enough for the estimation algorithm to see the whole dynamics. This results in very high estimation errors. Whereas, high noise in the system makes necessary that the estimator requires more number of samples to give a good estimate.

As the results for the heater are validated, the elementary model and aggregate

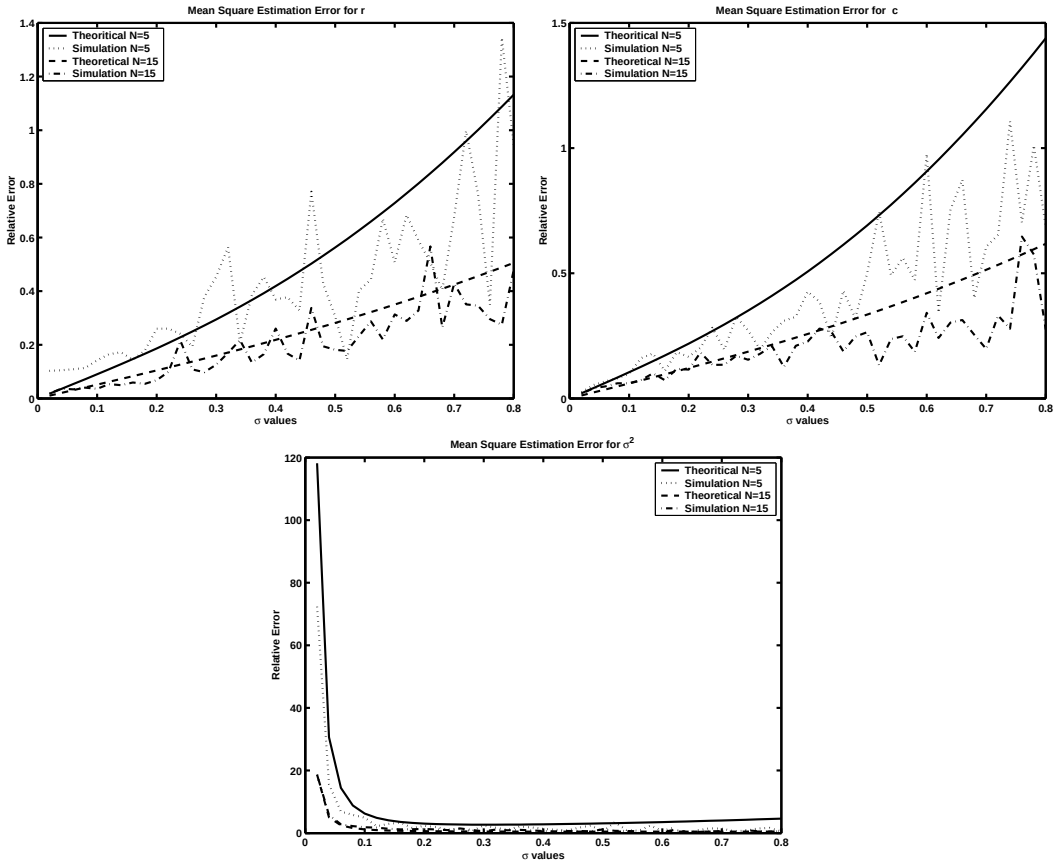

Figure 3.8: MSE as a Function of σ and Number of Samples for Heater.

Air-Conditioner model are developed. This is presented in the following section.

3.4 Air-Conditioner Case

By modifying the model of the Heater, the following model for the Air-Conditioner is obtained.

3.4.1 The Hybrid Stochastic Model for Air-Conditioner

Equation (3.1) is modified and the hybrid stochastic differential equation model obtained represents the Air-Conditioner. The continuous stochastic differential equation for the A/C is as follows:

$$Cdx(t) = \acute{a}(x_a(t) - x(t))dt - \acute{R}m(t)b(t)dt + d\acute{v}(t) \tag{3.75}$$

which could be modified by dividing through out by C as

$$dx(t) = a(x_a(t) - x(t))dt - Rm(t)b(t)dt + dv(t) \tag{3.76}$$

with the discrete state equation modified as

$$m(t) = m(t) + \Pi(x(t) : x^+, x^-) \tag{3.77}$$

$$\Pi(x(t) : x^+, x^-) = \begin{cases} 0 \ \text{ for } x^- \leq x \leq x^+ \\ m(t-1) \ \text{ for } x \leq x^- \\ 1 - m(t-1) \ \text{ for } x \geq x^+ \end{cases} \tag{3.78}$$

where $\acute{R}$ would represent the rate of cooling given by the Air-Conditioner. This is the primitive model as illustrated in the Figure 3.9, to which aggregation methodology is applied wherein an aggregate model representing a certain class of system is constructed.

3.4.2 The Aggregate Model for A/C

Following the same aggregation methodology as described in section 3.2.2 the aggregate model of the A/C is obtained. The dynamical system for the A/C reverses

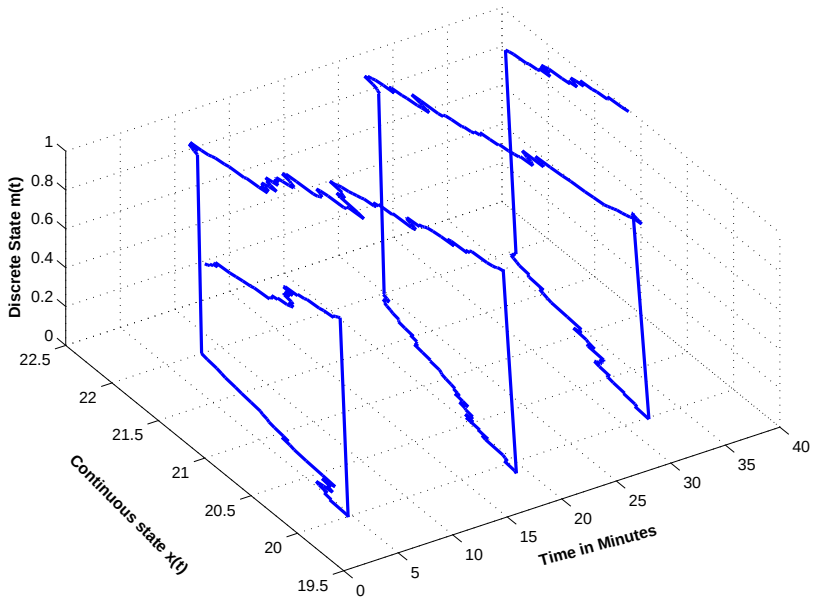

Figure 3.9: Continuous State and Discrete State as Function of Time (A/C).

as shown in the Figure (3.10). The Coupled Fokker-Planck equations (CFPE) as follows:

$$T_{\lambda,t}{}^{1}[f_1(\lambda,t)] = 0 \tag{3.79}$$

$$T_{\lambda,t}{}^{0}[f_0(\lambda,t)] = 0 \tag{3.80}$$

where

$$T^{k}_{\lambda,t}[f] = \frac{\partial}{\partial t}f - \frac{\partial}{\partial \lambda}[(a(\lambda - X_a(t)) - kb(t)R)f] - \frac{\sigma^2}{2}\frac{\partial}{\partial \lambda^2} \tag{3.81}$$

This is illustrated in Figure 3.10 with the boundary conditions for all 't' defined as follows

The absorbing boundary

$$f_{1b}(x_-,t) = f_{0b}(x_+,t) = 0 \tag{3.82}$$

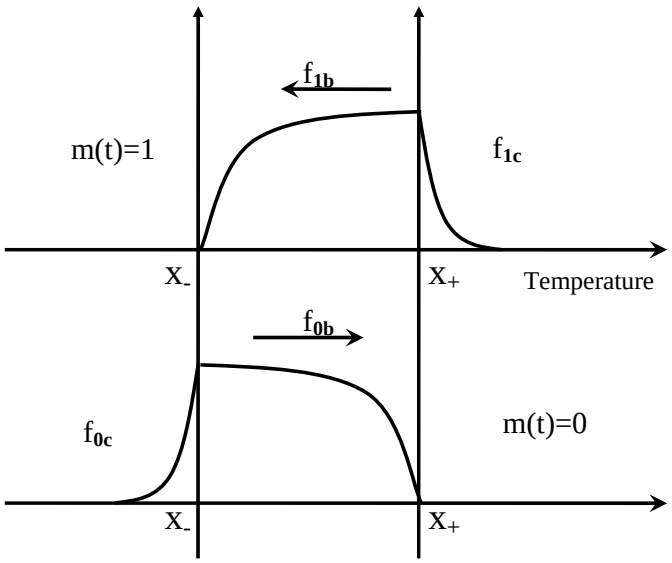

Figure 3.10: Illustration of Dynamical System (A/C).

The conditions at infinity

$$f_{1c}(-\infty, t) = f_{0a}(\infty, t) = 0 \tag{3.83}$$

The continuity conditions

$$f_{1b}(x_+, t) = f_{1c}(x_+, t) = 0 \tag{3.84}$$

$$f_{0a}(x_-, t) = f_{0b}(x_-, t) = 0 \tag{3.85}$$

Probability Conservation

$$-\frac{\partial}{\partial\lambda} f_{0a}(x_-, t) + \frac{\sigma^2}{2}\frac{\partial}{\partial\lambda} f_{1b}(x_-, t) + \frac{\sigma^2}{2}\frac{\partial}{\partial\lambda} f_{0b}(x_-, t) = 0 \tag{3.86}$$

$$\frac{\partial}{\partial\lambda} f_{1c}(x_+, t) - \frac{\sigma^2}{2}\frac{\partial}{\partial\lambda} f_{0b}(x_+, t) - \frac{\sigma^2}{2}\frac{\partial}{\partial\lambda} f_{1b}(x_+, t) = 0 \tag{3.87}$$

together with the equation

$$\bar{m}(t) = \int_0^t \frac{\sigma^2}{2}[\frac{\partial}{\partial\lambda} f_1(x_-, \tau) + \frac{\partial}{\partial\lambda} f_0(x_+, \tau)]d\tau + \bar{m}(0) \tag{3.88}$$

is the aggregate load model for the Air-Conditioners. The identification scheme is now developed for A/C.

3.4.3 Probability Density Functions

The 'On' and 'Off' time durations of the Air-Conditioners are opposite as defined for the heater i.e. the 'On' duration corresponds to first passage times from x_+ to x_- and x_- to x_+ for 'Off' duration. The time varying drift rates are r(t) and c(t) which are defined as heating and cooling rates are given as

$$r(t) = a(x_a - x(t)) \tag{3.89}$$

$$c(t) = a(x_a - x(t)) - R \tag{3.90}$$

Applying similar argument as in the case of heater where the probability density function is confined within a narrow range of temperature (typically $1.5 - 2^oC$), the above drift rates are practically constant(for constant weather conditions and for duration of control period). Referring to these as constants r and c, with x(t) replaced by the mean $\bar{x} = \frac{x_+ + x_-}{2}$, the probability density function for such passage times for this particular case are given by

$$p_{on}(T_{on}, \theta) = \frac{\Delta}{\sigma(2\pi T_{on}^3)^{\frac{1}{2}}} \exp - \frac{(\Delta - cT_{on})^2}{2\sigma^2 T_{on}} \tag{3.91}$$

$$p_{off}(T_{off}, \theta) = \frac{\Delta}{\sigma(2\pi T_{off}^3)^{\frac{1}{2}}} \exp - \frac{(\Delta - rT_{off})^2}{2\sigma^2 T_{off}} \tag{3.92}$$

where T_{on} and T_{off} are respectively the "on" and "off" durations, Δ is the temperature dead-band and θ is the scalar or vector parameter to be estimated. The probability density functions are same as that for the heater except for the interchange of 'r' and 'c'.

3.4.4 Identification Scheme for the A/C

Building on the same argument as described in section 3.2.4 same set of equations i.e. equations (3.32-3.34) determine the optimal estimators for the A/C model except for a small modification. These modifications are seen in equations for 'r_{opt}' and 'c_{opt}' which are as follows

$$r_{opt}(N) = \frac{N\Delta}{S_{off}(N)} \tag{3.93}$$

$$c_{opt}(N) = \frac{N\Delta}{S_{on}(N)} \tag{3.94}$$

$$\begin{aligned} \sigma^2_{opt}(N) &= \frac{1}{2}\Bigg[\frac{Q_{on}(N)}{N} - 2\Delta c_{opt}(N) + \frac{c_{opt}(N)^2 S_{on}(N)}{N} \\ &\quad + \frac{Q_{off}(N)}{N} - 2\Delta r_{opt}(N) + \frac{r_{opt}(N)^2 S_{off}(N)}{N}\Bigg] \end{aligned} \tag{3.95}$$

where

$$S_{on}(N) = S_{on}(N-1) + T_{on}(N)$$

$$S_{off}(N) = S_{off}(N-1) + T_{off}(N)$$

$$Q_{on}(N) = Q_{on}(N-1) + \frac{\Delta^2}{T_{on}(N)}$$

$$Q_{off}(N) = Q_{off}(N-1) + \frac{\Delta^2}{T_{off}(N)}$$

3.4.5 Theoretical Analysis for the Estimators

The asymptotic properties of estimators in case of limited samples for the Air-Conditioner (to be used in an online scheme) are discussed below.

The Laplace transformations of the probability functions of 'T_{on}' and 'T_{off}' are as follows

$$f_{T_{on}}(s) = exp\left[\frac{c}{\sigma^2} - \frac{\sqrt{c^2 + 2s\sigma^2}}{\sigma^2}\right] \tag{3.100}$$

$$f_{T_{off}}(s) = exp\left[\frac{r}{\sigma^2} - \frac{\sqrt{r^2 + 2s\sigma^2}}{\sigma^2}\right] \tag{3.101}$$

If 'X' and 'Y' are defined by

$$X = \sum_{i=1}^{N} T_{on}(i) \tag{3.102}$$

$$Y = \sum_{i'=1}^{N} T_{off}(i') \tag{3.103}$$

Then the different moments of 'T_{on}' that are to be computed are

$$E[T_{on}] = -\frac{\partial f_{T_{on}}(s)}{\partial s}\bigg|_{s=0} = \frac{\Delta}{c} \tag{3.104}$$

$$E[T_{on}^2] = \frac{\partial^2 f_{T_{on}}(s)}{\partial s^2}\bigg|_{s=0} = \frac{\Delta^2}{c^2} + \frac{\Delta\sigma^2}{c^3} \tag{3.105}$$

$$E\left[\frac{1}{T_{on}}\right] = \int_{s}^{+\infty} f_{T_{on}}(u)du|_{s=0} = \frac{c\Delta + \sigma^2}{\Delta^2} \tag{3.106}$$

$$E\left[\frac{1}{T_{on}^2}\right] = \int_{s}^{+\infty}\int_{v}^{+\infty} f_{T_{on}}(u)dudv|_{s=0} = \frac{c^2\Delta^2 + 3c\Delta\sigma^2 + 3\sigma^4}{\Delta^4} \tag{3.107}$$

$$E[X] = -\frac{\partial f_X(s)}{\partial s}\bigg|_{s=0} = \frac{N\Delta}{c} \tag{3.108}$$

$$E[X^2] = \frac{\partial^2 f_X(s)}{\partial s^2}\bigg|_{s=0} = \frac{N\Delta(Nc\Delta + \sigma^2)}{c^3} \tag{3.109}$$

$$E\left[\frac{1}{X}\right] = \int_s^{+\infty} f_X(u)du|_{s=0} = \frac{Nc\Delta + \sigma^2}{N^2\Delta^2} \tag{3.110}$$

$$E\left[\frac{1}{X^2}\right] = \int_s^{+\infty}\int_v^{+\infty} f_X(u)dudv|_{s=0} = \frac{N^2c^2\Delta^2 + 3Nc\Delta\sigma^2 + 3\sigma^4}{N^4\Delta^4} \tag{3.111}$$

Similarly, for 'T_{off}' we have

$$E[T_{off}] = -\frac{\partial f_{T_{off}}(s)}{\partial s}\bigg|_{s=0} = \frac{\Delta}{r} \tag{3.112}$$

$$E[T_{off}^2] = \frac{\partial^2 f_{T_{off}}(s)}{\partial s^2}\bigg|_{s=0} = \frac{\Delta^2}{r^2} + \frac{\Delta\sigma^2}{r^3} \tag{3.113}$$

$$E\left[\frac{1}{T_{off}}\right] = \int_s^{+\infty} f_{T_{off}}(u)du|_{s=0} = \frac{r\Delta + \sigma^2}{\Delta^2} \tag{3.114}$$

$$E\left[\frac{1}{T_{off}^2}\right] = \int_s^{+\infty}\int_v^{+\infty} f_{T_{off}}(u)dudv|_{s=0} = \frac{r^2\Delta^2 + 3r\Delta\sigma^2 + 3\sigma^4}{\Delta^4} \tag{3.115}$$

$$E[Y] = -\frac{\partial f_Y(s)}{\partial s}\bigg|_{s=0} = \frac{N\Delta}{r} \tag{3.116}$$

$$E[Y^2] = \frac{\partial^2 f_Y(s)}{\partial s^2}\bigg|_{s=0} = \frac{N\Delta(Nr\Delta + \sigma^2)}{r^3} \tag{3.117}$$

$$E\left[\frac{1}{Y}\right] = \int_s^{+\infty} f_Y(u)du|_{s=0} = \frac{Nr\Delta + \sigma^2}{N^2\Delta^2} \tag{3.118}$$

$$E\left[\frac{1}{Y^2}\right] = \int_s^{+\infty}\int_v^{+\infty} f_Y(u)dudv|_{s=0} = \frac{N^2r^2\Delta^2 + 3Nr\Delta\sigma^2 + 3\sigma^4}{N^4\Delta^4} \tag{3.119}$$

These are the higher moments of 'T_{on}' and 'T_{off}' for the Air-Conditioner. These are computed for obtaining first and second moments of the estimation errors.

Mean and Variance of 'T_{on}' and 'T_{off}'

The mean and variance which are useful in validating the simulation algorithm for Air-Conditioners are given as follows:

$$Mean(T_{on}) = E[T_{on}] = \frac{\Delta}{c} \tag{3.120}$$

$$Mean(T_{off}) = E[T_{off}] = \frac{\Delta}{r} \tag{3.121}$$

$$\begin{aligned} Variance(T_{on}) &= E[T_{on}^2] - [E(T_{on})]^2 \\ &= \frac{\Delta^2}{c^2} + \frac{\Delta\sigma^2}{c^3} - \left(\frac{\Delta}{c}\right)^2 \\ &= \frac{\Delta\sigma^2}{c^3} \end{aligned} \tag{3.122}$$

$$Variance(T_{off}) = \frac{\Delta\sigma^2}{r^3} \tag{3.123}$$

Bias of the estimators

The expected values of the optimal estimators with the bias for the Air-Conditioners are given as follows

$$\begin{aligned} E[(c_{opt}(N)] &= E\left[\frac{N\Delta}{\sum_{i=1}^{N} T_{on}(i)}\right] \\ &= N\Delta E\left[\frac{1}{\sum_{i=1}^{N} T_{on}(i)}\right] \\ &= N\Delta\left[\frac{Nc\Delta + \sigma^2}{N^2\Delta^2}\right] \\ &= c + \frac{\sigma^2}{N\Delta} \end{aligned} \tag{3.124}$$

Similarly,

$$E[(r_{opt}(N)] = r + \frac{\sigma^2}{N\Delta} \tag{3.125}$$

$$E[(\sigma^2_{opt}(N)] = \sigma^2 - \frac{\sigma^2}{N} \tag{3.126}$$

From the above expected values of the estimators it could be said that as the number of observations are increased, i.e. as $N \to \infty$, the bias is eliminated but for finite samples it would be significant.

The Mean Square Convergence parameters

For N samples, mean square estimation errors are given by various entries in Matrix M(N) where:

$$M(N) = E[(\widehat{\theta}_{opt}(N) - \theta)(\widehat{\theta}_{opt}(N) - \theta)^T] \tag{3.127}$$

with the error terms given by

$$m_{11}(N) = E[(c_{opt}(N) - c)^2] \tag{3.128}$$

$$m_{22}(N) = E[(r_{opt}(N) - r)^2] \tag{3.129}$$

$$m_{33}(N) = E[(\sigma^2_{opt}(N) - \sigma^2)^2] \tag{3.130}$$

The above mean square estimation errors can be written in terms of r, c, σ^2 as

$$m_{11}(N) = \frac{\sigma^2 c}{N\Delta} + \frac{3\sigma^4}{N^2\Delta^2} \tag{3.131}$$

$$m_{22}(N) = \frac{\sigma^2 r}{N\Delta} + \frac{3\sigma^4}{N^2\Delta^2} \tag{3.132}$$

and

$$
\begin{aligned}
m_{33}(N) &= \frac{2}{4N}\left(r^2\Delta^2 + c^2\Delta^2 + \sigma^2 r\Delta + \sigma^2 c\Delta + 2\sigma^2\right) \\
&\quad -\frac{3}{2N^2}\left(\sigma^2 r\Delta + \sigma^2 c\Delta\right) \\
&\quad -\frac{1}{N-1}\left(r^2\Delta^2 + c^2\Delta^2 + \sigma^2 r\Delta + \sigma^2 c\Delta\right) \\
&\quad -\frac{1}{(N-1)^2}\left(\sigma^2 r\Delta + \sigma^2 c\Delta + 2\sigma^4\right) \\
&\quad +\frac{N^3}{4(N-1)^4}\left(r^2\Delta^2 + c^2\Delta^2 + \sigma^2 r\Delta + \sigma^2 c\Delta\right) \\
&\quad +\frac{5N^3}{2(N-1)^5}\left(r\sigma^2 + c\sigma^2 + 2\sigma^4\right) \\
&\quad +\frac{45N^3}{4(N-1)^6}\left(\frac{\sigma^6}{r\Delta} + \frac{\sigma^6}{c\Delta} + 2\sigma^4\right) \\
&\quad +\frac{105N^3}{4(N-1)^7}\left(\frac{\Delta^4\sigma^8}{r^2} + \frac{\Delta^4\sigma^8}{c^2} + \frac{\Delta^5\sigma^6}{r} + \frac{\Delta^5\sigma^6}{c}\right) \\
&\quad +\frac{105N^3}{4(N-1)^8}\left(\frac{\sigma^6}{\Delta^3 r^3} + \frac{\sigma^6}{\Delta^3 c^3}\frac{\sigma^4}{\Delta^2 r^2} + \frac{\sigma^4}{\Delta^2 c^2}\right) \\
&\quad +\sigma^4\left(\frac{1}{4N} + \frac{3}{2N^2}\right)
\end{aligned} \tag{3.133}
$$

The root mean square relative estimation error on the estimators are given by

$$
\rho_i(N) = \frac{\sqrt{m_{ii}(N)}}{\theta_i}, i = 1, 2, 3 \tag{3.134}
$$

where $\theta = [r, c, \sigma^2]$ and $\rho_i(N)$ is the relative estimation error associated with the parameter θ_i for the Air-Conditioner Case.

Till now, the theoretical results were presented, these results are validated using simulation in the following section.

3.5 Simulation and Identification for the Air-conditioner

3.5.1 Simulation

Based on equation (3.76-3.78), simulation was conducted with the assumption of Weiner Noise as discussed in section 3.3.1.

With the Weiner noise defined, the simulation was carried out for the Air-Conditioner with the following parameters:

$a = 0.0262min^{-1}, R = 0.5958^oCmin^{-1}, x_+ = 22^oC, x_- = 20^oC, x_a = 35^oC$, with noise variance as $\sigma^2 = 0.04^oC^2min^{-1}$. A typical simulation is shown in Figure 3.11 where the system has already reached steady-state.

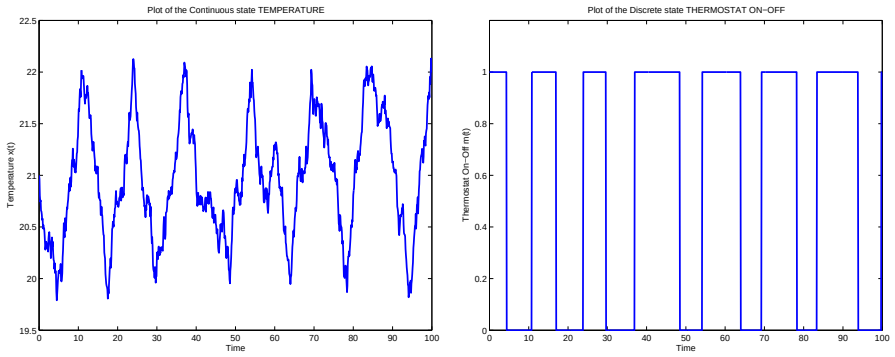

Figure 3.11: Simulation for a System already in Steady State (A/C).

Different simulations were carried out to verify the theoretical results for the air-conditioner as done for the heater. The statistics like the mean and the variance were verified against the theoretical ones derived in section 3.4.5 for the simulation algorithm. The vertical simulation and the horizontal simulation as presented for

the heater case were also verified for the Air-Conditioner.

Tables (3.7-3.8) refer to the results obtained through horizontal simulation. The same parameters that were previously defined were used in this simulation. The theoretical mean was calculated as given by equation (3.120) and compared with mean obtained through simulation of the system and the relative error between the two were calculated. Similarly, the theoretical variance as calculated by equation (3.122) and variance obtained through simulation compared for relative error.

Table 3.7: Statistics for Horizontal Simulation for 'T_{on}' (A/C).

Sample	Δ/c	Mean	Rel. Err.	$\Delta * \sigma^2/c^3$	Variance	Rel. Err.-Var
10	8.7336	9.62	0.1015	6.6617	11.3151	0.6985
20	8.7336	8.82	0.0099	6.6617	7.7396	0.1618
30	8.7336	8.7533	0.0023	6.6617	8.0074	0.202
40	8.7336	8.48	0.029	6.6617	7.1437	0.0724
50	8.7336	8.398	0.0384	6.6617	5.9822	0.102
60	8.7336	8.485	0.0285	6.6617	5.3816	0.1921
70	8.7336	8.6329	0.0115	6.6617	6.2927	0.0554
80	8.7336	8.7713	0.0043	6.6617	5.9537	0.1063
90	8.7336	8.9833	0.0286	6.6617	7.6252	0.1446
100	8.7336	8.906	0.0197	6.6617	7.4095	0.1123

In the horizontal simulation, it could be observed that the relative error that is generated by the simulation for mean and variance of samples of 'T_{on}' is less than 3% and 11% respectively and the mean and variance for samples of 'T_{off}' is less than 3% and 5% respectively. The mean and variance of 'T_{on}' and 'T_{off}' in general converges to the theoretical mean and variance as the number of samples are increased. But we can observe that the relative error between theoretical mean and simulation of 'T_{on}' and 'T_{off}' first increased and then it decreased. It might be due to system

Table 3.8: Statistics for Horizontal Simulation for 'T_{off}' (A/C).

Sample	Δ/r	Mean	Rel. Err.	$\Delta * \sigma^2/r^3$	Variance	Rel. Err.-Var
10	5.4526	5.87	0.0766	1.6211	1.3823	0.1473
20	5.4526	5.9	0.0821	1.6211	1.7421	0.0747
30	5.4526	5.75	0.0546	1.6211	1.6364	0.0094
40	5.4526	5.6075	0.0284	1.6211	1.7694	0.0915
50	5.4526	5.578	0.023	1.6211	1.5528	0.0421
60	5.4526	5.5767	0.0228	1.6211	1.5161	0.0648
70	5.4526	5.5943	0.026	1.6211	1.5913	0.0184
80	5.4526	5.6425	0.0348	1.6211	1.6832	0.0383
90	5.4526	5.6478	0.0358	1.6211	1.5762	0.0277
100	5.4526	5.615	0.0298	1.6211	1.535	0.0531

starting in steady state and therefore initial samples were closer to the theoretical mean.

The next set of Tables (3.9-3.12) refer to the results obtained through vertical simulation. Tables (3.9,3.10) represents the individual results obtained in each vertical run and Tables (3.11,3.12) represents the consolidated or the cumulative results. The simulation parameters were same as for the horizontal simulation, but the number of samples were limited to small number of ten due to simulation and computational time.

At one glance, the results show that individual runs for sample length of ten produces an average mean and variance relative error for 'T_{on}' as 5% and 41% respectively and for 'T_{off}' as 6% and 48% respectively.

The cumulative results of the vertical simulation are more important than the individual runs. As observed from tables (3.11,3.12) the relative error in the mean and variance of both 'T_{on}' and 'T_{off}' converges to the theoretical mean and variance as

Table 3.9: Statistics for Vertical Simulation for 'T_{on}' (A/C).

Sample	$\frac{\Delta}{c}$	Mean	Rel. Err.	$\frac{\Delta\sigma^2}{c^3}$	Variance	Rel. Err.-Var
10	8.7336	7.29	0.1653	6.6617	2.0166	0.6973
10	8.7336	8.36	0.0428	6.6617	7.6093	0.1423
10	8.7336	8.95	0.0248	6.6617	5.9517	0.1066
10	8.7336	9.14	0.0465	6.6617	10.0893	0.5145
10	8.7336	9.13	0.0454	6.6617	4.9779	0.2528
10	8.7336	7.99	0.0851	6.6617	11.5743	0.7375
10	8.7336	8.76	0.003	6.6617	6.5649	0.0145
10	8.7336	8.87	0.0156	6.6617	5.1734	0.2234
10	8.7336	8.96	0.0259	6.6617	13.0827	0.9639
10	8.7336	8.78	0.0053	6.6617	3.5018	0.4743

Table 3.10: Statistics for Vertical Simulation for 'T_{off}' (A/C).

Sample	$\frac{\Delta}{r}$	Mean	Rel. Err.	$\frac{\Delta\sigma^2}{r^3}$	Variance	Rel. Err.-Var
10	5.4526	5.91	0.0839	1.6211	1.1499	0.2907
10	5.4526	4.91	0.0995	1.6211	0.6721	0.5854
10	5.4526	5.4	0.0096	1.6211	1.32	0.1857
10	5.4526	6.2	0.1371	1.6211	1.6956	0.0459
10	5.4526	5.77	0.0582	1.6211	2.0646	0.2736
10	5.4526	5.61	0.0289	1.6211	3.4032	1.0994
10	5.4526	6.09	0.1169	1.6211	3.2921	1.0308
10	5.4526	5.45	0.0005	1.6211	2.7917	0.7221
10	5.4526	5.81	0.0656	1.6211	1.8188	0.122
10	5.4526	5.58	0.0234	1.6211	1.0084	0.3779

the number of runs(i.e. the number of samples) are increased. For 'T_{on}' the relative error in the mean and Variance goes to less than 1.5% and 5%. Similarly for 'T_{off}' the relative error in the mean and Variance is less than 4% and 19% respectively. The high value of variances in cumulative result is due to the limited samples of ten in individual runs. More samples of 'T_{on}' and 'T_{off}' are needed to converge in variance.

These results were obtained to verify the simulation algorithm and to check the

Table 3.11: Cumulative Statistics for Vertical Simulation for 'T_{on}' (A/C).

Sample	$\frac{\Delta}{c}$	Mean	Rel. Err.	$\frac{\Delta\sigma^2}{c^3}$	Variance	Rel. Err.-Var
10	8.7336	7.29	0.1653	6.6617	2.0166	0.6973
20	8.7336	7.825	0.104	6.6617	4.8129	0.2775
30	8.7336	8.2	0.0611	6.6617	5.1925	0.2205
40	8.7336	8.435	0.0342	6.6617	6.4167	0.0368
50	8.7336	8.574	0.0183	6.6617	6.129	0.08
60	8.7336	8.4767	0.0294	6.6617	7.0365	0.0563
70	8.7336	8.5171	0.0248	6.6617	6.9691	0.0462
80	8.7336	8.5612	0.0197	6.6617	6.7447	0.0125
90	8.7336	8.6056	0.0147	6.6617	7.4489	0.1182
100	8.7336	8.623	0.0127	6.6617	7.0542	0.0589

Table 3.12: Cumulative Statistics for Vertical Simulation for 'T_{off}'(A/C).

Sample	$\frac{\Delta}{r}$	Mean	Rel. Err.	$\frac{\Delta\sigma^2}{r^3}$	Variance	Rel. Err.-Var
10	5.4526	5.91	0.0839	1.6211	1.1499	0.2907
20	5.4526	5.41	0.0078	1.6211	0.911	0.438
30	5.4526	5.4067	0.0084	1.6211	1.0473	0.3539
40	5.4526	5.605	0.028	1.6211	1.2094	0.254
50	5.4526	5.638	0.034	1.6211	1.3804	0.1485
60	5.4526	5.6333	0.0332	1.6211	1.7176	0.0595
70	5.4526	5.6986	0.0451	1.6211	1.9425	0.1983
80	5.4526	5.6675	0.0394	1.6211	2.0486	0.2638
90	5.4526	5.6833	0.0423	1.6211	2.0231	0.248
100	5.4526	5.673	0.0404	1.6211	1.9216	0.1854

convergence with respect to the theoretical results. The convergence is considered acceptable for the simulation algorithm to be used further for obtaining the optimal estimators.

The sensitivity analysis for Air-Conditioner for mean square error is described in the next section.

3.5.2 Sensitivity Analysis for the A/C Case

Sensitivity analysis was conducted to verify the theoretical results for root mean square convergence(MSE) as described by the equations(3.129-3.133) with the one obtained through simulation. Root mean square convergence with respect to simulation is obtained on the same patterns as described for the heater case in section 3.3.2. The RMS values thus obtained are compared with the results calculated through theoretical expressions.

The three kind of sensitivity analysis performed for heater were repeated for the Air-conditioner. The first kind of analysis consists of observing the behavior of the optimal estimators as the number of samples are changed. In the second kind of analysis, we focus on the convergence characteristics with respect to the changes in the parameters of the system. Finally the convergence behavior with respect to noise variance was carried out. The results are shown as follows:

Effect of Number of Samples

With the parameters defined previously, the effect of the number of samples on identification are studied on the quality of the estimators. Figure 3.12 represents the plot of root mean square relative error as functions of number of samples compared for theoretical and simulation. For the verification, about twenty five parallel simulations where carried out and the results obtained from each simulation about the estimates r, c, σ^2 was taken and the root mean square relative error was compared

with the ones obtained theoretically.

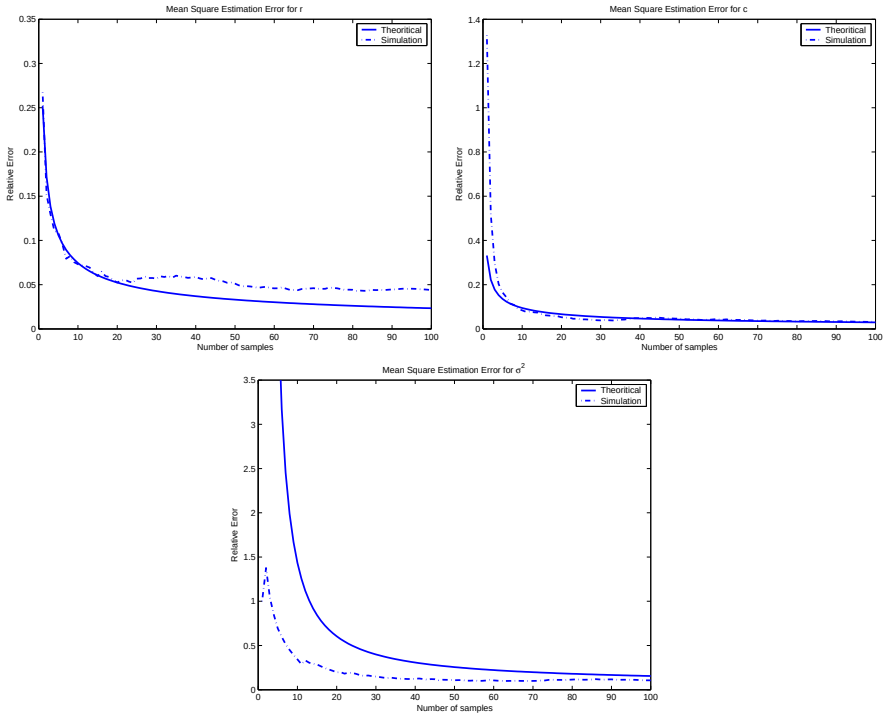

Figure 3.12: MSE as a Function of Number of Samples for A/C.

As seen in the figure the simulation showed almost the same trend when compared to theoretical results. The convergence in heat drift rate and noise variance is slightly different with the theoretical. This variation in the result for simulation could be explained as follows: the theoretical results were calculated for aggregated load and during simulation, limited horizontal simulation were carried out which results in the deviation. Also, it could be observed that the convergence of the estimators improves with the number of samples. The more measurements we use, the better is the result, which is what was expected.

Effect of Thermal Heat Loss and Power Rating

In the nextset of simulation, the theoretical root mean square relative convergence error and the one obtained through simulation was calculated as a function of thermal heat loss 'a' and Heating rate 'R'. In the simulation, the values of the parameter 'a' was varied from $0.005min^{-1}$ to $0.03min^{-1}$ and for two different values of the parameter 'R' i.e. 0.5^oCmin^{-1} and 0.7^oCmin^{-1}. Also the simulation was carried out for twenty five different parallel runs under steady-state and the results averaged and compared with the theoretical results. The results are shown in the Figure (3.13). As seen from the figure, the simulation follows the trend in theoretical results. The plots also suggest that the estimate of 'c' becomes difficult for high values of 'R' and 'a' which could be attributed to longer values of 'On' times which suggests the necessity to increase the sampling set. Similarly the estimation of 'r' becomes better because of stable values of 'off' times as the parameter 'a' is increased. As for the estimation of σ^2, small values of 'a' makes the 'on' time very small and comparable to noise and high estimation errors and large values of 'a' makes 'r' small and hence poor estimates. The estimation errors produced by simulation as compared to theoretical estimation error is less and does not increase as 'a' values is increased. As already discussed in case of sensitivity analysis with respect to number of samples, that the deviation in simulation and theoretical results is because the theoretical results are derived for aggregated loads. Also we can observe that for higher values

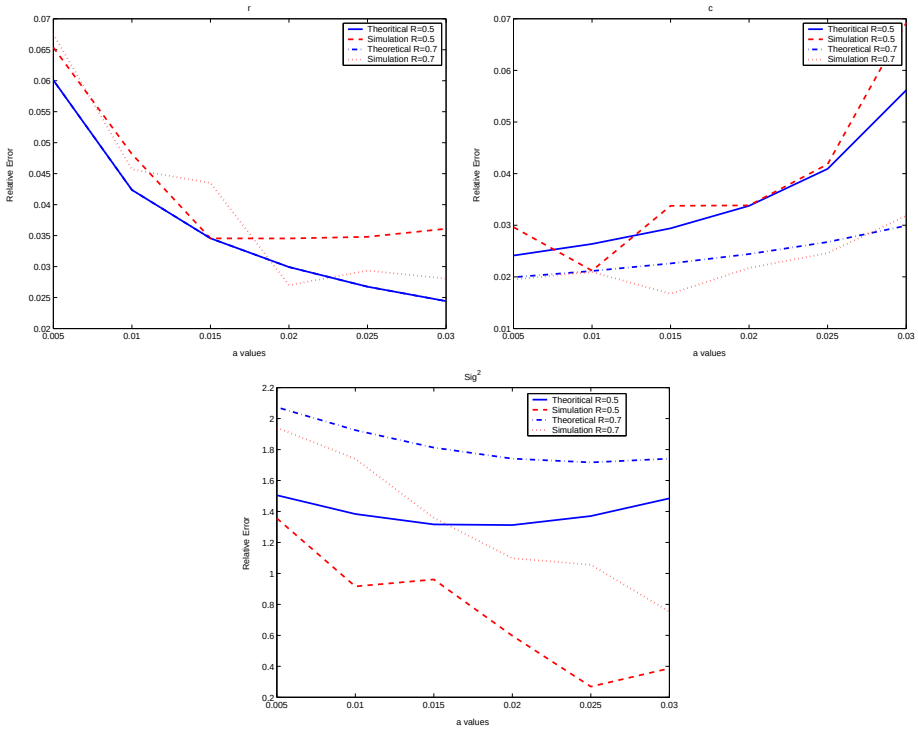

Figure 3.13: MSE as a Function of Thermal Heat Loss 'a' and Power Rating 'R' for A/C.

of 'R' the MSE for noise variance is higher.

Effect of Noise Parameter 'σ'

Finally, the theoretical root mean square estimation errors and the one obtained through simulation were compared as a function of different values of σ for different samples of 'On' and 'Off'. In this particular simulation the noise parameter σ was varied from $0.05^oC^2min^{-1}$ to $0.6^oC^2min^{-1}$ for two different sample lengths of 5 and 15 'On-Off' samples respectively. Also for the simulation, 20 different parallel runs under statistically steady-state were carried out. The root mean square is then

computed and is compared with the theoretical results, which could be seen in the Figure (3.14). From the figures, it could be observed that as the noise parameter σ

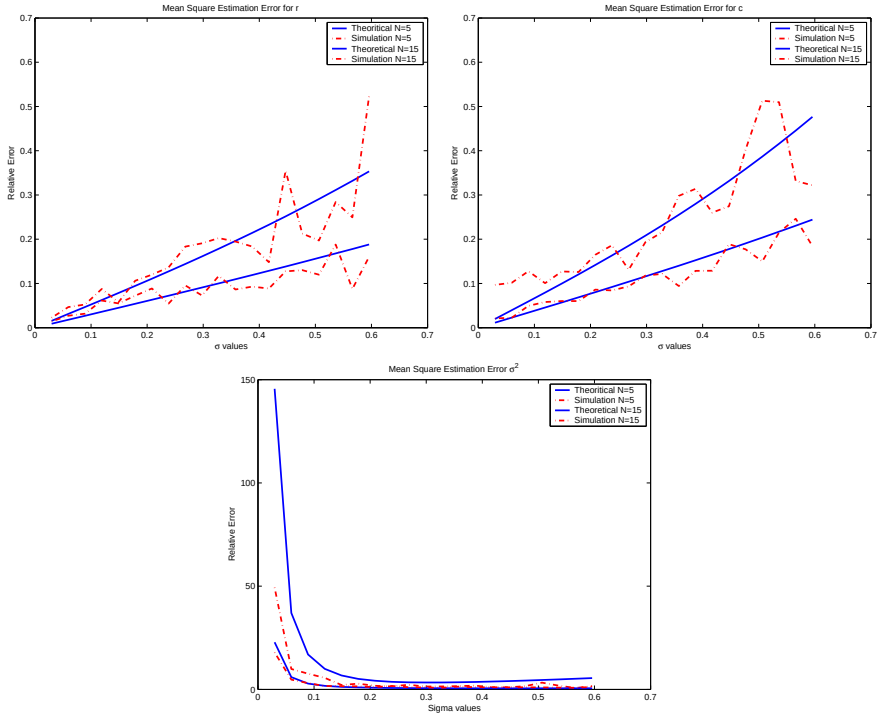

Figure 3.14: MSE as a Function of σ and Number of Samples for A/C.

is increased, the relative error in the estimation of 'r' and 'c' for fixed sample size also increases. This is because the noise pollutes the estimation and the estimation error increases. As for the estimation of σ^2 the relative error is very high for small values of σ because the systems dynamics are not excited enough for the estimation algorithm to see the whole dynamics. This results in very high estimation errors. High noise in the system makes necessary that the estimator requires more number of samples to give a good estimate.

The results validate the results obtained theoretically and hence validate the identification scheme presented for Air-Conditioner. The aggregate simulation model that will be used throughout this work will be validated for Cold Load pickup in the following section.

3.6 Simulation of Homogenous Groups of A/C

Simulation was also carried out to validate the classical cold load pickup response (response when all the load is switched off for certain time and then reconnected) of one homogenous group in simulation containing 1000 a/c's. The result obtained is compared with [10].

The parameters as in [10] are given by:

R'=5600 Btu/h; C=300000 J/^{o}C; a'=120 W/^{o}C; noise variance as $\sigma^2 = 0.01$ with the constant ambient temperature Xa = 34^{o}C and thermostat setting at 24^{o}C with the deadband set at 1.1^{o}C. The result is shown in Figure 3.15. The simulation depicted the same behavior as expected. The system settles down to about 64% in about 4 hours. Power supply to the homogenous group was cut off for 10 minutes and then restored back. This simulation endorses the use of aggregate simulation model for DLC strategy application. The control scheme where this model is used is discussed in the next Chapter.

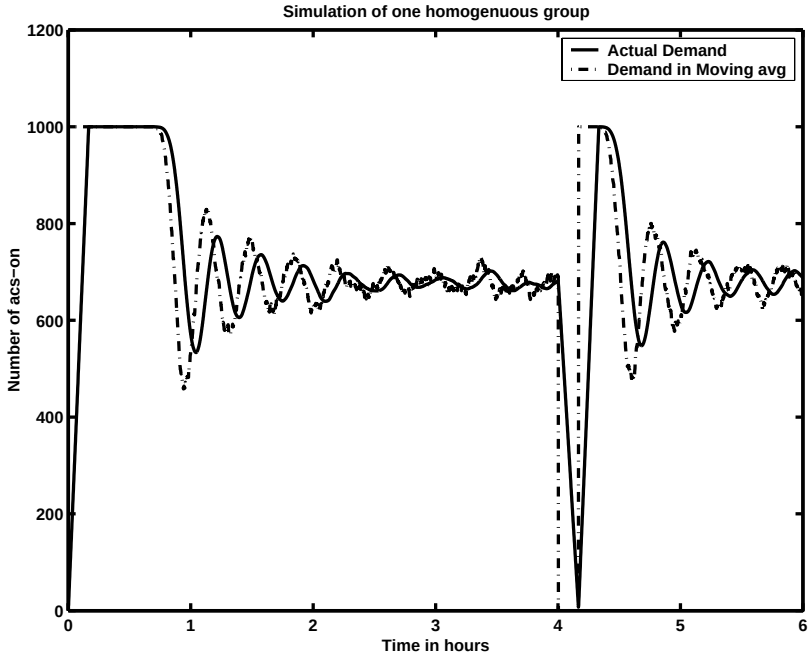

Figure 3.15: Simulation of A/C Homogenous group.

3.7 Summary

In this Chapter, the A/C model and its identification scheme was developed after presenting the validation results for the Heater. Later sections presented the validation for the Air-Conditioner model, its identification scheme and the sensitivity results. The aggregate simulation model for a load of A/C's in homogenous group was implemented and its result was validated in the last section. The next Chapter addresses the controller formulation and presents a Modified MPC controller.

Chapter 4

CONTROL STRATEGIES

4.1 Introduction

Control Strategies are methodologies whose aim is to influence the demand of the power system according to what is desired by the utilities. These strategies provide, means of getting the desired results by governing the decision variables that are to be controlled in the system. The decision variables here are the switching of the power supply to particular thermostatic loads arranged in some kind of homogenous groups. Major types of control strategies along with multivariable predictive control strategy are presented and discussed in the following section.

4.2 Major Types of Control Strategies

4.2.1 Dynamic and Linear Programming

Many of the control strategies based on Dynamic and Linear Programming are found extensively in the literature. These strategies were part of initial efforts in implementation of control strategies for demand reduction. With an objective of integrating Direct Load Control schedules with unit commitment and maximizing fuel cost saving, Hsu and Kuo [15] used dynamic programming algorithm to produce both generation schedule and amount of load control at each control interval.

According to Hsu and Kuo if a day is divided into N intervals and control period in M stages so that it covers $(k+1)$ to $(k+M)$ periods then the amount of load reduction at stage 'n' is given by

$$\begin{aligned} y_{DLC}(n) &= x_{DLC}(n) C_{DLC} \\ & 0 \leq x_{DLC}(n) \leq P, k+1 \leq n \leq k+M \end{aligned} \tag{4.1}$$

where C_{DLC} is the capacity of each cycling group divided into P specific address-specific group and x_{DLC} are the group under direct control at stage 'n'. Each stage was taken as 30 minutes and during control stage, x_{DLC} was supplied with power and rest of the group was not supplied power. Taking payback ($z_{payback}$) for three stages as the percentages of load control, the modified load profile L(n) is obtained

as follows

$$L(n) = L'(n) - y_{DLC} + z_{payback}(n-1) + z_{payback}(n-2) + z_{payback}(n-3) \quad (4.2)$$

Wei and Chen [16] presented their algorithm to overcome the limitation of time horizon and memory in the previous case using the multi-pass dynamic programming methods. Using the multi-pass dynamic programming they were able to schedule DLC dispatch of Air-conditioners for 8 days with very less computation time and memory. Chen et al. [17] presented a method which first identified a set of candidate control patterns for feasibility and cost benefit and then gives an optimal DLC dispatch via a binary network flow model. But both Wei and Chen and Chen et al. considered a constant controllable load and specified fixed candidate schedules in there formulation. Kurucz, et al. [13] used linear programming for reducing peak load demand and concluded that linear programming was a powerful and effective tool for scheduling load control. The paper did not consider possibilities of all control duration strategies that could be used. This was rectified by Ng and Shebé [14] who considered all the control duration strategies using linear programming. But the method used an assumption of constant controllable load to achieve load reduction which is a drawback by itself. Moreover the aforementioned strategies did not include the customers comfort index in their formulation which is considered equally important when compared to demand reduction.

4.2.2 Pulse Width Modulation

Pulse width modulation (PWM) based technique was presented by Navid and Banakar [18] and Canbolat Ucak and Ramazan [24] to reduce the controlled appliances power demand in accordance with a predefined load reduction profile or target curve. In PWM, a signal described in Figure 4.1 is used as a control signal. The control

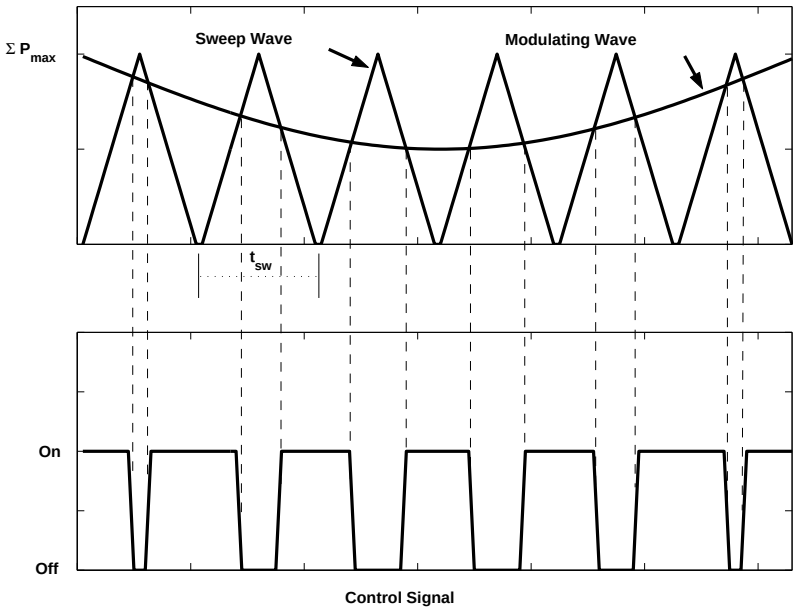

Figure 4.1: Control Signal in a PWM Technique.

signal is a series of varying pulses obtained when a sweep wave is compared directly with the modulating wave. That is when the modulating wave is less than the sweep wave the control signal is 'On', otherwise its 'Off'. The sweep wave is obtain by varying it from zero to sum of all the power's of participating controllable loads. This control strategy had the advantage of scheduling controllable loads with the

basic information of peak demand and thermostat cycling which are easily available. The scheduling technique was computationally easy to implement on a normal Intel Personal Computer. While this strategy helped in getting a more flexible load management program, and an effective use of more sophisticated equipments, it was just applied during control period and a different control strategy was opted after the control period in order to reduce the payback. Also for this strategy to be implemented a target curve or a modulated curve is defined based on controllable loads and not on the total load. Apart from this, customer comfort is not taken into consideration which could always lead to customer dissatisfaction.

Canbolat and Ramazan in addition studied the load parameter dispersion and concluded that thermal capacity and dead-band do not alter the magnitude of an aggregated load but the thermal resistant, rating of air-conditioner and the thermostat setting are important parameters in determining the aggregated load level for steady state.

4.2.3 Fuzzy Logic

In the previous type of control strategies, customer's preferences and desires were not taken into consideration. Anticipating the need to implement this in the utility based control, fuzzy logic was introduced in Direct Load Control by Bhattacharya and Crow [27]. They pointed out that the previous methods applied in DLC are good for analysis but are not good for them to be easily implemented. Using fuzzy logic

approach, they tried to optimize the trade-off between customer preferences, utility resources and uncertainty in load. Huang et al. [28] suggested a fuzzy dynamic programming structure to reduce load as well as total operating costs for scheduling the DLC. Taking the uncertainties of load variations on the basis of the previous load prediction errors made their method more robust in its structure. Salehfar et al. [36] have also suggested fuzzy approach in their control strategies for DLC of water heaters and Air-conditioners by incorporating customer's desires. They showed that implementing a fuzzy based strategy shifted the average demand of customers loads and thus improves utility load factor.

4.2.4 Genetic Algorithm in DLC

The use of modified genetic algorithm (GA) called recursive GA was proposed by Leether and Hsieh [29] to optimize the scheduling of direct load control strategies. They showed that recursive GA tends to level off the accumulated shedding time of each controllable load group which can avoid customers complain about the fairness of scheduling. Although this strategy works with good results, it requires the optimal schedules to be setup manually in the load management system. Moreover, it looked at the controllable load profile without taking into consideration the global or the total load profile.

4.3 Multivariable Predictive Control

With an objective of scheduling the DLC in accordance with the global or total load curve, Molina et al. [19] described a new constrained multivariable predictive control strategy to be applied in residential HVAC Direct Load Control. This control algorithm provided multiobjective framework taking into account customers comforts, HVAC limits, utility limitations etc., to minimize the discrepancies between controlled load curve and the predefined target load curves. The control problem suggested in [19] was to optimally control the residential HVAC to modify the global load curve according to target load profile prefixed at the optimization formulation. For this strategy the controllable loads are divided into homogenous groups having similar parameters, target load curves for different objectives are defined and important DLC contract values such as minimum 'On' time and maximum 'Off' time are taken. The control period is then divided into 'm' periods and forced duty cycles for each homogenous group for each period is computed. These forced duty cycles are the control actions and they are computed for each period and the whole optimization process is then performed again during the next interval.

The control strategy could be described by Figure 4.2. At the starting period of the control duration, the simulation of distribution system is done based on models presented in [10]. The responses were then fed to the optimizing controller. Control decisions are then calculated where only decisions for the next period are fed to

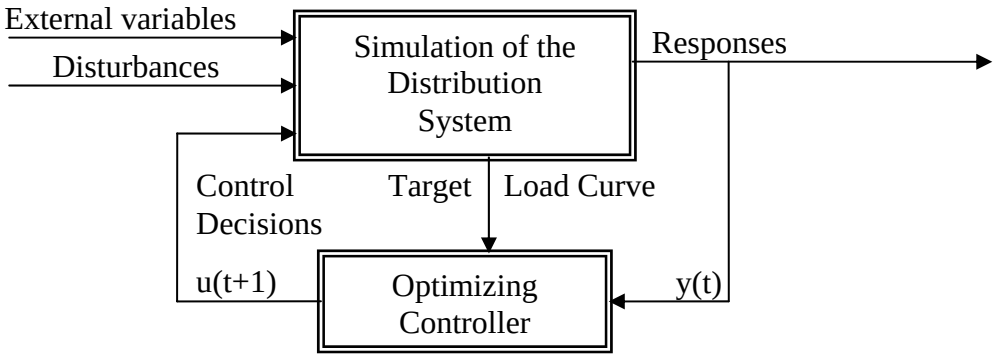

Figure 4.2: MPC Control Strategy.

the system along with external parameters and disturbances. At the next period, the optimization is carried out again to produce the control actions at that control period. This continues till the last period of the control horizon.

In the next sub-section, the formulation of the multivariable Model Predictive Control (MPC) strategy based on [19] is presented.

4.3.1 Controller formulation

Nomenclature

a - Parameter to control rapidity in close loop behavior

m - number of periods of control horizon

ij - suffix to denote group 'i' at period 'j'

CL_{ij} - Controllable load

CLD_{ij} - Controllable deferred load

CT_j - total load at period 'j'

MCL_{ij} - Maximum controllable load

MCD_{ij} - Maximum controllable load deferred

MPl_i - Maximum peak load of group 'i'

MPb_i - Maximum peak load of group 'i'

NL_{ij} - Noncontrollable load

Pb_i - Payback of group 'i' after controlling

RC_j - The reference curve for period 'j'

y_{r_j} - The Target Load curve

u_{ij} - The control actions

Wf_i - Weighing vector for prioritizing future control

Wc_{ij} - Weighting matrix to step changes in control actions

The controller objective is stated as follows

$$Min\left[\sum_{j=1}^{m} Wf_j(CT_j - RC_j)^2 + \sum_{j=1}^{m}\left(\sum_{i=1}^{N} Wc_{ij}(u_{ij} - u_{ij-1})^2\right)\right] \tag{4.3}$$

where

$$RC_j = aRC_{j-1} + (1-a)y_{r_j} \tag{4.4}$$

$$CT_j = \sum_{i=1}^{N}(NL_{ij} + u_{ij}Min\{MCL_{ij}; CL_{ij} + CLD_{ij-1}\}) \tag{4.5}$$

$$CLD_{ij} = CLD_{ij-1} + CL_{ij} - u_{ij}Min\{MCL_{ij}; CL_{ij} + CLD_{ij-1}\} \tag{4.6}$$

The objective here is to minimize both the weighted tracking error as well as the weighted step changes in control decisions subjected to the following constraints.

$$0 \leq a \leq 1 \tag{4.7}$$

$$0 \leq u_{ij} \leq 1 \tag{4.8}$$

$$0 \leq CLD_{ij} \leq MCD_{ij} \tag{4.9}$$

$$0 \leq Pb_i = CLD_{im} \leq MPb_i \tag{4.10}$$

$$0 \leq NL_{ij} + u_{ij}.Min\{MCL_{ij}; CL_{ij} + CLD_{ij-1}\} \leq MCD_{ij} \tag{4.11}$$

Equation (4.7) controls the rapidity towards the close-loop behavior of the controller system. Equation (4.8) gives the limits within which the control actions are computed. Equation (4.9) represents the constraint for the deferred load where the deferred load cannot be more than MCD_{ij} the maximum deferred controllable load

for group 'i' in period 'j'. The MCD_{ij} is computed taking into account the maximum 'Off' durations and the customer comfort levels(average temperatures inside the homogenous groups) that are to be maintained during the control period. Equation (4.10) is the constraint introduced to minimize the payback. This constraint ensures that the cumulative deferred load is close to zero in the last control period. Finally, equation (4.11) limits the secondary peaks that are generated during the control strategy.

The control system has a closed-loop behavior to accommodate modelling errors and other disturbances. Also the control algorithm allowed for dynamic modification of target load profile according to real-time system behavior.

In this formulation, the responses of the system are first calculated and on these responses the optimization is carried out. One drawback is that deferred load is calculated as the difference between Off-control power demand and the supplied power under control irrespective of the A/C's thermostat state. This difference is added on to the next period load. But the actual deferred load is different for a real case. For a real case if average power is computed during each control period, the deferred load is slightly less than the one actually deferred. In the next subsection we will show that this will not lead to the best result. Accordingly, a modification of the original implementation is proposed.

4.3.2 Modified Multivariable Predictive Control

Figure 4.3 shows a simulation of a homogenous group consisting of 5 A/C's. In this,

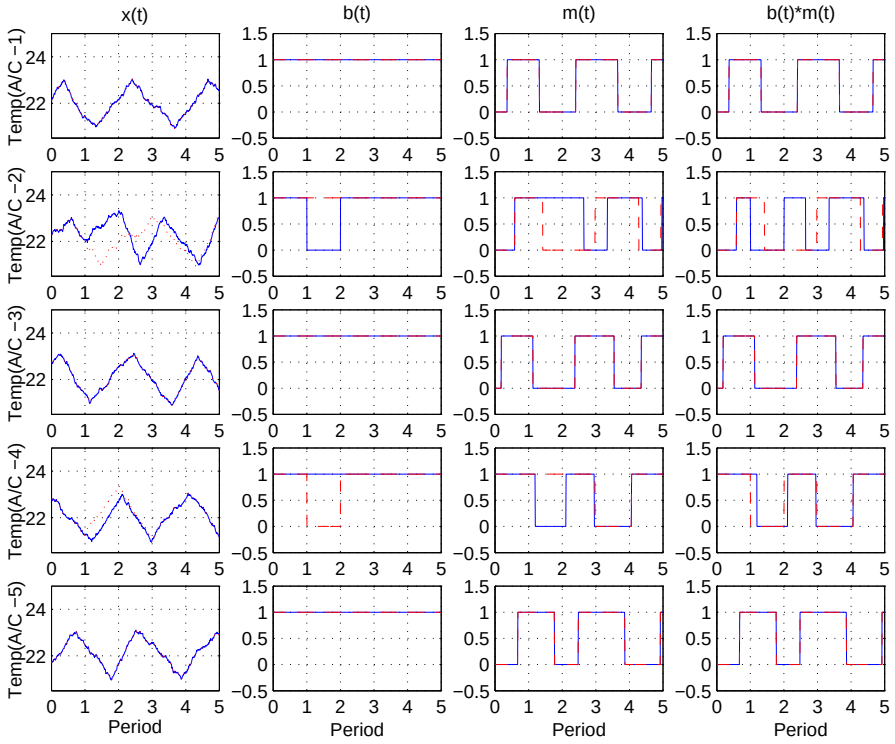

Figure 4.3: Illustration of Load Deferred in Homogenous group.

the total control duration was one hour with 12 minutes of control period each. It is required in the second period that the total load to be around 80% of the total load. This could be done by switching the power supply at one of the five A/C's. Two cases are discussed over here. Lets assume in the first case the second A/C is switched off. This is shown by the solid line in all the plots. It could also be observed in the plot of b(t)*m(t) that the load deferred should be added on to the next period i.e. in the third period. When the average power is used in calculating the loads

we observe that the load deferred is different. That means that the deferred load is actually a percentage of the load during that control period. Therefore the actual deferred load seen during the next period is between the actual load for the third period and actual load for the third period plus 100% of deferred load at the second period.

The percentage of the load that is deferred will also depend on the A/C that is selected. Now for the second case if the fourth A/C in the group is switched off, the deferred load will be totally different when compared to the previous case. This case is shown by the dotted curve in all plots. This shows that the deferred load is not just a difference between the actual Off-control load and the load under control for the same period.

So, under such average computation of loads, the deferred load that is reflected during the control strategy is different taking the control strategy away from real case. To achieve more reality in the scheme, a modification in the strategy is proposed as discussed in the next subsection.

4.3.3 The Simulation Approach

A better approach would be to apply the optimizing controller by simulating the network during the optimizing routine itself. This type of controller optimization is explained in Figure 4.4. So in this control strategy the network is simulated until the starting period of control duration, and the controllable load along with noncontrol-

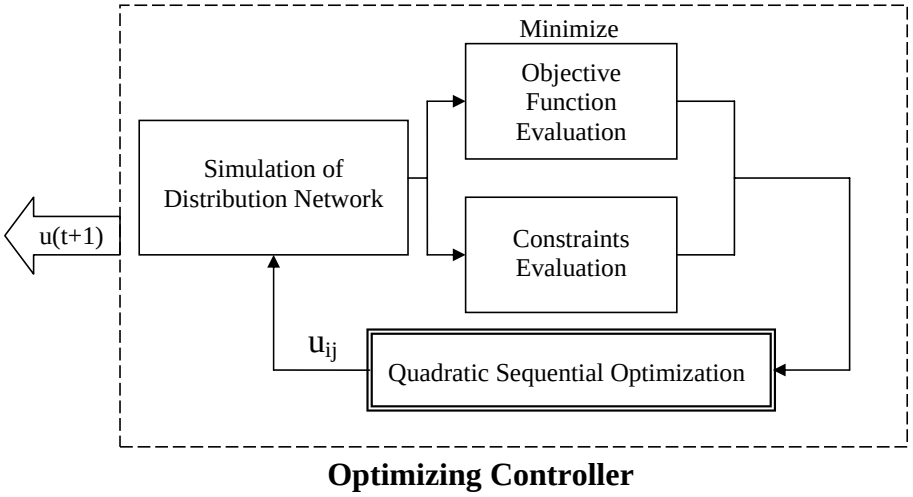

Figure 4.4: Modified Optimizing Controller.

lable are then computed for the whole of the control horizon. This load obtained is what we call controllable load without control or the Off-control load profile. Based on this load the various constraints of maximum deferred load, maximum peak load and maximum payback period are computed.

The optimization is then performed to obtain the control decisions. During the optimization routine, a complete monitoring of temperatures and states of A/C is maintained and only those A/C units which are 'On' and have temperatures near there thermostatic settings are switched off during control. Thus, control actions that are obtained are close to real when compared to the one obtained in Molina's case.

4.4 Power Saving Analysis

4.4.1 Simulation Parameters

Simulation was carried with the above scheme. Two homogenous groups were created with 25 air-conditioners each with average thermal capacity 'C' of 398798 and 390000 J/^{o}C respectively, average loss coefficient 'a' of 175 and 160 W/^{o}C respectively and average power rating of air-conditioners as 3960 and 3800 Watts. These parameters used for the first homogenous group are taken from a real air-conditioner system located at Rabee Courts, KFUPM, Dhahran, KSA. Noncontrollable loads were then generated for the whole day along with controllable load. The day was divided in different periods of 12 minutes each. The thermostat setting of each A/C in the group was assumed to be the same with minimum setting of 21^{o}C and a temperature deadband of 2^{o}C. The ambient temperature that was also taken from a real data collected during the month of August. The profile of the ambient temperature for 21^{st} of August is shown in Figure 4.5 where the average temperature was 36.67^{o}C.

4.4.2 Peak Reduction

The simulation was carried out for 4 hours from 10 a.m. to 14 p.m. with the objective of reducing just the peak load. The result could be seen in Figure 4.6. To obtain the reduction of peak during the same hours, a reference curve as shown in Figure

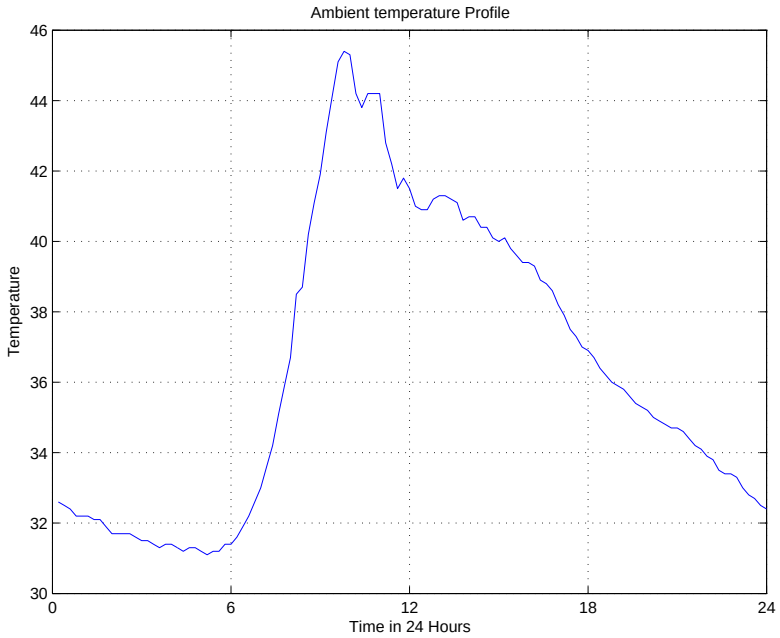

Figure 4.5: Ambient Temperature for Simulation.

4.6 was defined. Various constraints were calculated where maximum deferred load was kept at 10% of the controllable load, peak load could not exceed 96% of the total load without control and payback was 2% of total load that would be deferred during the whole control period. These constraints are shown with dotted line in Figure 4.7. The simulation was carried out as described in the previous section. In Figure 4.7, the dotted line shows the actual load demand that is seen during control, this load is higher than that of load without control. This demand profile is the one on which the control decisions are implemented. The dashed dotted line represents the optimized load. The maximum temperature for all A/C's during control was just 25.6^{o}C whereas the average temperature that exceeded the comfort index was about 23.76^{o}C, which is acceptable. The peak load reduction of about 5% was achieved.

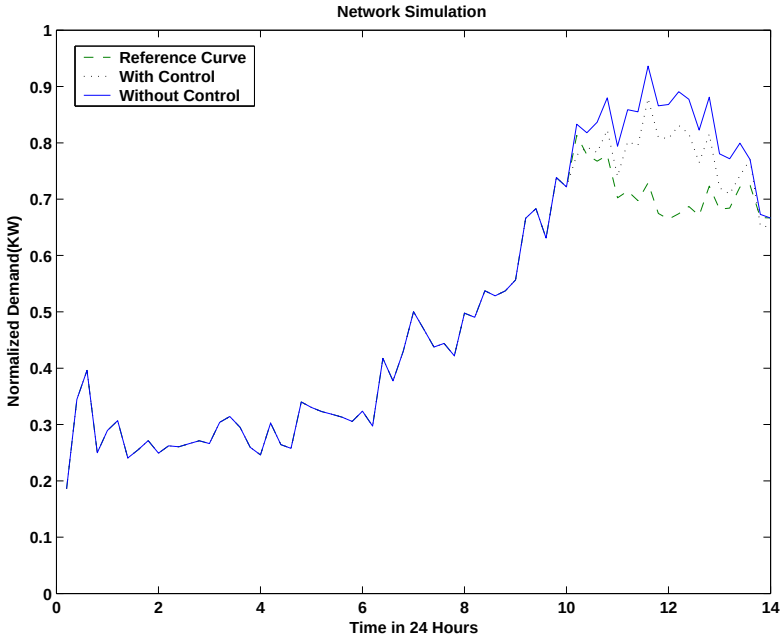

Figure 4.6: Simulation Result for Network for Peak Reduction.

Another simulation with the same parameters was performed with a change of control duration and deferred load. In this result, the control decision are evaluated every 15 minutes instead of 12 minutes. This was done to reduce the computation time as the number of control periods per unit hour is reduced. Also the maximum deferred load was increased from 10% to 12% and payback constraint at last period reduced to 1%. The response of the network to the control strategy is shown in Figure 4.8 and the responses of individual homogenous groups is shown in Figure 4.9. The simulation was continued till the end of the day for both cases, i.e. before control and after control. The load profile after control merges easily and traces almost the same profile as before control because of the more stringent payback constraint.

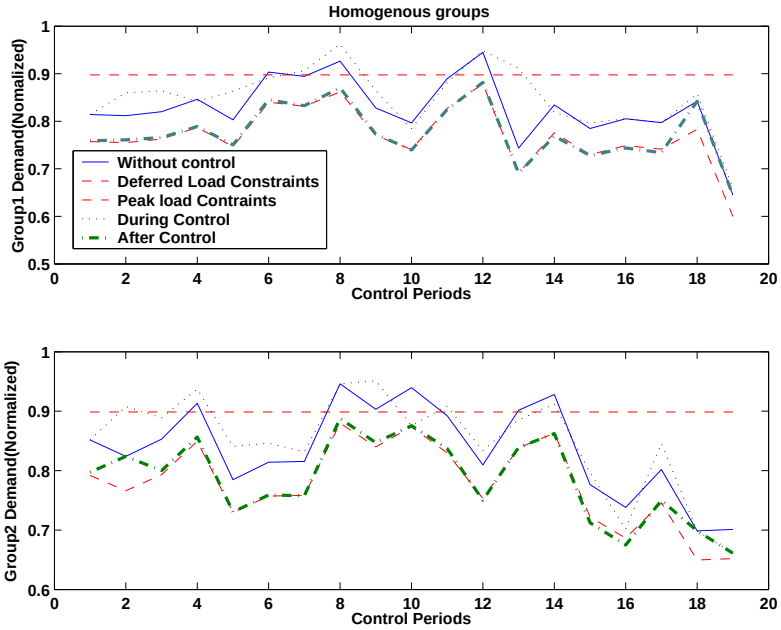

Figure 4.7: Homogenous Groups During Peak Reduction.

For this simulation, the maximum temperature that was seen during control was 26.07^{o}C and the average temperature that exceeded the comfort index was 23.85^{o}C. This increase in the average temperature could be attributed to increased control periods. Energy saving were also calculated for this simulation as the ratio of difference in energy before control and after control to energy before control. Peak load reduction of 2.53% in the load profile was observed, this reduction in load was due to the payback constraint.

Finally, the above simulation was repeated with same payback constraint but with a different maximum deferred load constraint. The maximum deferred load was increased from 12% to 20% in this simulation. The result of optimization for the

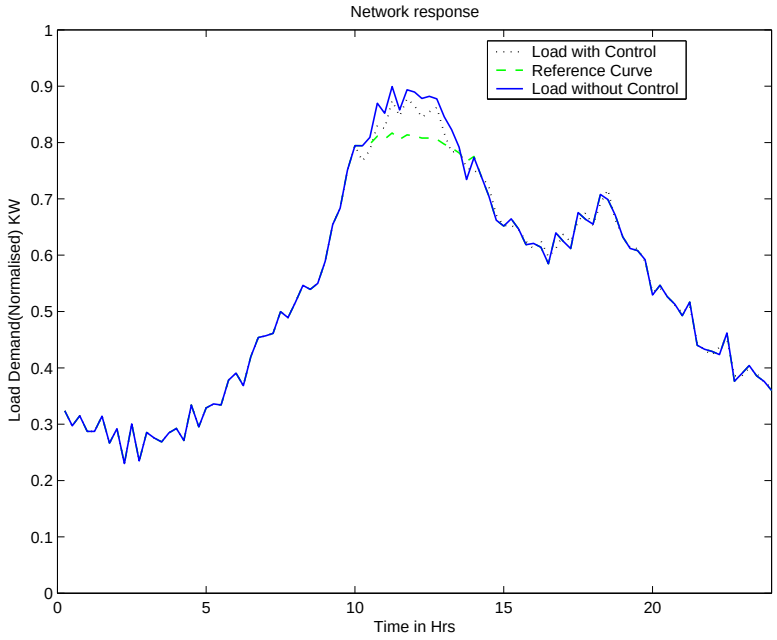

Figure 4.8: Network Simulation Result for Peak Clipping(Payback-1%).

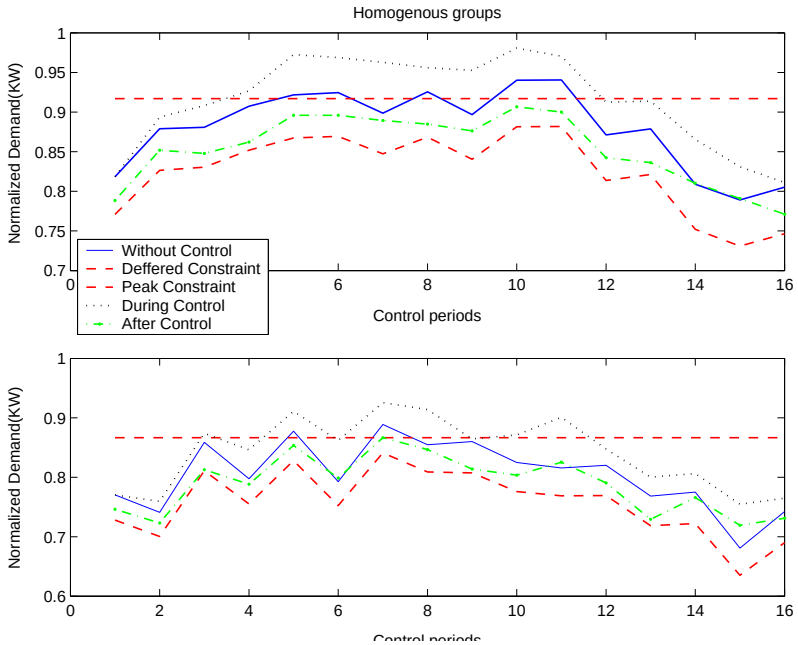

Figure 4.9: Homogenous Groups During Peak Clipping(Payback-1%).

network is seen in Figure 4.10 and for the two different homogenous groups in Figure 4.11.

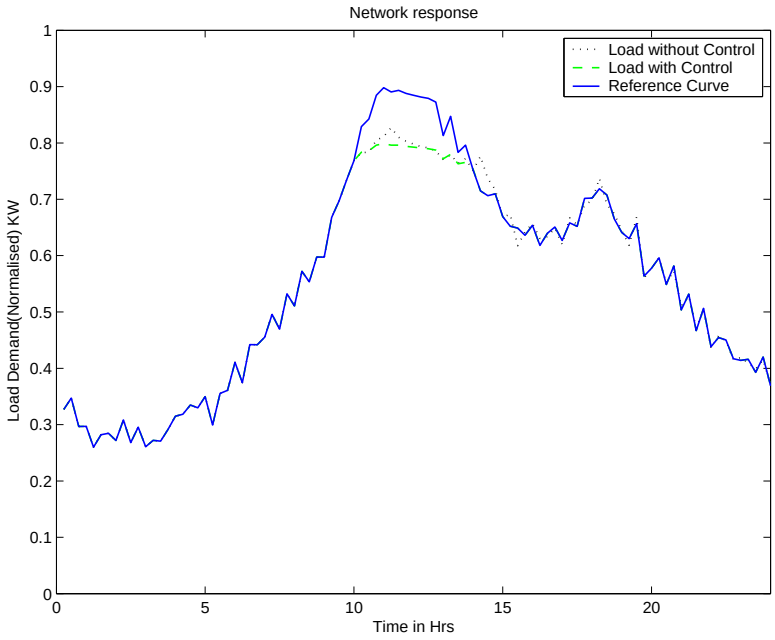

Figure 4.10: Network Simulation Result for Peak Clipping(Max. Deferred Load-20%).

It can be observed here that by relaxing the deferred load constraint the optimization was able to trace the reference curve. But this was done at the cost of the comfort index.

The maximum temperature that was observed during control was 27.29^{o}C which is quite high compared to thermostatic setting of 23^{o}C. The average temperature that exceeded the comfort index was observed to be 24.28^{o}C. The load profile in the homogenous groups traces the maximum deferred load except for the last period due to the payback constraint. After the control, a slight increase in the total load was

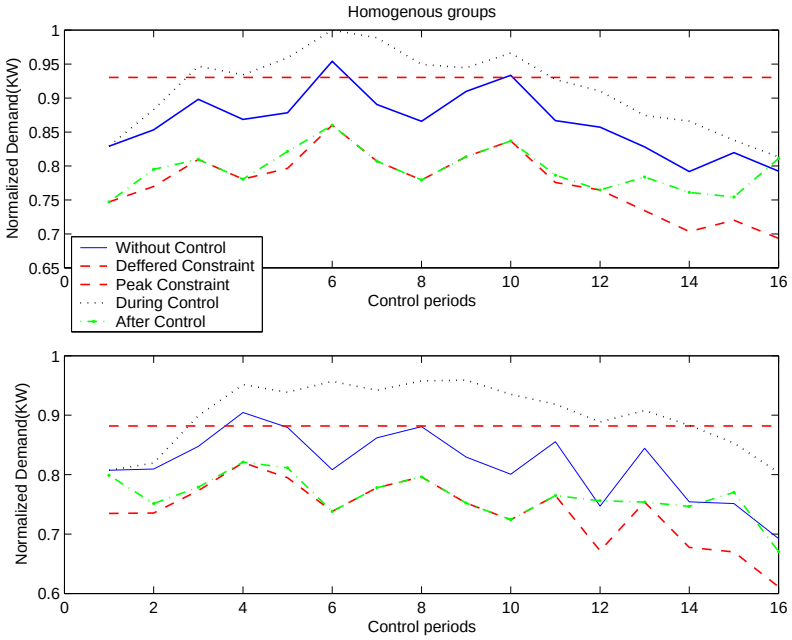

Figure 4.11: Homogenous Groups during Peak Clipping(Max. Deferred Load-20%).

observed. A total of 7.89% reduction in the peak load was achieved in this simulation. Therefore, a balance between the payback constraints and the deferred load constraint has to be achieved for maintaining the comfort index inside the dwelling of the house.

4.5 Summary

This Chapter presented a brief overview of the major control strategies that has been applied in DLC. The Model Predictive Control strategy was explained in the subsequent sections and its liabilities were discussed. A modified approach was then developed for the same controller scheme and its results presented.

Chapter 5

IMPLEMENTATION ON A REAL A/C

5.1 Setup and Instrumentation

To analyze the identification scheme and study the control strategy, a residential housing was used. Data was collected from the residential house 2213 of Rabee courts on the KFUPM University campus. This residential house is a single storey house whose layout is shown in Figure 5.1.

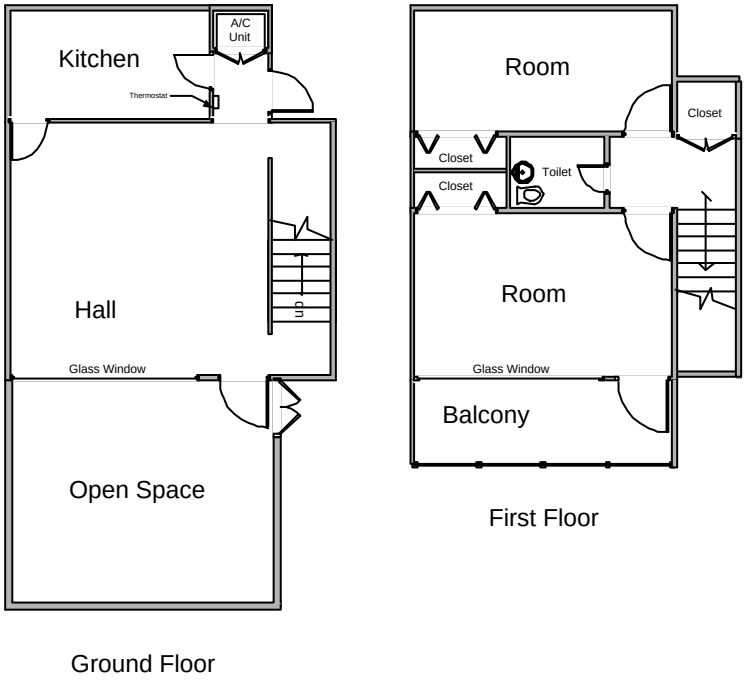

Figure 5.1: Plan of the Residential House, Rabee Courts, KFUPM.

5.1.1 Instrumental setup

There were three computers with two different instruments used in the collection of data from the residential house. These instruments were FLUKE 43-power quality analyzer and VELOCICALC Plus. The instruments setup plan inside the house is shown in Figure 5.2.

The FLUKE 43 was kept near the power panel with the sensor measuring the current and voltage readings inside the panel as seen in Figure 5.2. Two VELOCICALC instruments used to measure the temperature and other parameters were placed on the ground floor near the thermostat and on the first floor balcony to measure ambient parameters respectively. Computer 1 recorded the readings from FLUKE

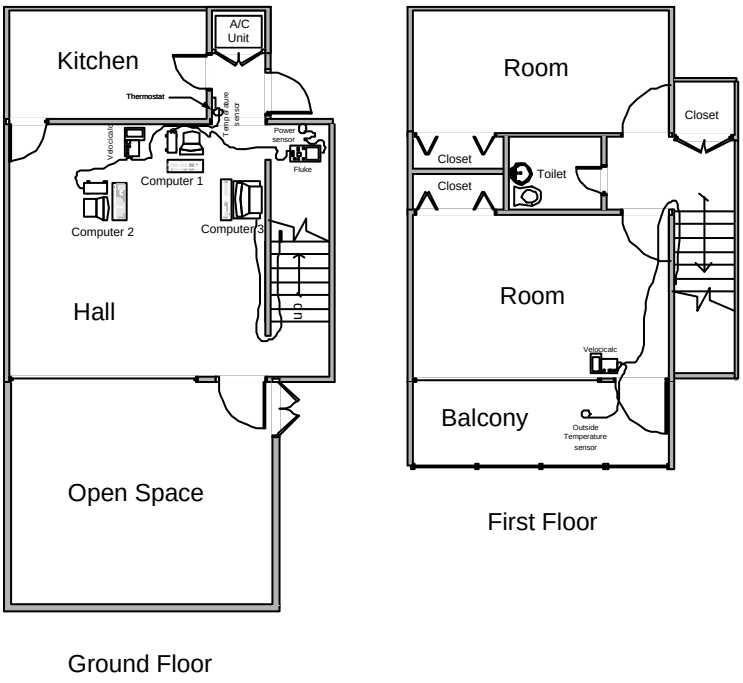

Figure 5.2: Instruments Setup Plan at Residential House, Rabee Courts, KFUPM.

while computers 2 and 3 recorded readings from internal and external VELOCICALC instruments respectively.

5.1.2 Data Collection

The VELOCICALC Plus was used to collect data related to temperature, humidity, air-velocity and air-pressure. It was hooked to the computer through a RS232 serial port. Commands are sent to VELOCICALC Plus through a software interface and the instrument responds by sending a data sequence. The software interface used are Labview and Matlab. The different readings that are provided by VELOCICALC

Plus are air-velocity in m/sec, volumetric flow rates in m^3/hr, pressure in Pa, temperature in ^oC, relative humidity in %, dew point temperature in ^oC and wet-bulb temperature in ^oC. Two readings, the temperature and the humidity, are the most important for our experimental study. A Genuine Pentium with 128Mb RAM running Windows 98 and Labview program was used to collect the outside data at a two second interval (Figure 5.3). The probe instrument used to measure the

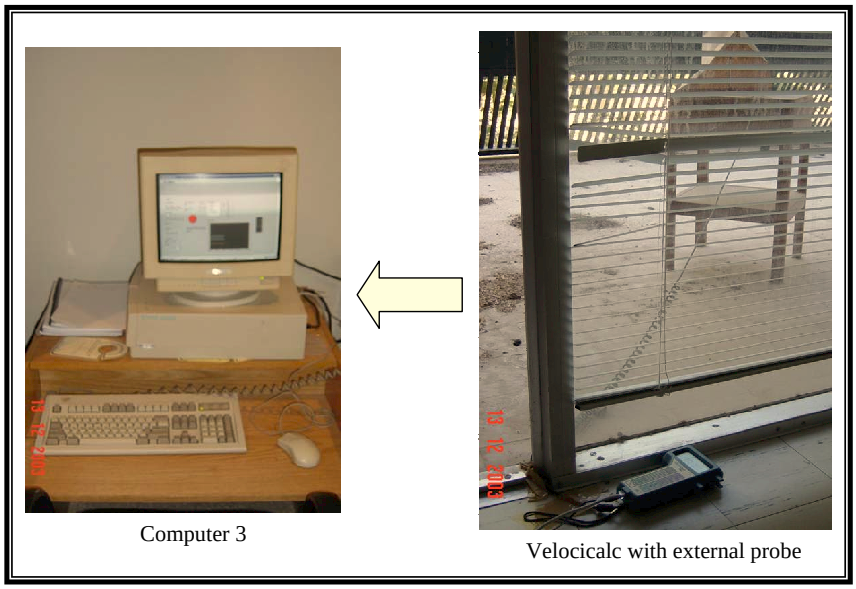

Figure 5.3: Setup of Computer 3 for External Parameters Acquisition.

external atmospheric parameters was kept at a 3 feet height without exposing the it directly to sunlight.

Another VELOCICALC Plus, used to measure the internal house temperature and humidity was hooked to a Pentium IV 2.4 GHz, 504Mb RAM computer(Figure 5.4. A Matlab program was developed to collect and store the data in an Excel

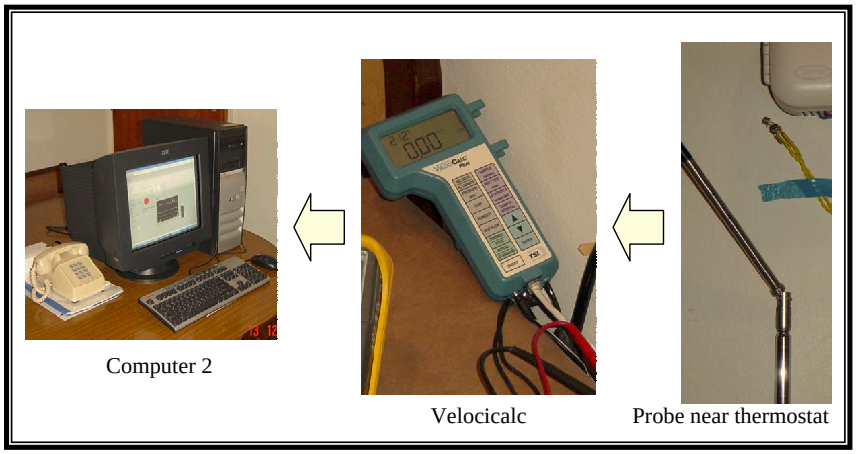

Figure 5.4: Setup of Computer 2 for Internal Parameters Acquisition.

sheet format. The probe of the instrument used to measure the inside temperature was kept very close to the thermostat, so as to ensure that data collected shows the temperature as seen and perceived by the thermostat. The sampling of this instrument was done at around 5 seconds while the average reading time for the instrument through the program was 2 to 3 seconds.

The FLUKE 43-power quality analyzer was used to collect data from the power line like voltage, current, power frequency, its related harmonics, etc. The data was collected through the RS232 serial port of the computer. A Matlab routine is used to acquire data through three different screens displays of the FLUKE 43 through a serial port. The different parameters that are read from analyzer are as follows. From the first screen of Volts/Amps/Hertz mode, the RMS voltage, RMS current in amps, Line Frequency on trigger channel, Crest factor on channel 1 and Crest factor on channel 2 are measured. From the second screen, i.e. the

power mode; the real power, the apparent power, reactance power, total power factor (TPF), displacement power factor (DPF) and line frequency are read. Finally from the last screen of the harmonics mode, the total harmonic distortion (THD), total RMS reading, K-factor, frequency of selected harmonic component, absolute RMS of selected harmonic component, relative RMS and phase of selected harmonic component are read. The sampling was done to suit the analyzer's data transmission capacity which was taking an average of 28-29 seconds to move through three screens collecting 18 parameters through the serial port. Taking into account this required time for data transmission, it was sampled at 30 seconds.

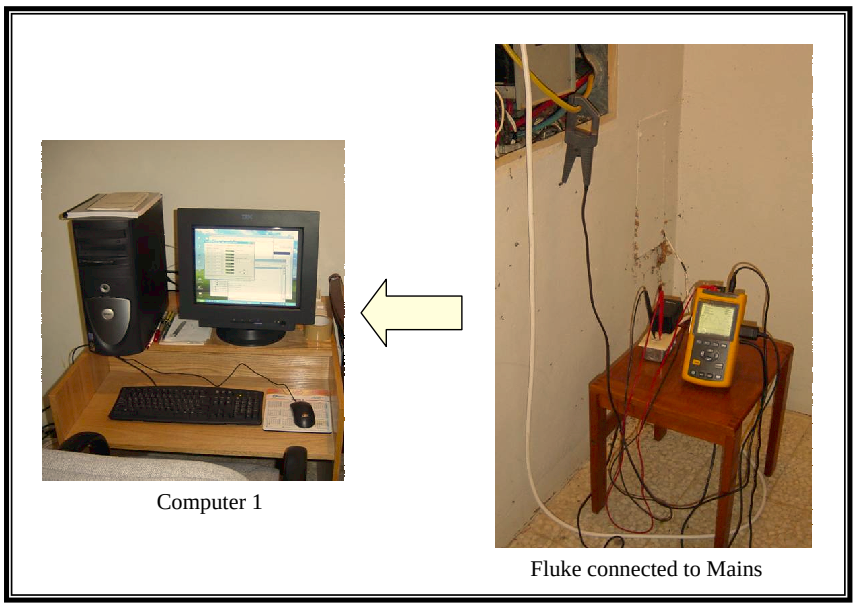

Figure 5.5: Setup of Computer 1 for Power Measurements.

The FLUKE 43 measures directly the load from the main lines (Figure 5.5). Since

only the A/C unit was switched "On" and all the other devices were switched "Off", the measurement from the main lines reflected the power usage by the A/C unit only.

5.1.3 Power Consumption

The typical power consumption pattern for the residential A/C unit for a single day can be seen in Figure 5.6. In Figure 5.7 we can observe the power consumption

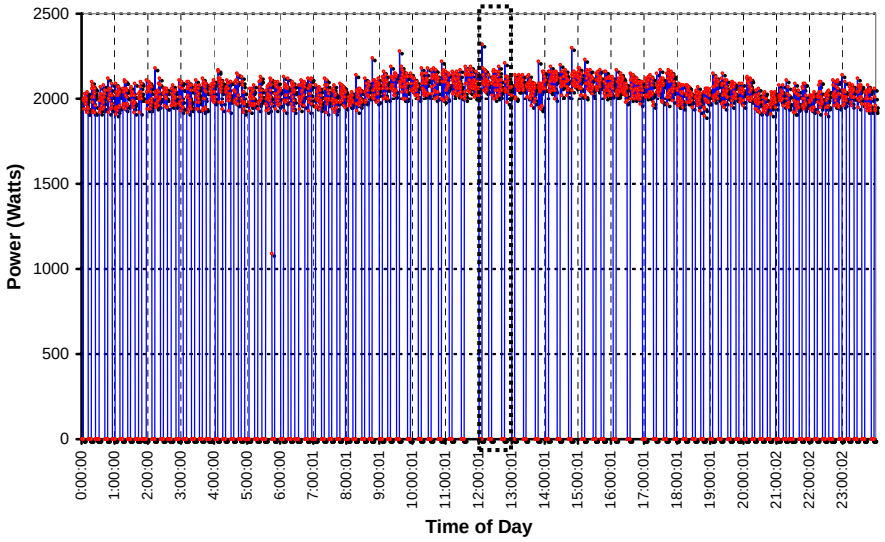

Figure 5.6: Typical Day Power Consumption for a Residential A/C at Dhahran.

pattern for just one hour of that particular day as shown by the dotted rectangle in Figure 5.6. We can see that the power consumption moves from zero to full power capacity of the A/C. As observed in Figure 5.7 there are variations of power consumption when the A/C is in its "On" state.

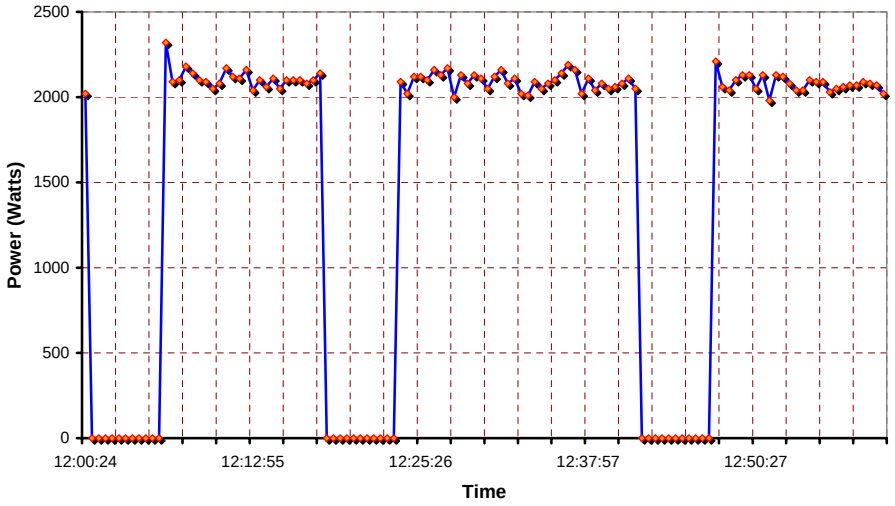

Figure 5.7: Typical Power Consumption for Residential A/C for One Hour.

5.1.4 Climate

The University campus where the readings were taken is located at Dhahran. The summer in Dhahran is marked by very high humidity (upto 95% and above) and very high temperature (average of 44^oC). This usually lasts for four months every year from June to September. The temperature pattern for one day during these months can be seen in the Figure 5.8. Similarly, the humidity pattern for one day at Dhahran is shown in Figure 5.9. The temperature and humidity pattern for two months, i.e. July and August, were collected during the summer of 2003. Data from the months of September and October were used to validate the previous results. The data related to the power consumption of the A/C during these months was also done. The necessary data of "On-Off duration" for the identification scheme to be implemented was then extracted from this data collection.

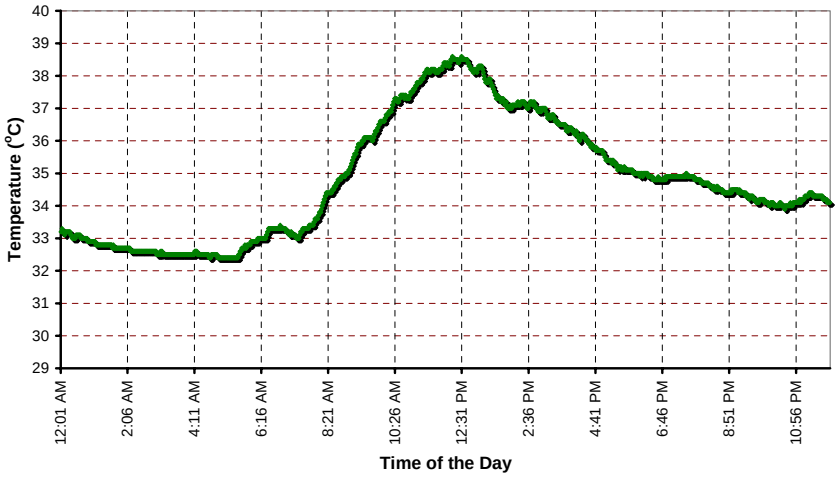

Figure 5.8: Typical Temperature Pattern for a Single Day at Dhahran.

The real power reading from the FLUKE 43 was used to extract the "On" and "Off" durations for the identification scheme.

5.2 Calculation of Actual Heat gain and Thermal Capacity

The calculation of the heat gain and the thermal capacity of the residential house of Rabee Courts, King Fahd University of Petroleum and Minerals was done as discussed in the following section.

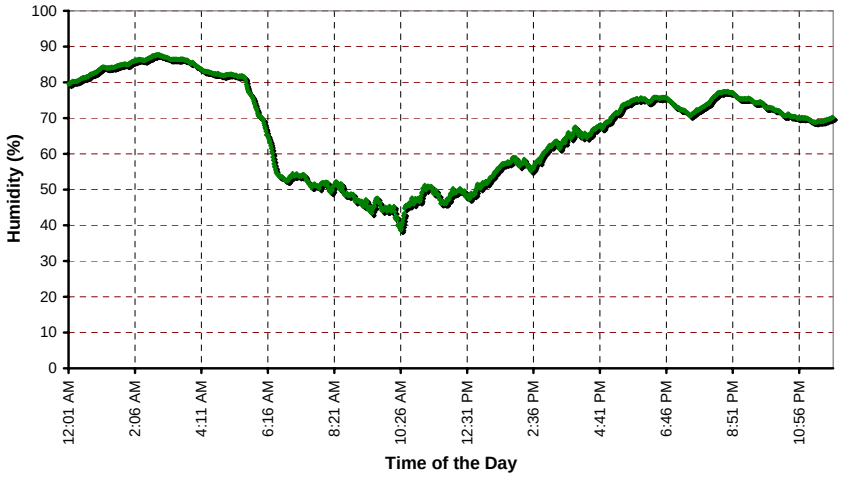

Figure 5.9: Typical Humidity Pattern for a Single Day at Dhahran.

5.2.1 Thermal Capacity

The thermal capacity is defined as the amount of heat energy required by the system to raise its temperature by 1^{o}C. The unit of thermal capacity is J/^{o}C.

To find the thermal capacity of any system, we need to find the mass of the system. In our case the system is a house containing mainly air as its content. So we need to find the mass of air inside the house. Once we know the mass of air present inside the house, we can find the thermal capacity of the system.

To calculate the mass of air inside the house we can calculate the volume of air present and multiply by a factor of 1.2 as

$$1\ m^3 \text{ of air} = 1.2 \text{ Kg}.$$

The plan shown in Figure 5.1 could be used to calculate the volume of air inside the house. The height of the wall for the ground floor is 2.5 m and the height of the

house at first floor is 3 m. The volume of air at ground and first floor is calculated as follows.

$$\text{Volume of air at ground floor} = 8.5 \text{ x } 6 \text{ x } 2.5 = 127.5 \text{ m}^3. \quad (5.2)$$

$$\text{Volume of air at first floor} = 10.5 \text{ x } 6 \text{ x } 3 = 189 \text{ m}^3. \quad (5.3)$$

$$\begin{aligned} \text{Total volume of air inside the house} &= \text{Volume at ground} + \text{Volume at first floor} \\ &= 127.5 + 189 = 316.5 \text{ m}^3. \end{aligned} \quad (5.4)$$

$$\begin{aligned} \therefore \text{ The weight of air inside the house} &= 1.2 \text{ x volume of air} \\ &= 1.2 \text{ x } 316.5 \\ &= 379.8 \text{ Kg} \end{aligned} \quad (5.5)$$

The specific capacity of air is 1.05 x 10^3 J/Kg-K.

Therefore, the thermal capacity of the house is given as

$$\begin{aligned} \text{Thermal Capacity of the house (C)} &= \text{weight of air in the house} \\ &\text{x specific capacity of air} \\ &= 379.8 \text{ x } 1.05 \text{ x } 10^3 \\ &= 398790 \text{ J/K}. \end{aligned} \quad (5.6)$$

5.2.2 Heat capacity of the House

The heat gain inside the house could be due to conduction, convection and radiation. The heat gained by the house is mostly through the walls and the roof. The

residential house has one side totally of glass as shown in the plan of the house (Figure 5.1).

Therefore, we need to calculate the heat gain through each wall and the roof. To find the heat gained through walls we need to find the thermal conductivity of section of the wall and the roof. The section of each wall is given in Figure 5.10.

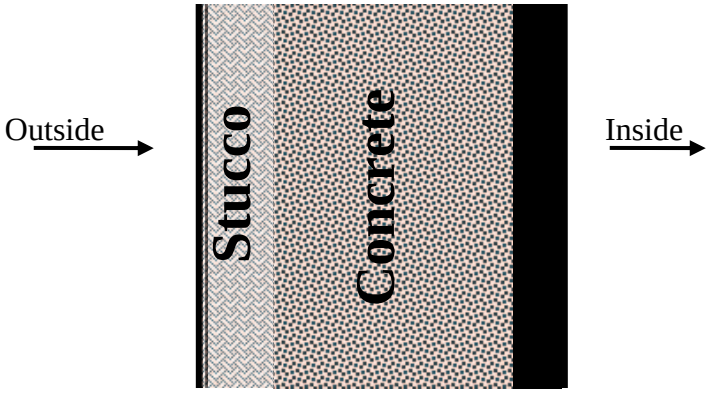

Figure 5.10: Wall section of Residential House, Rabee Courts.

The arrow in the section diagram shows the flow of heat inside the house. To find the 'U' value i.e. the thermal conductivity of the wall we need to find the thermal resistance of each and every section of the wall. The wall comprise of the external resistance, 2.5 cm of stucco, 30 cm of low density concrete, 2 cm of plaster and finally the inside resistance. These resistance values could be obtained from the standard table of thermal properties of common building material which are summarized in the Table 5.1. These values obtained from standard tables are always measured on the 21^{st} of every month at 4 pm. For summer the value is then obtained at 4 pm

Table 5.1: Thermal Resistances Table.

Type of section (material)	Thickness (cm)	Thickness (mm)	Resistance of the section (m3-K/W)
Inside resistance	-	-	0.059
Stucco	2.5	25	0.037
Low density Concrete	30	300	2.200
Plaster	2	20	0.026
Outside resistance	-	-	0.121

on 21^{st} of April. Otherwise the resistances through out the day change according to the ambient temperatures.

$$\begin{aligned} \text{Therefore the total resistance of the wall 'R'} &= 0.059 + 0.037 + 2.200 + 0.026 + 0.121 \\ &= 2.443 \text{ m}^2\text{-K/W} \end{aligned} \tag{5.7}$$

The thermal conductivity is defined as the reciprocal of the thermal resistance.

$$\begin{aligned} \text{Therefore the thermal conductivity 'U'} &= 1/\text{R} \\ &= 1/2.443 \\ &= 0.409 \text{ W/m}^2\text{-K} \end{aligned} \tag{5.8}$$

Now the heat gained per unit temperature through each and every wall on the ground and the first floor could be calculated. First the total area of the wall and the roof are calculated as shown in the Tables 5.2, 5.3 and 5.4. The total area that is involved in terms of heat gained is the sum of area of the entire wall on the ground floor, first floor and the roof.

$$\text{Total area through which heat is gained} = 201.5 \text{ m}^2 \tag{5.9}$$

Table 5.2: Areas of Walls on the Ground Floor.

Face of the wall on ground floor	Dimension of the wall(m)	Area of the wall (m^2)
Southeast	8.5 x 2.5	21.25
Southwest	6 x 2.5	15
Northwest	8.5 x 2.5	21.25

Table 5.3: Areas of Walls on the First Floor.

Face of the wall on first floor	Dimension of the wall (m)	Area of the wall (m^2)
Southeast	10.5 x 3	31.5
Southwest	6 x 3	18
Northwest	10.5 x 3	31.5

Therefore the heat gain through the wall from the ground floor and the first floor and the roof is given as follows

$$\text{Total heat gained through walls and roof} = 201.5\text{m}^2 \text{ x } 0.409\text{W/m}^2\text{-K} \quad (5.10)$$

$$= 82.41 \text{ W/K} \quad (5.11)$$

The heat gained through the glass from the second and first floor is computed as follows:

The glass used in the house is double glazed with the thermal conductivity given as

Table 5.4: Area of the Roof.

Roof	Dimension of the roof (m)	Area of the roof (m^2)
Roof	10.5 x 6	63

Table 5.5: Total Area of Glass Side of the House.

Floor of House	Dimension of the wall(mts)	Area of the wall(m^2)
Ground Floor	6 x 2.5	15
First Floor	6 x 3	18

2.78 W/m^3-K.

$$\begin{aligned} \text{The total heat gained through the glass} &= 2.78 \text{ x } 33 \\ &= 91.71 \text{ W/K} \end{aligned} \tag{5.12}$$

$$\begin{aligned} \text{The heat gained by the house} &= 82.41 + 91.71 \\ &= 174.15 \text{ W/K} \\ &= 174.15 \text{ x } 60 \text{ J/min-K} \\ &= 10449 \text{ J/min-K} \end{aligned} \tag{5.13}$$

5.2.3 Calculation of actual cool drift rate and heat drift rate

To calculate the heat drift rate and cool drift rate associated with the house we need the actual power rating of the Air-Conditioner. We can get this from the FLUKE power analyzer reading. Since the A/C working on 220V consumes around 18 Amps of current as an average, therefore the power rating of the A/C is 3960 Watts. The power rating of the A/C in Joules per minute is 237600 J/min.

According to the model, we calculate 'a' as the ratio of heat gained through the house to the thermal capacity of the house and 'R' as the ratio of power rating of

the A/C to the thermal capacity of the house. Therefore the model parameters 'a' and 'R' are given as follows

$$a = a'/C = 10449/397890 = 0.0262 \tag{5.14}$$

$$R = R'/C = 237600/397890 = 0.5958 \tag{5.15}$$

To calculate the heat drift rate and the cool drift rate we use the equations 3.89 and 3.90. Using the average ambient temperature(X_a) as 34^o and the average temperature inside the house($\bar{X}$) as 21^o we get the following values of cool drift rate and heat drift rate.

$$c = R - a * (X_a - \bar{X}) = 0.5958 - 0.0262 * (34 - 21) = 0.2551 \tag{5.16}$$

$$r = a * (X_a - \bar{X}) = 0.0262 * (34 - 21) = 0.3406 \tag{5.17}$$

These values of cool drift rate and heat drift rate vary with ambient temperatures. The above calculations were made taking the average ambient temperature for 21^{st} August. The actual values vary depending on the average ambient temperature for that particular day if the thermostat temperature is always kept constant.

5.3 Online Identification and Control at the Physical System

For the purpose of online identification of the parameters of the system as well as providing the utility the monitoring and control of each and every air-conditioners in

the homogenous group, a simple prototype electronic circuit was developed. The aim was to design a self running circuit which uses the power provided to the thermostat along with a data acquisition card. The circuit should also measure vital data like the temperature, state of the air-conditioner and transmit it to the data acquisition card. It would also translate signals from the data acquisition card for means of controlling the on-off cycle of the air-conditioner.

The thermostat

The thermostat in general has the following terminal configuration.

R - The 24VAC power supply to be given to this wire connection

Y1 - The output of the thermostat to the air-conditioner

Y2 - The output of the thermostat to the second stage of the air-conditioner

C - Common connection to 24V ac supply

W1 - The output of the thermostat to switch on the heater

W2 - The output of the thermostat to switch on the second stage of the heater

G - Output of the thermostat to switch the fan on/off.

The thermostat switches on the power supply of the air-conditioner for cooling and heating at the terminals 'Y1' and 'W1' respectively. The terminals 'R' and 'C' are the power connections that are given a 24VAC supply from a transformer at the Air-Conditioner. The terminal 'G' is to switch the fan 'on' and 'off'.

Circuit for a single A/C

The circuit that was developed is shown in Figure 5.11. It had to measure temperature, state of the A/C and control its 'On' Cycles using a data Acquisition Card.

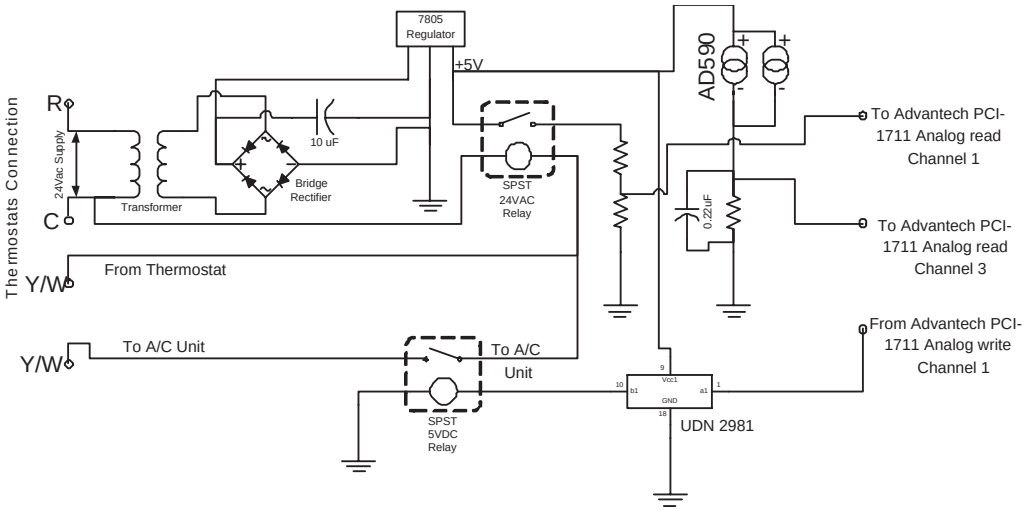

Figure 5.11: Circuit Diagram of Circuit connected to Single A/C.

Components used:

1. PC1711 Advantech Data-Acquisition Card
2. An isolating transformer(1:1 or 1:2)
3. Bridge rectifier BC125
4. Regulator IC 7810
5. AC Relay (24Vac SPST)

6. AD590 temperature transducer IC
7. 5VDC Relay (SPST)
8. UDN 2981 Driver Chip
9. Capacitors
10. Resistors

Description : The aim here is to use the power supply of the thermostat itself to provide power to the circuit. The thermostat has a power supply of 24VAC given to its 'R' and 'C' terminals. Using the same power supply from the terminals, it is connected to a transformer which isolates the thermostat's current with the circuit and also provides the power source to drive the circuit. The output of the transformer is then connected to the bridge rectifier which gives a rectified DC supply. The DC supply is then regulated to +5V by means of voltage regulator IC 7810. The thermostat gives an output of 24VAC at its terminal 'Y1' when the A/C is to be switched on and the same output at its terminal 'W1' when the heater is to switched on but not both at the same time. If one terminal is closed to complete the circuit, the other terminal remains open. These terminals of the thermostat are connected to the coil of the relay of 24VAC SPST, so that coil gets energized when either of the terminals is powered. The relay closes the regulator switch so that this +5V can pass through and could be measured by a voltage signal across the resistor

at the Advantech PC1711 analog channel-1 as shown in Figure 5.11.

Another circuit is the one which measures the temperature. For this purpose, the integrated circuit temperature transducer AD590 is used. AD590 is a two-terminal integrated circuit temperature transducer that produces an output current proportional to absolute temperature. For supply voltages between +4V and +30V the device acts as a high impedance, constant current regulator passing 1 μA/K. Laser trimming of the chip's thin-film resistors is used to calibrate the device to 298.2 μA output at 298.2K (+25^{o}C). A simple circuit would comprise of AD590 connected in series with the resistor. Since AD590 produces a current proportional to the absolute temperature there is a corresponding voltage drop across the resistor. This voltage is measured by the analog channel-2 of the PCI1711 Advantech card as shown in the circuit diagram.

Finally, we require that the circuit could switch off the A/C based on the control decisions taken at the utility end. For this purpose, the 'Y1' terminal that goes back from the thermostat to the A/C unit was intercepted with a relay which is connected to a pin which is always in the closed position. This relay required a driver circuit for which the 9-pin UDN 2981 driver chip was used. Signals from the analog output of the Advantech Card channel '0' could be then converted to control actions on the A/C. This did not affect the measurement for 'On' cycles of A/C as the thermostat still provided the signal of 24VAC but that was routed through this circuit which drives the relay connected to it.

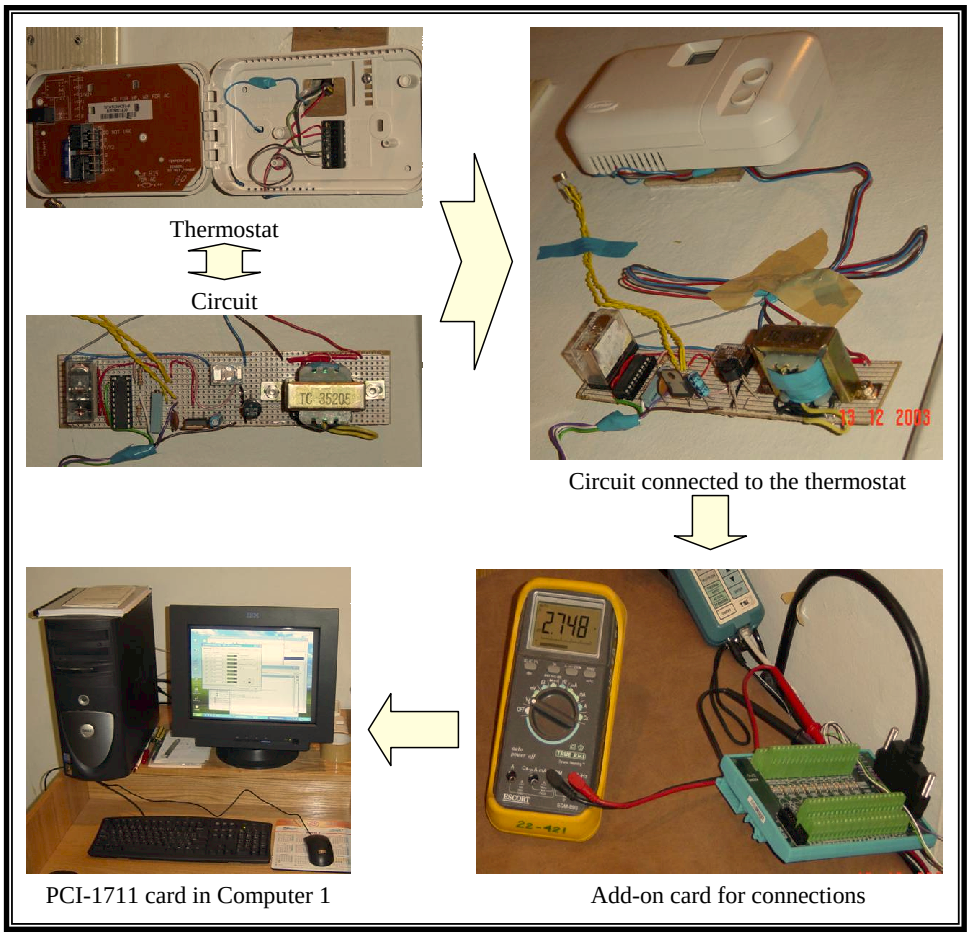

Figure 5.12: Connections for Single A/C for Online Scheme.

The whole circuit was tested on actual A/C system shown in the Figure 5.12.

5.4 Summary

In this chapter we discussed the data acquisition carried out for the identification and control. The instrumental setup was discussed, along with weather characteristics of the location. The calculation of actual parameters for the house was done. Finally

the circuit developed for the online scheme was presented. Results for data acquired are presented in next chapter along with some sensitivity analysis with respect to environmental parameters.

Chapter 6

VARIATIONS DUE TO ENVIRONMENTAL PARAMETERS

6.1 Results for Identification

The implementation of the identification scheme using the instrument setup and circuit developed was carried out. Using the computational scheme described in Chapter 3, the results obtained from a real Air-Conditioner's will be presented in this chapter.

6.2 Identification Results for the A/C

Data collected over a duration of three days, i.e. from 3rd August to 5th August 2003, was used to implement the identification scheme. The result could be seen in Figure 6.1.

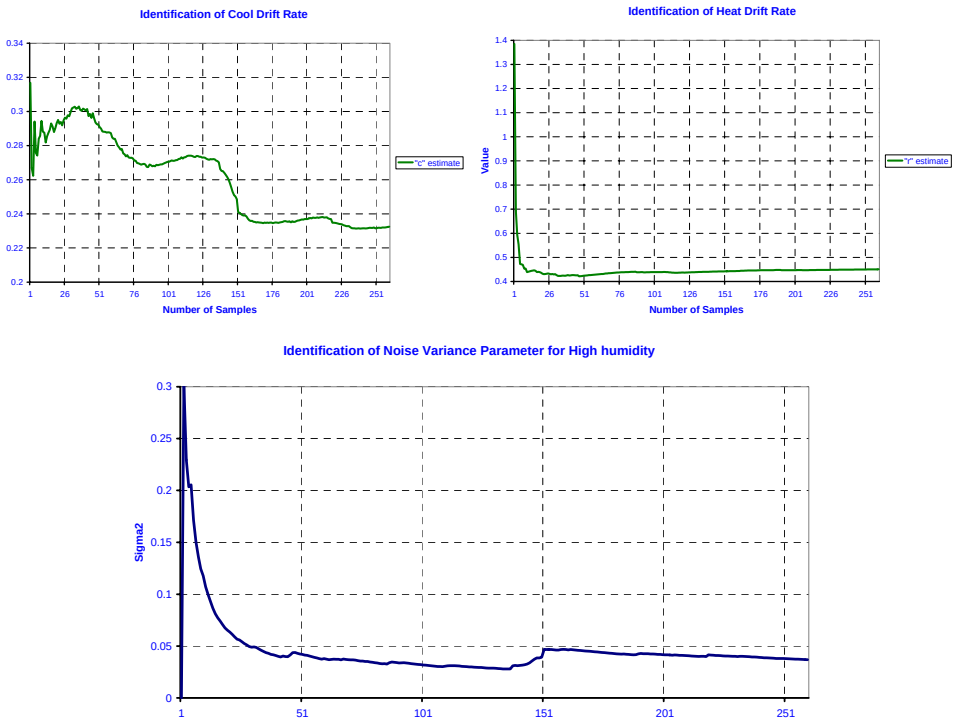

Figure 6.1: Identification of Parameters r, c and σ.

It can be seen that the identification for different parameters reaches a steady-state value at different samples. The cool drift rate "c" does not settle down until 150 samples of "On" times, while the heat drift rate has reached a steady-state pattern within 20 samples of "Off" time duration. Similarly the noise variance parameter "σ^2" also requires 75 samples of data points to converge to a one percent of its value.

There is a slight increase in steady-state pattern of the identification seen in noise parameter identification. This effect could also be seen in the identification pattern of cool drift rate i.e. "c" around the 150th sample. One explanation of this is the shift of average "On" duration. This could be explained in more detail if we look at Figure 6.2 which shows the average temperature of house.

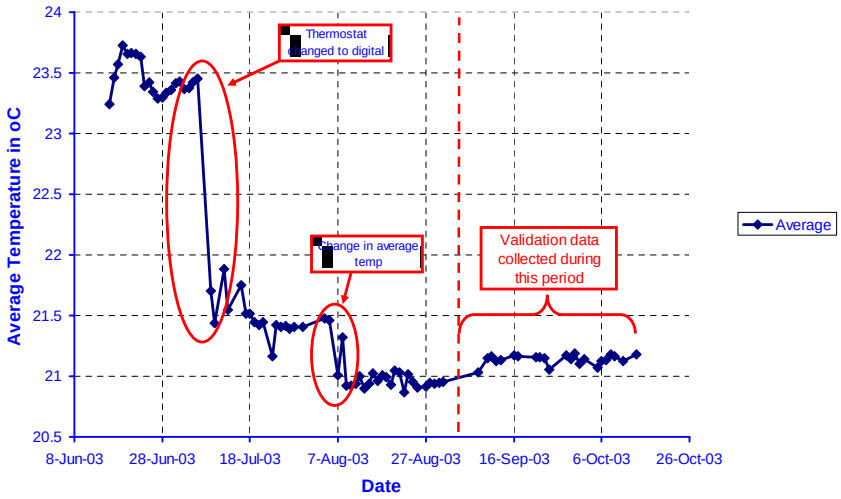

Figure 6.2: Average Temperature of the House.

We can observe from the average temperature reading of the house for five months that the average temperature of house shifts from 23.5^oC to 21.5^oC from 5th July 2003. This could be attributed to the change in the thermostat carried out during that day. The old thermostat was removed and a new digital thermostat installed in its place. The deadband was also calculated and the new deadband for this installed thermostat was 2.54^oC when compared to 2^oC for the old mercury type. Another important change could also be seen in the average temperature. This change is due

to changes in the thermostat minimum temperature setting. A change was done on 7th August in the minimum comfort temperature of the house. This change is the one which is reflected in Figures 6.3, 6.4 and 6.5.

In Figure 6.3 we could observe the cool drift rate changes due to the installation of new thermostat in the house on 9th July. At this point, the identification scheme was reset to accommodate the change in the thermostat with new dead-band i.e. delta (Δ). Further, we see that the identification scheme had settled down to its steady-state but when the thermostat minimum comfort temperature was changed on 7^{th} August, it reflected in the identification's steady-state value. This change in the identification was due to the shift in the average "On" duration of the A/C. Since the comfort temperature was decreased, the average "On" periods were increased and the value of the cool drift rate which is inversely proportional to the "On" period decreased.

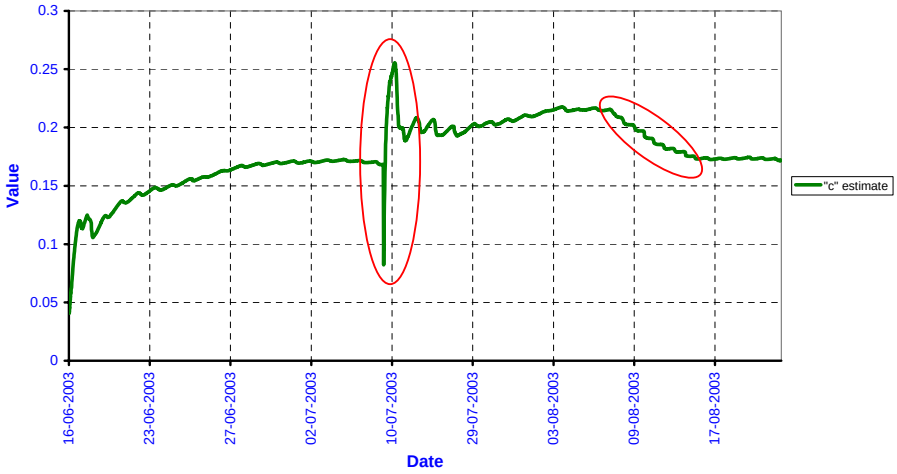

Figure 6.3: Identification of the Cool Drift Rate.

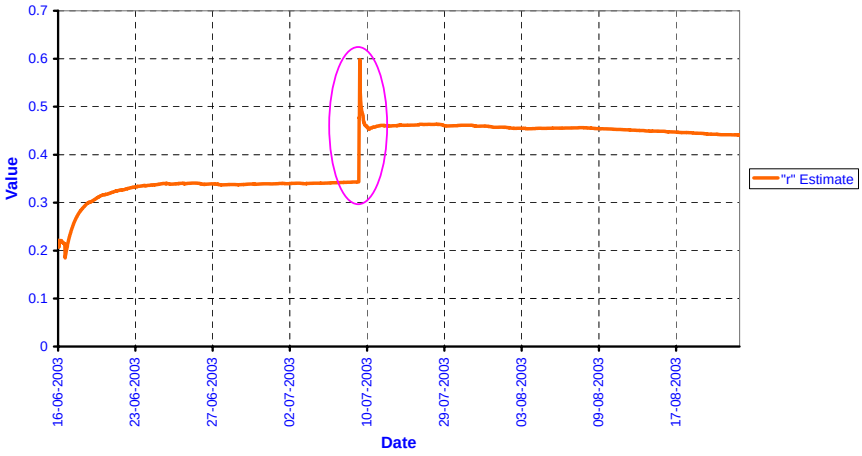

Figure 6.4: Identification of the Heat Drift Rate.

In Figure 6.4, where the heat drift rate is identified, there is no change seen except for a change which occurred during the changing of the thermostat. This could be explained as follows. The heat drift rate depends on the "Off" period of the A/C unit. And since this duration is just a factor of external heat pumped into the house we observe no shift in average "Off" duration. The average value of the heat rate is changed due to a change (increase) in delta (Δ) because of the new thermostat installed.

In Figure 6.5, where the noise parameter in the house was identified we observe that the change in the thermostat is seen as a reset on 9^{th} July. Also one can observe that the average value identified for the noise variance also increases after the reset. The small circle at the end of the identification curve indicates that the increase in average "On" period had an effect in increasing the value of noise parameter identified. This change occurs from August 7^{th} where the minimum

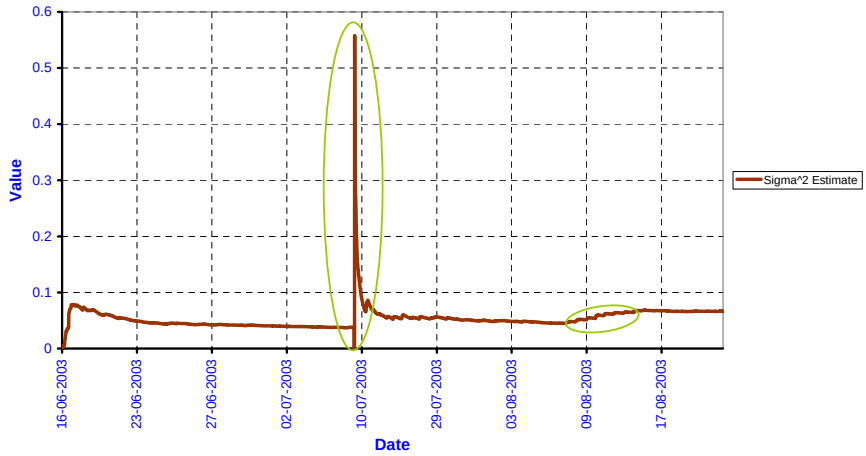

Figure 6.5: Identification of the Noise Variance Parameter σ^2.

comfort temperature was changed to lower setting.

6.3 Effect of Humidity

To study the effect of humidity on identification scheme, two sets of data were prepared. The first set of data corresponds to the extraction of "On-Off" durations for the days where the humidity was less and the second set which included days having similar patterns of high humidity.

For the first set to be implemented, days from the month of August with low humidity pattern were selected. The typical temperature and humidity pattern for those days is depicted by the Figure 6.6. As we can notice from Figure 6.6, the temperature is high but the humidity is less than 40%. The selected days from August had very similar weather patterns and the identification scheme was implemented on

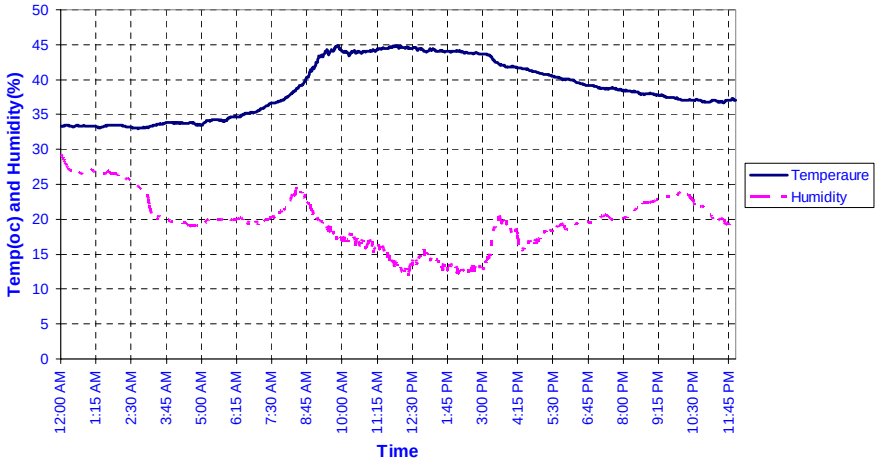

Figure 6.6: Low Humidity Pattern for 17^{th} July.

the samples of "On" and "Off" time duration. The days that were included in the identification scheme are 27^{th}, 28^{th}, 29^{th}, 30^{th}, 31^{th} August and 2^{nd} & 3^{rd} September. Similarly days with high humidity patterns during August were selected to include into the identification scheme. The typical humidity patterns for high humidity days could be seen in Figure 6.7. As seen from Figure 6.7, the temperature profile is the

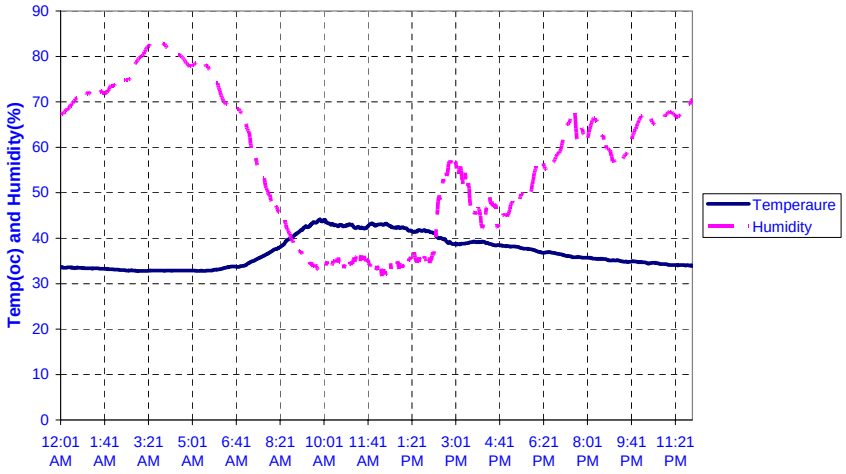

Figure 6.7: High Humidity Pattern for 17^{th} July.

same with the humidity almost above 40%. Days with similar humidity pattern were selected and the identification was applied using "On" and "Off" durations. The days selected for the high humidity were $7^{th}, 8^{th}, 9^{th}, 17^{th}, 18^{th}$ and 21^{st} August.

6.3.1 Comparison for Low and High Humidity

The identification was compared for low humidity and high humidity and the results could be seen in the following figures. From Figure 6.8, we can observe that the cool

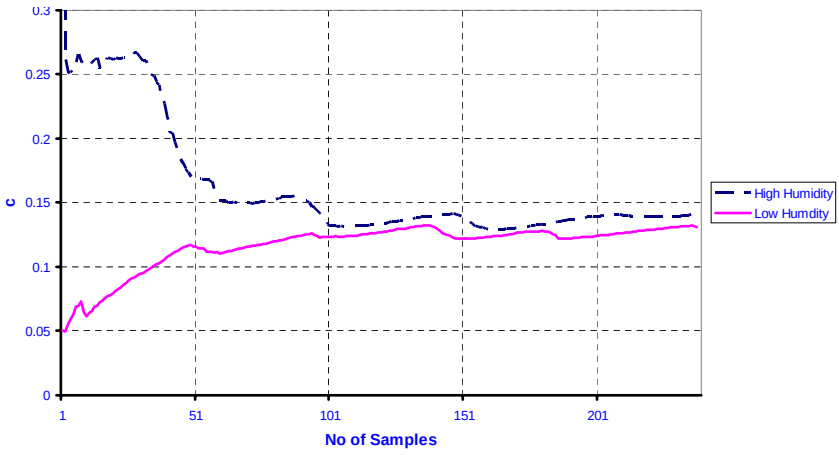

Figure 6.8: Identification of 'c' for Low and High Humidity.

drift rate for high humidity is high when compared to the identified cool drift rate of the low humidity. Similarly the heat drift rate for low humidity as seen in Figure 6.9 reaches a steady-state value higher than that of high humidity. This could mean that during the low humidity days, the "On" duration is lengthier and during the high humidity days the "On" durations are smaller. As for the heat drift rate, it is quite opposite. This could be explained as follows, during the low humidity days the

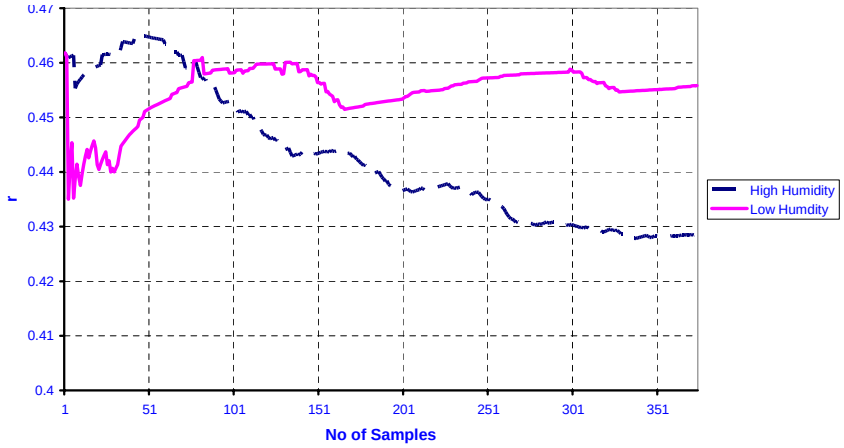

Figure 6.9: Identification of 'r' for Low and High Humidity.

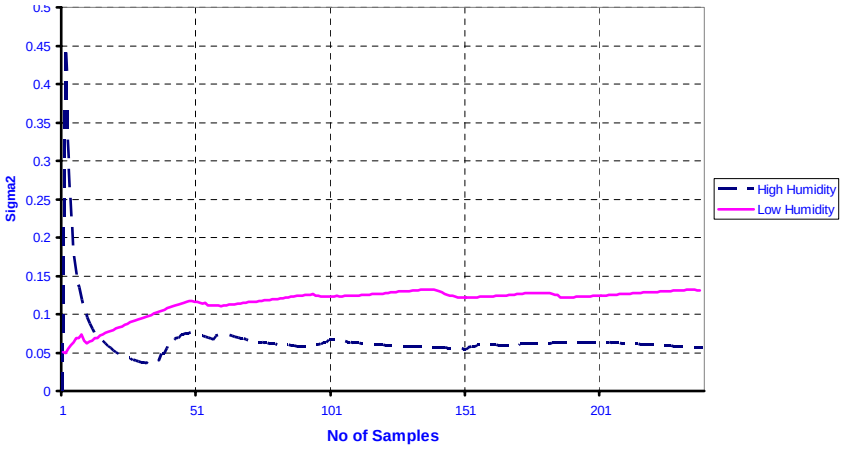

Figure 6.10: Identification of 'σ^2' for Low and High Humidity.

heat that is pumped into the house is more and hence longer "On" durations and lesser "Off" durations, whereas during the high humidity days the heat infiltration into the house is less and mostly absorbed by the ambient humidity around the house. The result for the identification of noise variance parameter σ^2 as seen in Figure 6.10. The steady-state value for noise variance parameter σ^2 is more for low humidity and less for high humidity.

6.3.2 Validation

To validate the above results data from the months of September and October was also analyzed. The days selected for low humidity are 6^{th}, 7^{th}, 18^{th}, 19^{th}, 20^{th} and 24^{th} September where the humidity was less than 40%. And the days that were selected for the high humidity patterns are 14^{th} and 15^{th} September, 4^{th}, 10^{th} and 14^{th} October where humidity is more than 40%.

The results for the cool drift rate, heat drift rate and the noise variance parameter are given below. These results verify the results obtained from previous data as seen in Figures 6.11, 6.12 and 6.13.

When we compare the results for cool drift rate in Figure 6.11 with the results in Figure 6.8, we observe that the results pattern is the same i.e. for low humidity, the identified parameter is low while for the high humidity it is high. But the value to which it converges is different i.e. in previous results the value converges at 0.15 (Figure 6.8) where as for the present result the convergence is around 0.24 (Figure

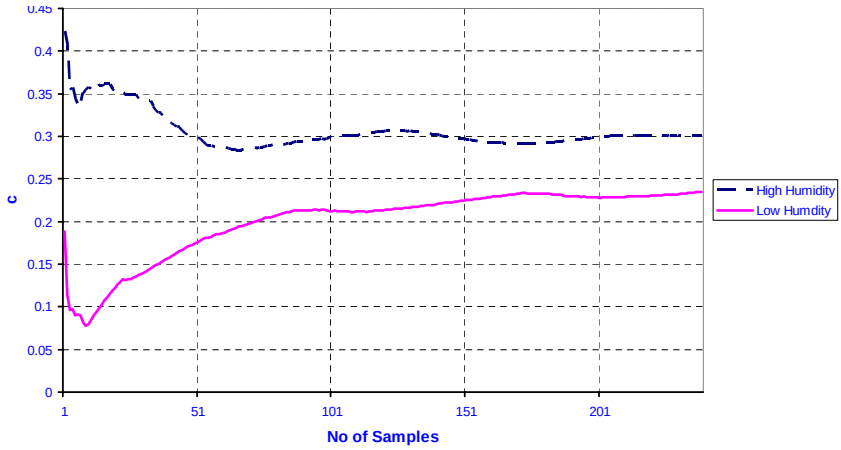

Figure 6.11: Identification of 'c' for Low and High Humidity (Validation).

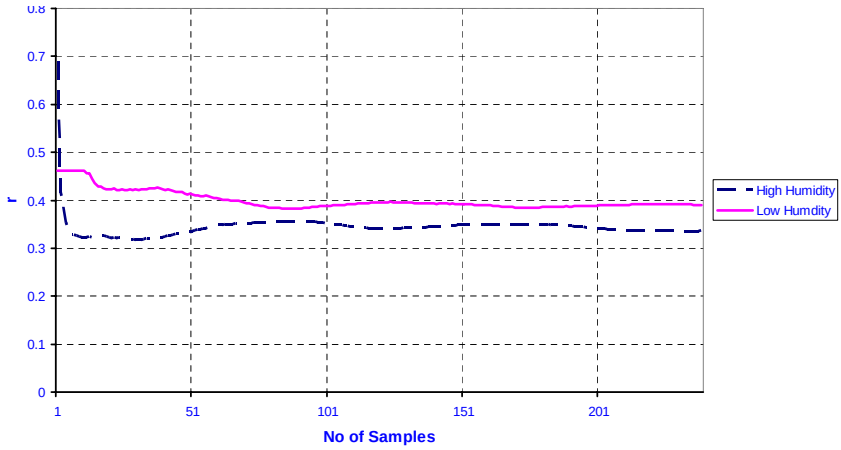

Figure 6.12: Identification of 'r' for Low and High Humidity (Validation).

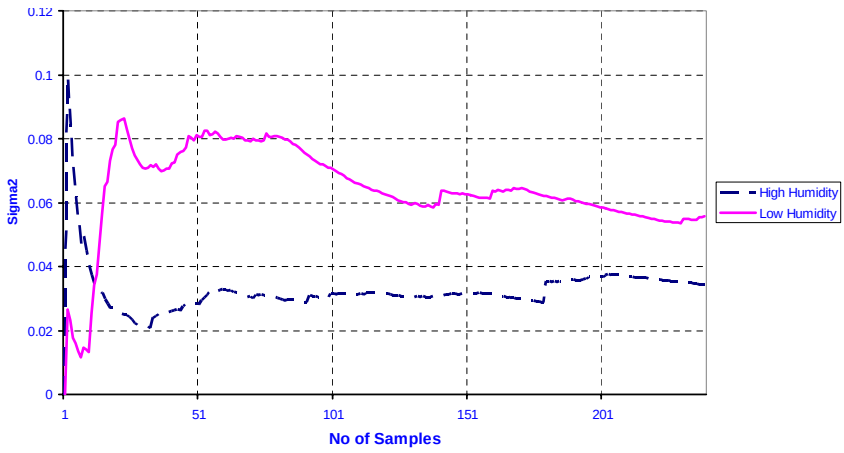

Figure 6.13: Identification of 'σ^2' for Low and High Humidity (Validation).

6.11). Similarly we can observe the same trend in the result of heat drift rate 'r' i.e. for low humidity it is high and for high humidity it is low. The convergence values for these are different when compared to previous results in Figure 6.9. A similar occurrence could also be seen in the noise variance parameter.

6.3.3 Explanation for Drift in Convergence

This deviation in the convergence in the results for validation and previous result could be explained if the average temperatures during the days of August and during the days of September and October are compared.

As seen in Figure 6.14 and Figure 6.15 the average temperature during the month of August is higher when compared to the average temperature in September and October. This could explain the difference in the estimated values of 'c', 'r' and σ^2. Since during the months of September and October the average temperature was

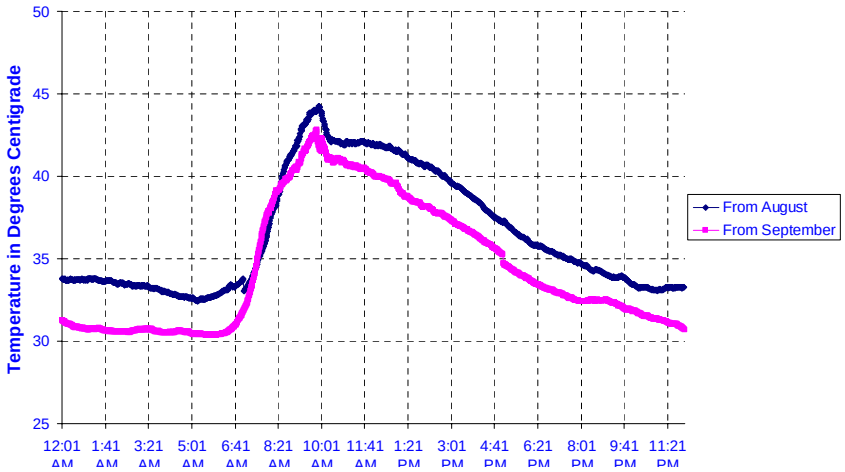

Figure 6.14: Comparison of Temperatures for Low Humidity Days.

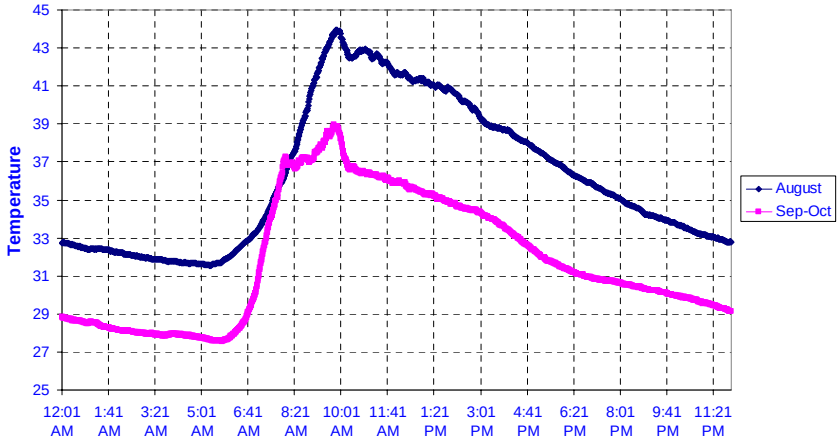

Figure 6.15: Comparison of Temperatures for High Humidity Days.

low, it means the average 'On' duration would change. During August, the average 'On' period was 17 minutes while during the months of September and October it was almost half of 8 minutes. As a result the estimation of parameters in the month of September and October are different with 'c' being slightly higher, 'r' converging to smaller values and σ^2 estimation settling to still lower values. The variations in σ^2 could also be attributed to the noise added due to solar radiation, since during the month of August, solar radiation is at its peak, while during the month of September the solar radiation falls to a comparatively low level which results in convergence to still lower values.

6.4 Effect of Solar Radiation

The effect of solar radiation on the identification pattern was also analyzed and the result for its effect on the identification was done for both low humidity and high humidity.

For low humidity, the results were obtained for night and day. The night time was selected to be between 7:00 pm to 4:00 am in the morning and rest of time was considered as day time. The days that were selected to obtain the result are same as those selected for low humidity days.

6.4.1 Comparison for Low Humidity

The identification of r, c and σ^2 patterns compared for night and day data are as follows. From Figure 6.16, we notice that the cool drift rate for night is high and

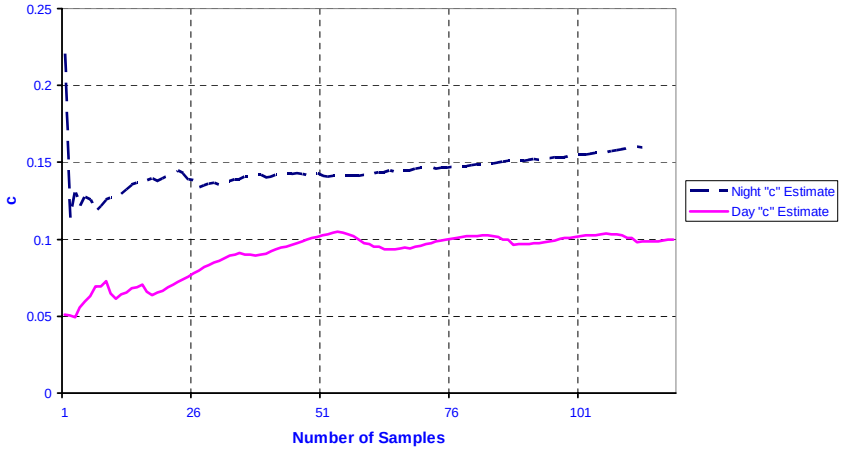

Figure 6.16: Identification of 'c' for Night and Day for Low Humidity.

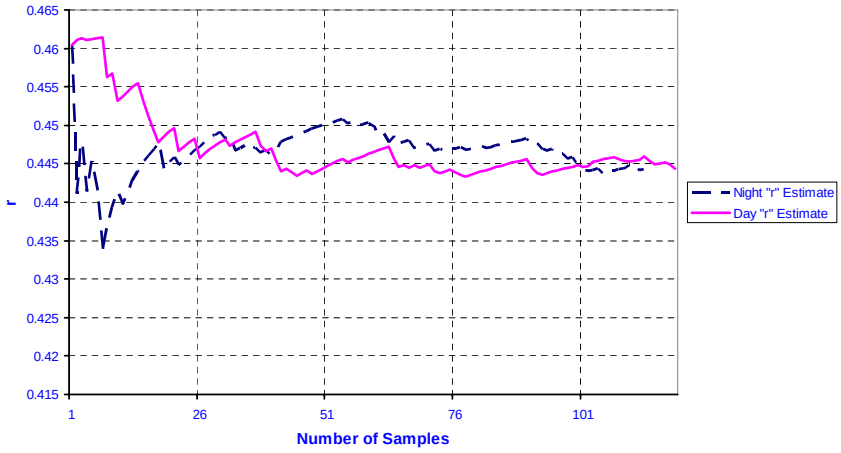

Figure 6.17: Identification of 'r' for Night and Day for Low Humidity.

that for the day is low. This could be due to the increased "On" durations during the day as more heat is swept into the house when compared to the night. This

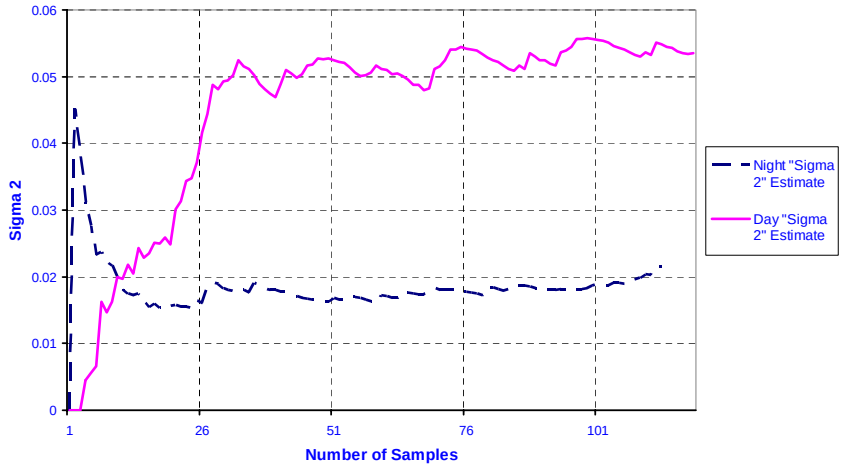

Figure 6.18: Identification of 'σ^2' for Night and Day for Low Humidity.

makes the A/C unit to cool for longer durations in the day than during the night. Thus, this effect is seen in the identification of cool drift rate "c".

In Figure 6.17, the effect on identification scheme is just due to external atmosphere. During the day, more heat is gained by the house, it results in higher value of the identified heat drift rate because of reduced "Off" duration. Where as during the night less heat gained i.e. more time spend by the A/C in "Off" state, decreases the value of the identified heat drift rate. As for noise variance parameter σ^2 associated with the house, we see in Figure 6.18 that the day estimation is very high and low for the night. This big difference in the values could only be explained if we consider the noise as solar radiation. Since during the day more fluctuations are introduced as solar radiation coming inside the house, we see a high jump in the value of noise variance.

6.4.2 Validation for Low Humidity

The results from the previous section are further supported by the results in Figures 6.19, 6.20 and 6.21. These figures were obtained from validation carried out from the data collected during the month of September.

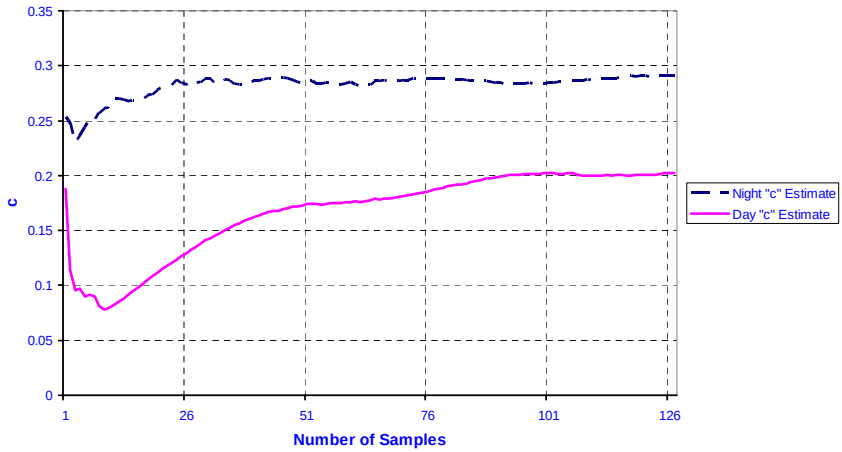

Figure 6.19: Identification of 'c' for Night and Day for Low Humidity (Validation).

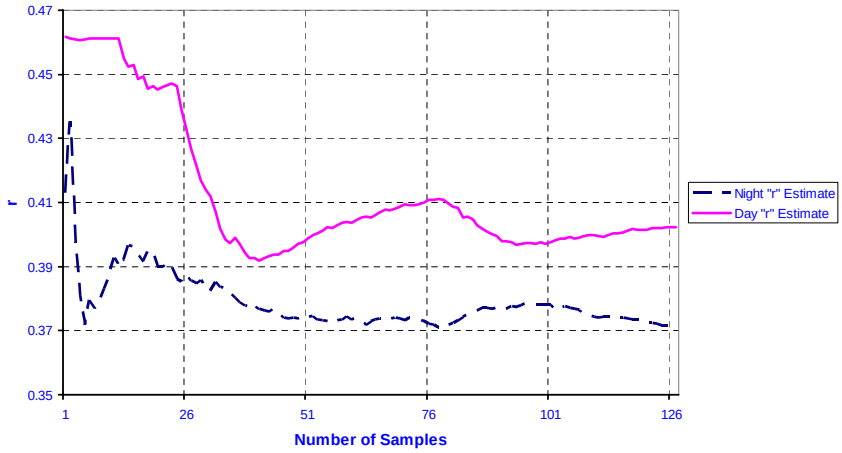

Figure 6.20: Identification of 'r' for Night and Day for Low Humidity (Validation).

We can observe the similar pattern for cool drift rate 'c' where the converged value

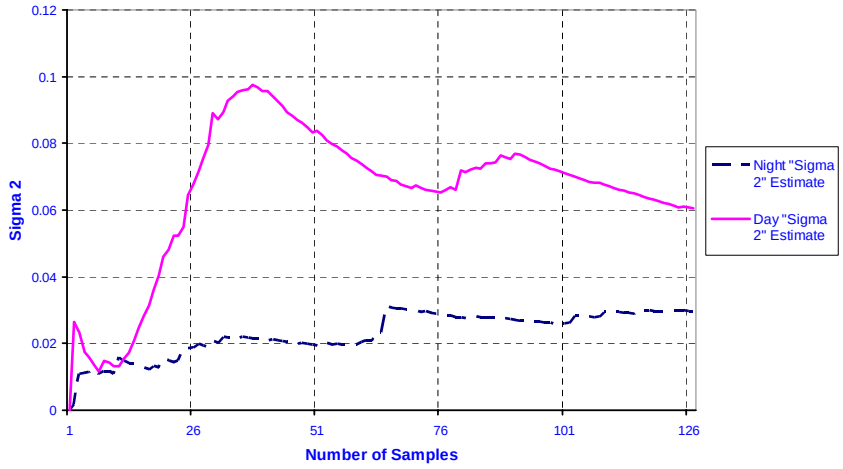

Figure 6.21: Identification of 'σ^2' for Night and Day for Low Humidity (Validation).

for day is less than that of night. But the converged values are different i.e. 0.2 for day and 0.3 for night whereas for previous results we had 0.1 for day and 0.15 for the night. The trends for the heat drift rate 'r' i.e. higher converged value for day and lower value of convergence during the night and noise variance parameter σ^2. This was high for day and low value for night. This could be seen in Figures 6.20 and 6.21. But the values to which the parameters i.e. 'c' and 'σ^2' converge are different. This discrepancy in results for convergence during validation could be attributed to difference in average temperatures during the months of collected data for validation and previous months. This has already been explained in section 6.3.3 with reference to Figures 6.14 and 6.15.

6.4.3 Comparison for High Humidity

The estimation of parameters was also done for the high humidity days. The days that were selected for night data included those used for high humidity days with 12^{th} and 15^{th} August added. This was done to increase the required number of sample data points to the same value as used for the day. The identification patterns for 'r', 'c' and σ^2 could be seen in the following Figures 6.22, 6.23 and 6.24.

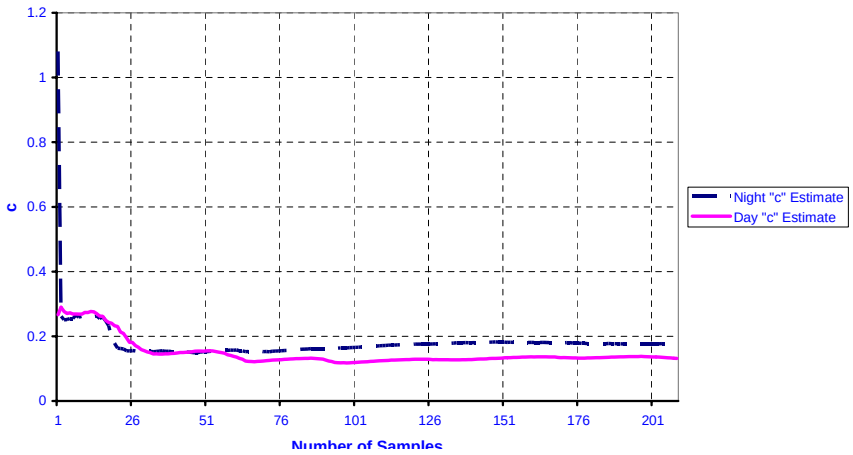

Figure 6.22: Identification of 'c' for Night and Day for High Humidity.

In Figure 6.22, the cool drift rate shows a similar pattern as seen for low humidity. The steady-state value for the cool drift rate is lower for day and high for the night, which means that the average "On" duration during the day is longer when compared to the night.

In Figure 6.23, the heat drift rate shows similar pattern when compared to the pattern shown during the low humidity days. That is the "Off" duration during the night is longer when compared to the day. This means that during high humidity

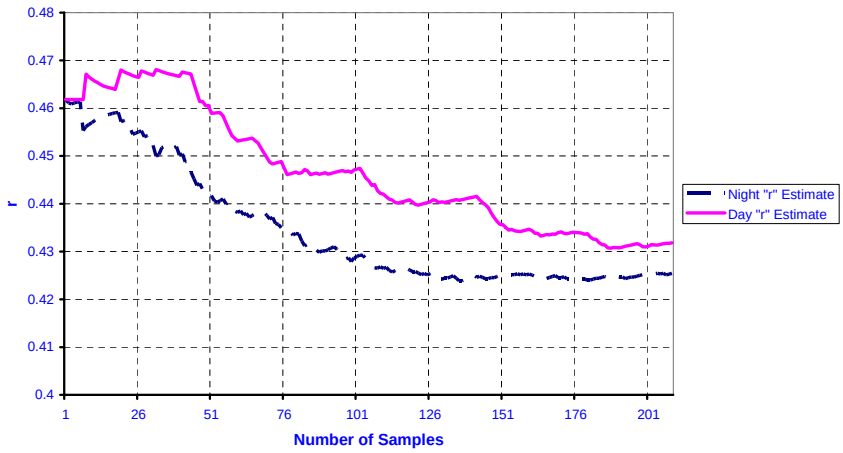

Figure 6.23: Identification of 'r' for Night and Day for High Hhumidity.

days, more heat is gained by the house during the day and so small average value of "Off" durations, while its opposite for the night. As such the identified steady-state value for high humidity days for the day is higher as observed.

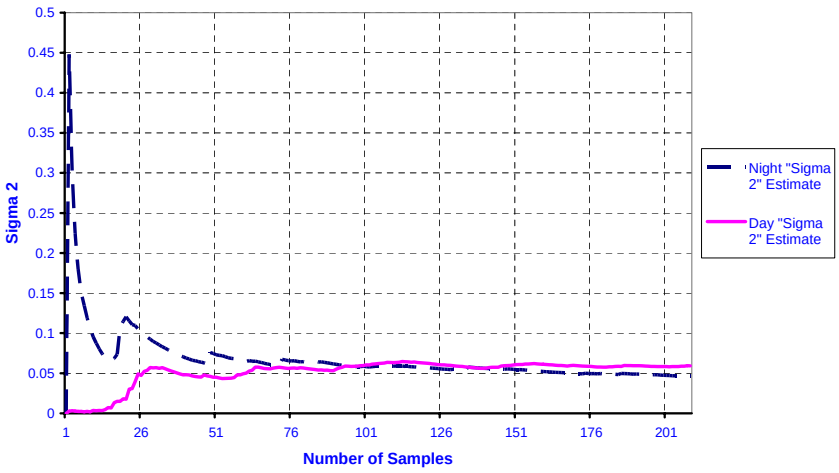

Figure 6.24: Identification of 'σ^2' for Night and Day for High Humidity.

In Figure 6.24, the identification pattern for the noise variance parameter for high humidity is shown. The behavior for the steady-state dynamics of this parameter is

different as that of low humidity days. It has low value for the night and high value for the day. But there is a marked difference in the convergence for day and night when compared to low humidity days. The night and day steady-state variances are almost the same when compared to that of low humidity days. This means that during the day, high humidity acts as buffer and prevents the thermal shocks that could be introduced inside the house as noise. As for low humidity, the solar radiation has a prominent effect as noise.

6.4.4 Validation for High Humidity

The results discussed in the previous section are verified and further supported by Figures 6.25, 6.26 and 6.27. These figures are the results obtained from the validation carried out on the data collected during the months of September and October. The days for which the data was collected are 14^{th} and 15^{th} September and 9^{th}, 10^{th} and 14^{th} October.

The results shown in Figure 6.25 for cool drift rate 'c' show the similar trend as shown for previous result i.e. the day convergence is lower than that of night. But the convergence for 'c' is around 0.3 where as for the previous result it was around 0.2. The results for heat drift rate 'r' shows that same trend that steady-state convergence during day is high and low for night. The noted difference in noise variance parameter that during night and day the convergence is almost the same. This con-

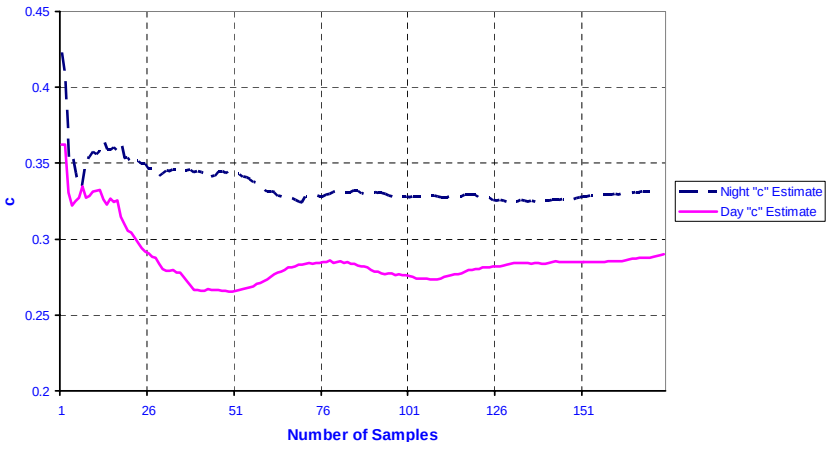

Figure 6.25: Identification of 'c' for Night and Day for High Humidity (Validation).

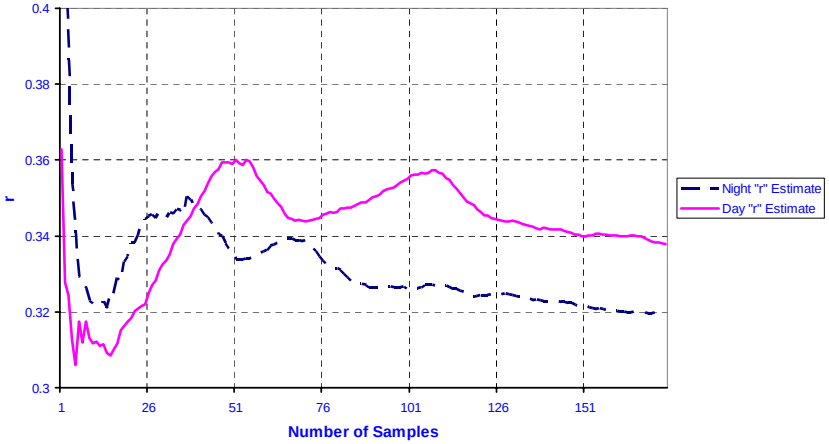

Figure 6.26: Identification of 'r' for Night and Day for High Humidity (Validation).

firms that during high humidity the humidity acts as buffer and prevents the solar radiation from inducing thermal shocks into the system. The trends shown by the Figures 6.26 and 6.27 are the same but the convergence values are different due to the different average temperatures as already discussed in validation subsection of section 6.3.3. The implementation of identification scheme using the instrument setup and circuit developed was carried out. The following results could be summa-

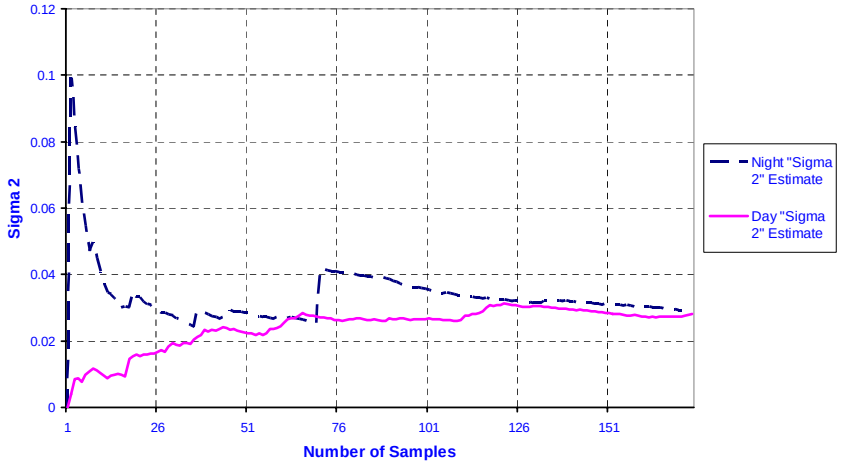

Figure 6.27: Identification of 'σ^2' for Night and Day for High Humidity (Validation).

rized. Using the above computational scheme for the On-Off duration obtained the results could be summarized in the following pages.

6.5 Summary

Results for identification scheme implemented for a real Air-Conditioner system were presented. The variation in the identification of parameter of the model with respect to Humidity were discussed. Also, variations in the identification of parameters due to solar radiation was obtained.

Chapter 7

CONCLUSIONS

7.1 Summary

The work presented in this thesis addressed the issue of Load Management under Direct Load Control strategy. The main aim here was to develop an environment that integrates identification, simulation and control all necessary for the implementation of DLC.

For this purpose the physical model proposed by Chong and Debs presented in Chapter 2 was used in the simulation of the individual A/C's. The typical test like the cold load pickup was used to validate the elementary load and compared successfully to [10]. Indeed, the models responded as expected and hence it confirmed the simulation carried out.

The identification scheme based on Maximum Likelihood algorithm presented in

Chapter 3 was first reproduced for the Heater and then extended to the A/C. The identification scheme was also extended to the Air-Conditioner's case. The mean square estimates were then derived for A/C and sensitivity analysis for limited samples were performed. The simulation results confirmed the theoretical results obtained.

The control scheme based on Model Predictive Control proposed by Molina et al. was scrutinized and a modified control strategy was proposed. Results were presented for peak load clipping. The simulation showed the potential for possibly reducing the power demand by 2.5% while taking into account the comfort index and the payback.

For implementation of DLC on a simple case, instrumentation was done on a real A/C in a residential setting. Data acquisition of internal parameters like temperature and humidity of the residential house along with external parameters like ambient temperature and ambient humidity and power reading from the A/C unit were implemented. The data collected was analyzed and used in the identification scheme.

In order to implement the direct control of the load, a low cost computer controlled prototype device was designed, developed and successfully tested. This device could be directly hooked without involving any change in the actual setting of the thermostat. This device has the following features:

- It monitors the internal temperature for implementing the control decision.

- It provides the "On-Off" duty cycles for identification scheme by observing the discrete state of the A/C.

- It could also be used to implement forced duty cycles on the A/C as part of load reduction.

Finally the sensitivity of the identification scheme as perceived by the utility was studied with respect to the environmental parameters like humidity and solar radiation. Results for those effects on the load parameters were presented.

7.2 Possible future development

Some avenues for future development could be summarized as follows:

- Sensitivity analysis showed that any environmental change effects the parameters of the model. Even though the identified load is seen by the utility, they lost their physical relation with the A/C. Use of physically based model which incorporates these effects of humidity and solar radiation where these parameters will explicitly appear as model parameters can be addressed.

- The matlab program computation time for optimization was observed to be very high. This time limitation could be improved by using a 'C' code structure of the same strategy or by parallel processing or a combination of artificial intelligence modelling and prediction.

- Peak Load Clipping in the load profile was presented in this work. Other strategies of Valley filling and Load shaving with the modified MPC control strategy can be addressed.

- Data acquisition was done as part of this work using a personal computer directly. For this DLC to be expanded to homogenous group, the issues related to data transmission, data loss and control delays could be addressed. Also a Lan, Wan or Internet based architecture could possibly be ventured.

- Using the developed electronic device presented in Chapter 6, a real-time control system for acquiring the data and controlling a complete residential, office buildings and Industrial Chillers could be developed with slight modifications.

- One important aspect would be to study the effect of control strategy on the starting frequency of the ac supply and on the cold inrush current.

- The effect of hard environmental conditions, like high humidity and high temperature, on the cooling rate is significant. The A/C stays "On" longer unusually. The control strategy as it is now may fail to save power without affecting the comfort index. A closer look to these situations is an important direction for future research.

Bibliography

[1] M. El-Amin, A.M. Al-Shehri, G. Opoku, H. Maghrabi and M.A. AbdulMajeed. "Opportunities for demand side management programs in Saudi Arabia". *Load Management and Energy conservation, GCC-CIGRE Tenth Symposium 10-11 November 1999*, pages 71–83, November 1999.

[2] Gupta P.C. and Yamada K. "Adaptive short-term forecasting of hourly load using weather information". *IEEE Transactions on Power Applications and Systems*, PAS-91, 1972.

[3] F.D. Galiana et. al. "Identification of stochastic electric load models from physical data". *IEEE Transactions in Automation Control*, AC-19:887–893, Dec. 1974.

[4] Poysti K. "Box-jenkins method in short-term forecasting of grid loads in finland". *In the Proceeding of 8th Power Systems Computation Conference*, pages 357–368, Aug. 1984.

[5] D. W. Bunn and E. D. Farmer. "Comparative models for electrical load forecasting". *John Wiley and Sons*, 1985.

[6] Ihara S. and Schweppe F.C. "Physically based modelling of cold load pickup". *IEEE Transaction on Power Apparatus and Systems*, PAS-100:4142–4150, September 1981.

[7] Mortensen R. E. and Haggerty K. P. "A stochastic model for heating and cooling loads". *IEEE Transactions on Power Systems*, 3(3):1213–1219, August 1988.

[8] Chong C. and Debs A. "Statistical synthesis of power system functional load models". *Proceeding of the IEEE conference on Decision and Control*, pages 264–269, 1979.

[9] Mortensen R. E. and Haggerty K. P. "Dynamics of heating and cooling loads: Models, simulation and actual utility data". *IEEE transaction on Power Systems*, 5(1):243–249, February 1990.

[10] Alvarez C., Malhame R.P. and Gabaldon A. "A class of models for load management application and evaluation revisited". *IEEE, Transactions on Power Systems*, 7(4):1435–1443, November 1992.

[11] Kamoun S. and Malhame R.P. "Convergence characteristics of a maximum likelihood load model identification scheme". *Automatica*, 28(5):885–896, Sept. 1992.

[12] Sami El-Ferik and Malhame R. "Identification of alternating renewal electric load models from energy measurements". *IEEE Transaction on Automatic Control*, 39(6):1184–1196, June 1994.

[13] C. N. Kurucz, D. Brandt and S. Sim. "A linear programming model for reducing system peak through customer load control programs". *IEEE Transactions on Power Systems*, 11(4):1817–1824, November 1996.

[14] Kah-Hoe Ng and Shebé G. B. "Direct load control - a profit based load management using linear programming". *IEEE- Transactions on Power Systems*, 13(2):688–694, May 1998.

[15] Y.-Y. Hsu and H.-C. Kuo. "Dispatch of capacitors on distribution system using dynamic programming". *Generation, Transmission and Distribution, IEE proceedings*, 140(6):433–438, November 1993.

[16] Deh chang Wei and Namming Chen. "Air conditioner direct load control by multi-pass dynamic programming". *IEEE Transaction on Power Systems*, 10(1):307–313, Febraury 1995.

[17] Jianming Chen, Fred N. Lee, Arthur M. Breipohl and Rambabu Adapa. "Scheduling direct load control to minimize system operational cost". *IEEE Transactions on Power Systems*, 10(4):1994–2001, November 1995.

[18] N. Navid-Azarbaijani and M. H. Banakar. "Realizing load reduction functions by aperiodic switching of load groups". *Power Systems, IEEE Transaction on*, 11(2):721–727, May 1996.

[19] Molina A., Gabaldon A., Fuentes J. A. and Fco. J. Canovas. "Approach to multivariable predictve control applications in residential hvac direct load control". *Power Engineering Society, Summer Meeting, 2000. IEEE,*, 3:1811–1816, 2000.

[20] Malhame R. and Chong C. Y. "Electrical load model synthesis by diffusion approximation of a high order hybrid-state stochastic system". *IEEE Transactions on Automatic Control*, AC-30(9):854–860, September 1985.

[21] Malhame R. and Chong C. Y. "On the statistical properties of a cyclic diffusion process arising in the modelling of thermostat-controlled electric power system loads". *SIAM, Journal of Applied Maths*, 48(2):465–480, April 1988.

[22] R.E. Mortensen. "Alternating renewal process models for electric power system loads". *Automatic Control, IEEE Transactions on,*, 35(11):1245, November 1990.

[23] Alvarez C., Malhame R.P. and Gabaldon A. "A class of models for load management application and evaluation revisited". *IEEE Power Engineering Review*, 12(11):45, November 1992.

[24] Canbolat Ucak and Ramazan Caglar. "Effects of load parameter dispersion and direct load control actions on aggregated load". *Power System Technology, 1998. Proceedings. POWERCON '98. 1998 International Conference on*, 1:280–284, 1998.

[25] Kamoun S. *"Synthese Dynamique de modeles statistiques a base physique bes charges electriques dans les Reseaux"*. PhD thesis, Ecole Polytechnique De Montreal, December 1989.

[26] Sami El-Ferik. *"Identification D'un modele stochastique de renouvellement pour charges thermiques sur un Reseau Electrique"*. PhD thesis, Ecole Polytechnique De Montreal, June 1991.

[27] K. Bhattacharya and M.L. Crow. "A fuzzy logic based approach to direct load control". *IEEE Transactions on Power Systems*, 11(2):708–714, May 1996.

[28] Huang K. Y., Yang H. T., Liao C.C. and Ching-Lien Huang. "Fuzzy dynamic programming for robust direct load control". *Energy Management and Power Delivery, 1998. Proceeding of EMPD '98.*, 2:564–569, 1998.

[29] Leehter Yao and Kai-Chin Hsieh. "Scheduling of direct load control by a recursive genetic algorithm". *Systems, Man and Cybernetics, 1998 IEEE Internaltional Conference on*, 3:2460–2465, 1998.

[30] Anibal T. and Edward L. Vine. "Advanced monitoring technologies for the evaluation of demand-side management programs". *Power Systems, IEEE Transaction on*, 9(3):1691–1697, August 1994.

[31] C. Y. Chang, C. J. Wu, C. T. Chang, C. H. Lin, J. L. Yen, T. G. Lu and W. C. Chang. "Experiences of direct load control using ripple signals in taiwan power system". *Advances in Power Systems Control, Operation and Management, 1997. APSCOM-97. Fourth Internaltional conference on*, 2:591–596, 1997.

[32] Ming Yuan Cho and Cha Win Hwang. "Development of PC based management system for electrical energy saving of high voltage customer". *Industrail and Commercial Power Systems Technical Conference, 2001. Conference Record: Papers presented at the 2001 Annual Meeting. 2001 IEEE*, pages 7–12, 2001.

[33] Shih Wei Gau, Ming Yuan Cho and Cha Win Hwang. "Development of microprocessors based demand control system for industrail and commercial customers". *Industrail and Commercial Power Systems Technical Conference, 2001. Conference Record: Papers presented at the 2001 Annual Meeting. 2001 IEEE*, pages 1–6, 2001.

[34] J. C. Hwang. "Assessment of air-condition load management be load survey in taipower". *IEEE Transactions of Power Systems*, 16(4):910–915, November 2001.

[35] Paul I-Hai Lin and Harold L. Broberg. "Internet-based monitoring and control for HVAC applications". *IEEE Industry Applications Magazine*, pages 49–54, Jan-Feb 2002.

[36] Salehfar H., Noll P. J., LaMeres B. J., Nehrir M. H. and Gerez V. "Fuzzy logic-based direct load control of residential electric water heaters and air conditioners recognizing customer preferences in a deregulated environment". *Power Engineering Society Summer Meeting, 1999. IEEE*, 2:1055–1060, 1999.

[37] Malhame R. and Chong C. Y. "Towards the solution of an optimal control problem in the load management of electric power systems". *Proceedings of Conference on Decision and Control*, pages 2–4, December 1980.

[38] El-Ferik, Sami and Malhame R. P. "Correlation identification of alternating renewal electric load models". *Decision and Control, Proceedings of the 31st IEEE Conference on*, 1:566–567, 1992.

[39] Malhame R. and Chong C.Y. "Towards the solution of an optimal control problem in the load management of electric power systems". *Proceeding of Conference on Decision and Control, IEEE*, December 1980.

[40] H.-T. Yang and K.-Y. Huang. "Direct load control using fuzzy dynamic programming". *Generation, Transmission and Distribution, IEE proceedings*, 146(3):294–300, May 1999.

[41] Hsu Y.Y. and Su C. C. "Dispatch of direct load control using dynammic programming". *IEEE Transactions on Power Systems*, 6(3):1056–1061, August 1991.

VITA

Syed Ameenuddin Hussain was born in Hyderabad, India on March 11, 1979. He received Bachelor's of Engineering in Mechanical Engineering from Osmania University in 2000. He joined the Department of Systems Engineering, King Fahd University of Petroleum & Minerals (KFUPM), as a Research Assistant in Fall 2000. He received the Master of Science degree in Systems Engineering from KFUPM in January 2004.